NKG2A is a Therapeutic Vulnerability in Immunotherapy Resistant MHC-I Heterogenous Triple Negative Breast Cancer

By

Brandie C. Taylor

Dissertation
Submitted to the Faculty of the
Graduate School of Vanderbilt University
in partial fulfillment of the requirements
for the degree of

DOCTOR OF PHILOSOPHY
in

Cancer Biology
May 10, 2024
Nashville, Tennessee

Approved:

Justin M. Balko, Pharm.D., Ph.D. (Advisor)

Vito Quaranta, M.D. (Chair)

Jin Chen, M.D., Ph.D.

Marjan Rafat, Ph.D.

John Wilson, Ph.D.

Dedication

For patients and loved ones impacted by cancer.

Acknowledgements

I am grateful for the opportunity to recognize those who have played an essential role in shaping my scientific education and development. Above all, I am deeply grateful to my exceptional mentor, Dr. Justin Balko, whose guidance has enabled me to evolve both personally and scientifically. I am indebted to him for his kindness, patience, and unwavering support. As a mentor, he consistently prioritizes the success of his trainees and actively seeks out opportunities to empower us for the future. I am thankful for members of the Balko Lab for their expertise and advice. Specifically, I would like to thank Xiaopeng Sun, this project would not have been possible without him.

I am grateful to the members of my thesis committee: Dr. Vito Quaranta, Dr. Jin Chen, Dr. Marjan Rafat, and Dr. John Wilson. Their unwavering support and guidance throughout my PhD journey have been invaluable. They challenged and motivated me to elevate the quality of my research, and for that, I am truly thankful.

Furthermore, I am so grateful to my partner Jake Hermanson for the unwavering support for all of my dreams. He has encouraged me to pursue my passions and has been there to celebrate my successes.

Lastly, I want to express my sincere gratitude to the patients and families who generously contribute their time, tissues, and data to cancer research. Their selflessness and willingness to participate in clinical trials are crucial in advancing cancer research. Without them, we would not be able to make significant progress in fighting this disease.

Contents

LIST OF TABLES

LIST OF FIGURES

CHAPTER I

Introduction[1]

Immunotherapy has emerged as a promising avenue for the treatment of cancer, with recent advances in immuno-oncology demonstrating the potential of targeting the immune system. Immune checkpoint inhibitors (ICI) have revolutionized cancer treatment by improving the prognosis and survival for select patients. However, ICI treatment remains limited due to intrinsic or acquired resistance to therapy, resulting in only a small percentage of patients benefiting from treatment. Despite extensive research, there are currently few clinically useful biomarkers of response, such as Programmed Death-Ligand 1 [PD-L1], tumor mutational burden, and microsatellite instability, and limited approved therapies to augment response to ICI. As the use of immunotherapies continues to grow, there is an urgent need to understand the mechanisms of ICI resistance and develop new therapeutic strategies to induce long-term responses.

CD8+ T cells are one of the primary effector cell types that mediate response to ICI and are activated following the recognition of peptide:major histocompatibility complex class I (MHC-I) complexes (pMHC-I) and co-stimulatory signals. T-cell receptors (TCRs) mediate cytotoxic CD8+ T cell activation by binding to their target through interactions with cognate pMHC-I which are ubiquitously expressed by all nucleated cells (1). The efficacy of ICI depends on T cell recognition of pMHC-I on the tumor surface. Activated CD8+ T cells can induce tumor cell death through injecting granzymes and other cytotoxic molecules through perforin-permeabilized membranes at an immunologic synapse. Thus, one mechanism whereby tumors can avoid T

[1] Selected from Taylor, B.C., and Balko, J.M. (2022) Mechanisms of MHC-I Downregulation and Role in Immunotherapy Response. *Frontiers in Immunology.* (**13);** DOI: 10.3389/fimmu.2022.844866

cell cytotoxicity is by downregulation of MHC-I. Loss and reduction of MHC-I expression has been correlated with worse overall prognosis and response to ICI in several cancer patient cohorts and clinical trials (2–6). Aberrant MHC-I expression may be reversible or irreversible because of genetic, epigenetic, transcriptional, or post-transcriptional alterations. The reversibility of some mechanisms of MHC-I downregulation creates a potential avenue for therapeutic strategies to restore MHC-I antigen presentation as a possible combinatorial approach with ICI in cancer. This chapter will address the current known mechanisms of MHC-I downregulation in cancer, implications in patient immunotherapy efficacy, and potential therapeutic MHC-I upregulation strategies to overcome ICI resistance in patients.

MHC-I pathway and regulation

MHC-I is a heterodimer consisting of two domains, a polymorphic human leukocyte antigen (HLA)-encoded heavy α-chain and an invariant light chain termed β2-microglobulin (β2M) (1). There are three classical HLA class I heavy chains, HLA-A, -B, and -C, which are encoded by three separate genes. MHC-I has a high degree of polymorphism derived from each heavy chain's peptide binding domain. The various HLA alleles have diverse peptide-binding specificities due to the sequence divergence between alleles (7). This diversity of MHC-I allows for a large repertoire of peptides, also known as the immunopeptidome, that can be recognized by CD8+ T cells.

Antigen presentation by MHC-I begins when endogenous proteins are ubiquitinated for proteasomal fragmentation into peptides (8). The peptides are then translocated from the cytosol into the endoplasmic reticulum (ER) through the transporters associated with antigen processing (TAP1/ TAP2) and undergo further processing by ER aminopeptidases (ERAP) (9,10). Processed peptides of 8 to 10 amino acids in length are required for stabilization of the MHC-I complex and are bound by their side chains through molecular interactions (6). The folding and assembly of the α-heavy chain and β2M is promoted by calnexin and this initial

complex is stabilized by the chaperone protein tapasin in complex with ERp57 via calreticulin (11). Interaction between TAP1/2 and tapasin permits exchange of peptides into the MHC-I binding groove, release of chaperone proteins, and stabilization of the MHC-I complex. Finally, the peptide:MHC-I complex travels via the Golgi apparatus to the cell surface and antigens are presented to CD8+ T cells (**Figure 1.1**). Cross presentation of exogenous antigens, normally presented by MHC-II on the surface of professional antigen presenting cells, can also be presented through the MHC-I pathway through endocytic mechanisms in which antigens are transported from the endosomal compartment into the cytosol and then degraded by the proteasome and transported into the ER (12). MHC-I expression is induced by both type I and type II interferons and this transcriptional activation is regulated by various conserved cis-regulatory elements at their promoters.

Transcriptional regulation of MHC-I is mediated by three major promoter elements; enhancer A bound by nuclear factor (NF)-κB, interferon-stimulated response element (ISRE) bound by multiple interferon regulatory factor (IRF) family members, and the SYX-module bound by NOD-like receptor CARD domain containing 5 (NLRC5) (13–15). NF-κB induced class-I expression is functional at the HLA-A and HLA-B loci, containing NF-κB binding sites at their Enhancer A regions. In contrast, HLA-C and the non-classical alleles are not transactivated by NF-κB (14,16).

The IRFs are upregulated in response to both type I interferons (IFNs) (e.g., IFNα and IFNβ) and type II IFNs (e.g., IFNγ) and signal through the JAK/STAT pathway (17). Following phosphorylation by JAK, STAT1/STAT2 dimerizes and translocate to the nucleus, where it binds to Gamma-activated sequence (GAS) elements of IFN-stimulated genes, including IRFs, which can subsequently activate the ISRE in the MHC-I promoter (13). It is important to note that studies show that IRF2 can be constitutively expressed and stable in the absence of IFN stimulation (18,19). Therefore, not only is the IRSE promoter region implicated under

inflammatory conditions, but it can also regulate basal MHC-I expression under non-inflammatory conditions. NLRC5 is a critical transcriptional regulator of MHC-I and its associated genes (e.g., β2M, TAP1/TAP2, and LMP2) (20). NLRC5 lacks a DNA-binding domain and is therefore dependent on the enhanceosome to connect to the promoter region of the SYX-module (21,22). Activation of each of these three promoter regions facilitates antigen presentation by MHC-I on the tumor cell surface and its accessory molecules β2M, TAP, and LMP2.

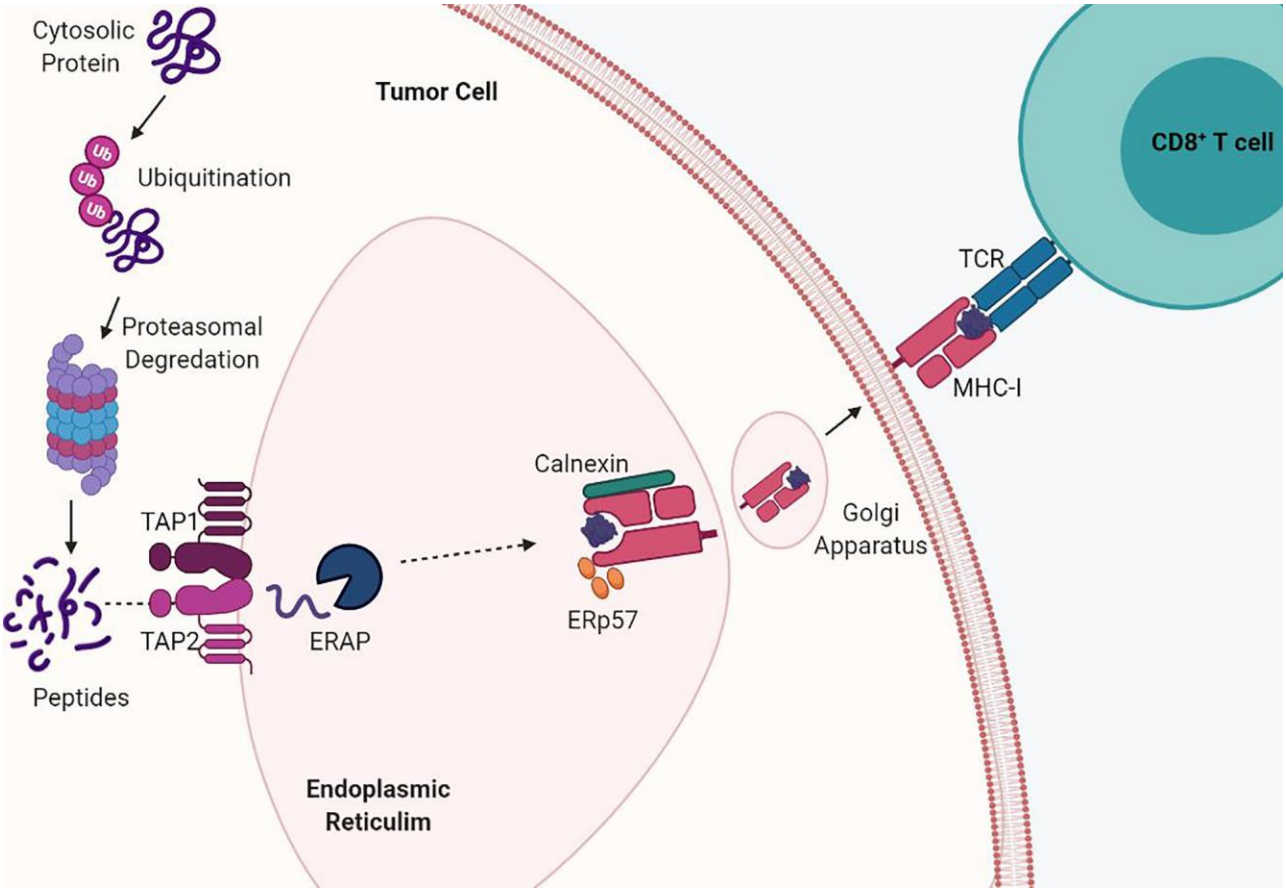

Figure 1.1 MHC-I antigen processing and presentation pathway. MHC-I presents endogenously derived peptide antigens to CD8+ T cells. Cytosolic proteins are degraded by the proteasome into peptides. These peptides are then shuttled into the endoplasmic reticulum (ER) by TAP transporter proteins. Antigen peptides are then loaded into the assembled MHC-I α-heavy chain and beta-2-microglobulin (β2M) complex and shuttled *via* the Golgi to the cell surface. Acquired mutations in the antigen presentation pathway drive loss of MHC-I.

Mechanisms of MHC-I downregulation in cancer

Tumor progression is shaped by immunoediting eventually leading to escape from anti-tumor immune responses. Tumor specific MHC-I (tsMHC-I) downregulation has been described in numerous tumor types such as melanoma, breast, colorectal, and cervical cancers (23–26). Loss of tsMHC-I expression is often correlated with shorter overall and progression free survival, and higher instances of metastasis (27–30). The clinical significance of MHC-I is due to the role of antigen presentation and immune control of cancers. Tumors can reduce antigen presentation through several mechanisms including reduced surface expression of tsMHC-I through genetic alterations, antigen depletion, and modulation of transcription. The types of defects that lead to MHC-I disfunction can be divided into two groups: hard lesions (i.e., therapeutically intractable) and soft lesions (i.e., therapeutically tractable) **(Figure 1.2).**

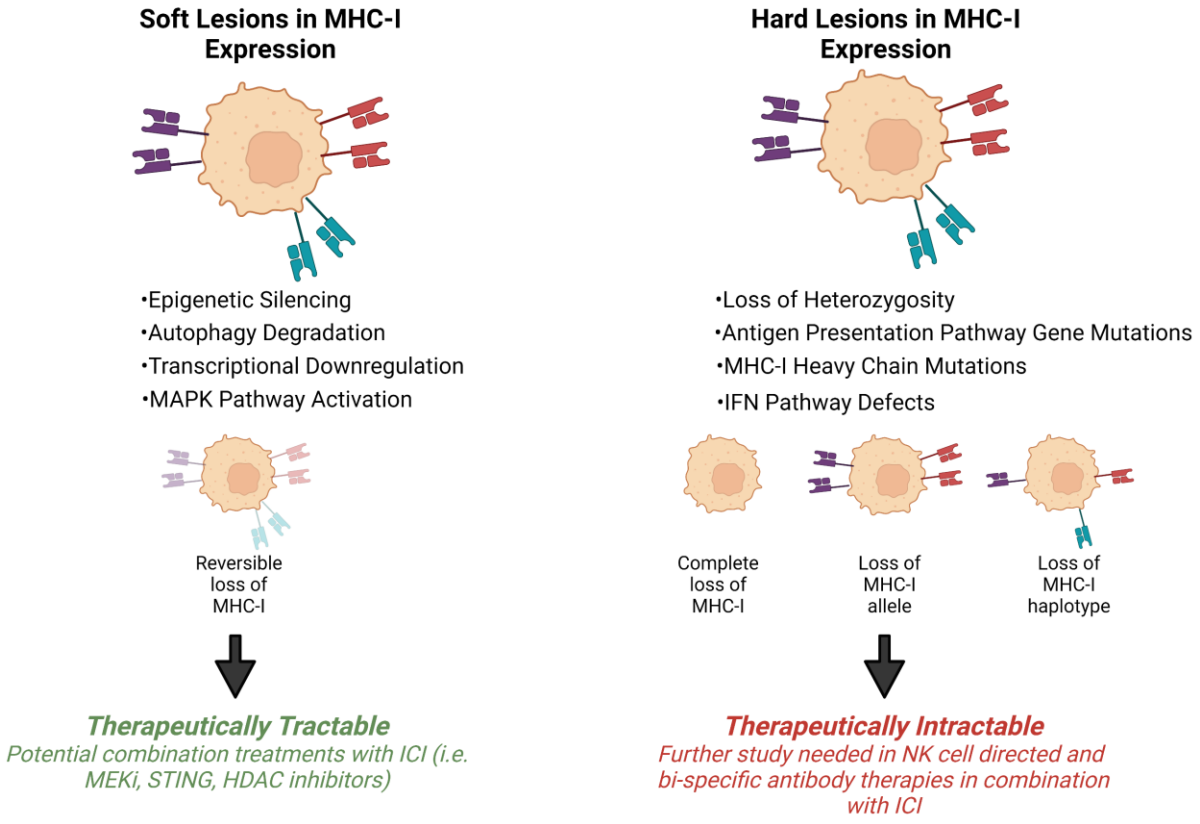

Figure 1.2 Mechanisms of MHC-I downregulation. Tumor specific MHC-I loss of expression can be classified into soft or hard lesions. MHC-I can be recovered *via* different treatment

approaches depending on the type of mutation. Hard lesions, such as *B2m* loss, cannot be therapeutically recovered, however, soft lesions, like epigenetic silencing, can be therapeutically reversed.

Antigen presentation pathway gene mutations

Defects in the MHC-I antigen presentation pathway are a common mechanism by which tumors can evade the immune response. Reduced levels and complete loss of TAP1/TAP2 expression have been documented in colorectal cancer, renal cell carcinoma, and melanoma resulting in reduced tsMHC-I stability and expression on the tumor surface (31–35). TAP loss has been attributed to a functionally defective allele of Tap1 in numerous solid tumors and cell lines resulting in defective peptide presentation (54). Similarly, studies have shown reduction of tapasin and ERAP have resulted in loss of antigen presentation on the tumor surface (24,36,37). Genetic structural alterations of the MHC-I complex are another common finding in tumors that exhibit reduced antigen presentation. Numerous studies document loss of heterozygosity (LOH) associated with chromosome 6p21 resulting in HLA haplotype loss in tumors (38–42). One clinical study designed to test adoptive transfer of T-cells revealed that downregulation of HLA-C was linked with immune evasion and lack of response to treatment (43). Further, a heterozygous deleterious mutation or complete loss of β2M can lead to reduced or absent surface levels of tsMHC-I. Some cancers, such as lymphomas, have high β2M mutation rates in more than 25% of patients (44,45). Additionally, truncating mutations of β2M were found in metastatic colon and melanoma cancers found to be resistant to the anti-PD1 therapy, pembrolizumab (23,46,47). These observations show that somatic mutations in MHC-I genes are a common mechanism of tumor immune evasion.

Transcriptional silencing

The MHC-I pathway can also be dysregulated through the modulation of various transcription factors. NF-κB, bound to the enhancer A region in the MHC-I promoter, is found to be constitutively active in most cancers (26). However, in some cancer types the loss of NF-κB expression results in MHC-I downregulation (19). This suppression of tsMHC-I expression via

NF-κB can be attributed to multiple proteins, specifically Nedd4 Binding Protein 1 (N4BP1) and tumor necrosis factor (TNF)α-induced protein 3 interacting protein 1 (TNIP1) (48). In addition to NF-κB, IFNs dimerize STAT1 resulting in IRF binding to ISRE therefore playing a key role in MHC-I upregulation during inflammation. Downregulation of both type I and II IFN pathways have been identified as mechanisms leading to resistance to ICI and adoptive T-cell therapies (38,49,50). Lastly, the expression of NLRC5, a key regulator of MHC-I transcription, has been found to be correlated with MHC-I expression and patient survival in several cancer types including ovarian, breast, and colorectal cancers as a mechanism of immune evasion (22).

The expression of antigen presentation pathway genes can also be downregulated through epigenetic silencing. This can occur from hypermethylation of the NLRC5 and MHC–I promoter regions (22,51–55). DNA hypermethylation has been shown to be reversible with the treatment of DNA methyltransferase inhibitors (DNMTi) leading to MHC-I upregulation in numerous cancer types (56–61). Another common defect resulting in reduced tsMHC-I antigen presentation is deregulation of histone deacetylases (HDACs), which removes acetyl groups from histones resulting in a more closed chromatin structure preventing the transcription of MHC-I (57,62,63). HDAC inhibitors increase the expression of MHC-I both *in vitro* and *in vivo*. Many of these drugs are already FDA approved (e.g., panobinostat and vorinostat) while others are in clinical trials to determine their efficacy in several types of cancer (60,62,64,65). Overall, these studies reveal the tumor-intrinsic role of epigenetic silencing to evade immune surveillance and the need for further study to understand the functional effect of these mechanisms in cancer.

Post-transcriptional silencing

In addition, loss of MHC-I in cancer can be due to post-transcriptional regulation mediated by non-coding RNAs. MicroRNAs (miRNA), a class of non-coding RNAs, can bind to the 3' untranslated region (UTR) of mRNAs. Upregulation of some miRNAs have been reported to repress expression of MHC-I in multiple cancers, including melanoma, esophageal carcinoma, and colorectal cancer (66–68). MiRNAs can affect various parts of the antigen presentation

pathway, including TAP1/TAP2 and calreticulin (66,68,69). For example, TAP2 expression has been shown to be inhibited in esophageal adenocarcinoma through miRNA 125a-5p and 148-3p which resulted in downregulation of HLA-A, -B, and -C (147). Furthermore, suppression of chaperone proteins by miRNAs (e.g., calnexin, tapasin, and calreticulin) involved in antigen presentation can downregulate MHC-I expression and CD8+ T cell infiltration (148–150). Taken together, miRNAs can negatively regulate MHC-I through post-transcriptional modification and further study may potentially lead to new therapeutic targets.

Implications of MHC-I downregulation in immunotherapy response

Recent developments in cancer therapy have shown clear advantages in targeting the immune system. Immunotherapies, such as ICI, have revolutionized the treatment for a range of cancer types, such as melanoma and non-small cell lung cancer (70,71). ICI increases anti-tumor immunity by blocking intrinsic checkpoints that have an inhibitory role in regulating T cell responses, such as cytotoxic T-lymphocyte antigen 4 (CTLA-4) and programmed cell death 1 (PD-1). Compared to previous standards of care (e.g., chemotherapy and surgery), ICI therapy has significantly improved overall and progression free survival in patients (72).

Despite these successes, ICI treatments still have many limitations and challenges. The benefits of ICI are still very low in some common tumor types, including breast and prostate cancer. ICI therapy is further complicated by observations of intertumoral heterogeneity in the degree of response to therapy. Additionally, a substantial percentage of cancer patients treated with immunotherapy experience intrinsic or acquired resistance, and many experience immune-related adverse events (73). There is currently a limited number of clinically approved multimodal treatments strategies to improve responsiveness to ICI. Furthermore, there are very few biomarkers that can predict immunotherapy benefit.

Acquired resistance to immunotherapy in several forms of cancer is associated with alterations in the MHC-I antigen presentation pathway. In several studies, downregulation of MHC-I is correlated with resistance to ICIs and adoptive T cell therapy (55,74,75). This is presumably

mediated by defects in the expression of tsMHC-I for tumor antigen presentation to CD8+ T cells. Analysis of somatic genetic alterations through transcriptomic sequencing and IHC in longitudinal samples of melanoma patients revealed LOH of β2M was found to be a common mechanism of acquired resistance to anti-CTLA and anti-PD-1 therapies (23,47,76). Mechanisms of transcriptional loss and evolutionary divergence of the class I heavy chain of specific alleles have been reported in patients which results in the loss of MHC-I polymorphism leading to ICI resistance (41,77,78). Whole exome sequencing and single-cell transcriptome analysis of colorectal patients resistant to ICI therapy have identified β2M biallelic deletions and truncating mutations in both primary and metastatic tumor lesions (46,79,80). Furthermore, a recent study *in vitro* found that β2M suppression in non-small cell lung cancer may be caused by KRAS mutations and STAT5 inhibition (112). Transcriptome and flow cytometric analysis of longitudinal melanoma biopsies collected from patients receiving PD-1 inhibitors identified downregulation of MHC-I to also be associated with TGFβ activity, SNAI1 upregulation, and cancer associated fibroblasts (74). Uncovering additional mechanisms of tsMHC-I and β2M downregulation as potential biomarkers for ICI response and strategies for restoring their expression are areas that merit further study.

Recent studies have demonstrated that in response to anti-PD-1/PD-L1 agents, non-responders have a much higher rate of genomic alterations in the IFNγ pathway as compared to patients that exhibit a clinical benefit. JAK1 or JAK2 were elucidated through whole exome sequencing of PD-1 resistant melanoma tumors (23,81). More specifically, one study determined that JAK1, not JAK2, is the primary mediator of IFNγ induced MHC-I expression and response to anti-PD-L1 therapy (82). Additionally, the transcription factor double homeobox 4 (DUX4) has been shown to block the IFNγ mediated upregulation of tsMHC-I in numerous cancer types *in vitro* resulting in failure to respond to anti-CTLA-4 and anti-PD-1 therapy and decreased overall survival (83). In addition, Ptpn2, was identified through an *in vivo* CRISPR screen to negatively regulate the JAK/STAT and antigen presentation pathways leading to ICI resistance (84). Taken

together, these studies suggest that negative regulation of the IFNγ pathway is a mechanism of primary resistance to ICI therapy and supports the design of therapeutic strategies to overcome IFNγ downregulation.

Therapeutic strategies to enhance MHC-I expression

TsMHC-I is associated with improved response to ICI and increased amounts of tumor infiltrating lymphocytes (41,77,79,82,85). Loss of MHC-I antigen presentation is common in cancers and allows tumors to evade immune surveillance. Although MHC-I loss due to structural genetic alterations such as β2M loss are irreversible, post-transcriptional downregulation of MHC-I can be reversed (**Figure 2)**. Therefore, novel strategies to upregulate tsMHC-I are anticipated to improve responses to immunotherapies.

One potential target of upregulating tsMHC-I is through the IFN signaling pathway. IFNγ has been shown to increase expression levels of various antigen presentation genes such as MHC-I and TAP (19,86). Additionally, NLRC5 has been identified as a key transcriptional coactivator of MHC-I and antigen presentation pathway gene expression (21). Genetic alterations, copy number loss, and somatic mutations of NLRC5 results in reduced MHC-I expression in various cancer types (87). In melanomas derived from patients responding to anti-CTLA-4 and anti-PD-1, there was a significantly higher expression of NLRC5 compared to non-responding patients (55). It has been demonstrated in breast cancer *in vitro* models that NLRC5 was promoted by IFNγ with upregulation of MHC-I suggesting a potential benefit to ICI treatment (88). Although IFN may have a beneficial effect on immunotherapy response, there are limitations to using them in cancer therapy due to potentially life-threatening toxicities seen in patients (89). One possibility of using IFNs for therapeutic upregulation of tsMHC-I without the associated toxicity is through antibody directed, dose-dependent cytokine release at the tumor specific site (90). However, this approach is yet to be tested in large clinical trials. Additionally, NF-κB pathway activation via immune receptors, such as the TNFα receptor, leads to downstream transcription of MHC-I by binding to the enhancer A regulatory element.

Stimulation of NF-κB signaling to induce MHC-I upregulation in cancer is a potential therapeutic target. Retinoids, which are clinically used in neuroblastoma through the induction of apoptosis, have been described to induce MHC-I expression through NF-κB signaling (91,92). Furthermore, in murine models of melanoma, in tumors with deficient IFN signaling MHC-I expression was restored by intratumoral injection of polyinosinic:polycytidylic acid, BO-112(93). BO-112 restored MHC-I expression through an NF-κB mediated mechanism and independent of NLRC5. A recent study used a CRISPR screening approach to identify factors that decouple the regulation of MHC-I and PD-L1(94). It was found that depletion of TRAF3 upregulated MHC-I through the NF-κB pathway and TRAF3 small molecule inhibitors increased immuno-sensitivity of cancer cells specifically through MHC-I expression. Stimulation of the NF-κB and IFN-pathways to induce MHC-I expression is further substantiated by studies of Stimulator of Interferon Genes (STING). STING stimulates both NF-κB and IFN-pathways and several STING agonists are being examined in clinical trials in several solid tumors in combination with anti-PD-1 (ClinicalTrials.gov Identifier: NCT04096638, NCT04144140). These studies demonstrate the potential for increasing tsMHC-I expression through transcriptional regulation and cytotoxic CD8+ T cell infiltration to improve patient responses to immunotherapy.

Numerous oncogenic pathways have been reported to affect the expression of MHC-I and related antigen presentation components, including the MAPK and EGFR (Epidermal Growth Factor Receptor) pathways (95,96). The MAPK pathway is thought to negatively influence MHC-I expression through decreased IRF and STAT1 expression resulting in reduced levels of tumor infiltrating lymphocytes (95,97,98). MEK inhibitors (MEKi), cobimetinib and trametinib, have been shown to enhance IRF1 expression and increased phosphorylation of STAT1 in human epidermal models (99). MEKi in breast cancer and non-small cell lung cancer models *in vivo* and *in vitro* have demonstrated an increase in MHC-I expression and combination of MEKi and ICIs may be a clinically relevant treatment option (75,98). Overexpression of EGFR has been associated with poor response outcomes to ICI in various cancer models, including non-small

cell lung cancer and neuroblastoma (100,101). Also, the EGFR family member, HER2, was shown to be inversely correlated with MHC-I expression in breast cancer and impairs T cell recognition of peptide: MHC-I complexes (102,103). Targeting EGFR receptors with antibodies and inhibitors has resulted in increased expression of MHC-I and antigen presentation components in several cancer cell lines, thus increasing their susceptibility to CD8+ T cell cytotoxicity (104–106). Together, these studies show the importance of targeting oncogenic pathways regulating MHC-I in cancer and the potential for therapeutically restoring anti-tumor immunity and improving immunotherapy response.

A recent study showed that in pancreatic ductal adenocarcinoma (PDAC) MHC-I molecules are selectively targeted for lysosomal degradation through an autophagy-dependent mechanism (107). This study demonstrated that MHC-I is decreased in PDAC through a NBR1-mediated autophagy-lysosomal pathway. It was found that autophagy inhibition using a clinically available antimalarial agent, chloroquine, increased surface levels of MHC-I and anti-tumor T cell responses when combined with ICI therapy (anti-PD-1 and anti-CTLA4). In breast cancer the gene MAL2, which encodes a transmembrane protein associated with protein endocytosis, promotes the turnover of pMHC-I complexes by modulating the interaction between RAB7 and MHC-I (108). MAL2 plays a critical role in the endocytosis-mediated protein degradation of the MHC-I complex and downregulates CD8+ T cell cytotoxicity. Depletion of MAL2 enhanced antigen presentation on tumor cells and activation of CD8+ cytotoxic T cells. Therefore, inhibition of MAL2 is a potentially effective strategy for increasing the efficacy of immunotherapy. Studies have also revealed that high calnexin expression can promote tumor proliferation and growth in lung cancer (109,110). In both *in vitro* and an *in vivo* melanoma model, Scaffold/ Matrix- Associated Region-1 (SMAR1) is directly involved in immune evasion mechanisms by positively regulating MHC-I expression through the downregulation of calnexin (111). Calnexin gene expression was found to be suppressed by the formation of a repression complex that binds to the matrix attachment region (MAR) site on the calnexin promoter. This

supports a therapeutic need for small molecule compounds for stabilizing SMAR1 expression, increasing CD8+ cytotoxic T cell infiltration to aid ICI treatment.

Other strategies to upregulate tsMHC-I expression are actively being investigated to ameliorate immunotherapy resistance. Current standards of care in oncology like chemotherapy and radiation are known to induce anti-tumor immune responses without stimulating immunogenic cell death. Studies on various tumor cells *in vitro* have shown that some chemotherapeutic agents augment tsMHC-I expression and *in vivo* further induce tumor CD8+ T cell infiltration. Docetaxel, a common chemotherapeutic agent, can increase expression of components of the antigen presentation pathway, such as TAP and tapasin, without inducing immunogenic cell death *in vitro* (112). Topoisomerase inhibitors (e.g., etoposide) and microtubule stabilizers (e.g., paclitaxel) have also been shown to stimulate MHC-I expression and Treg depletion in murine models (6,113,114). These pre-clinical studies indicate a therapeutic advantage to increasing tsMHC-I antigen presentation through combination of ICI and chemotherapeutic agents.

MHC-I loss and tumor infiltrating NK cells

Natural Killer (NK) cells play a crucial role in the innate immune response and are essential in the initial stages of host defense against infections and malignancies. These cells contribute to host defense by directly killing stressed cells, including tumor and virally infected cells, and releasing cytokines to coordinate the function and recruitment of other immune subsets.

NK cell activation is regulated by a repertoire of activating and inhibitory receptors that recognize germline-encoded ligands expressed by target cells (**Table 1.1**). The interplay between inhibition and activation are balanced against each other, such that inhibition can be overcome by strong activation signals.

Table 1.1. List of NK cell activation and inhibitory ligands and their receptors

Receptors	Ligands
Activating	
NKG2D	MHC-I chains related protein A and B, UL16-binding proteins
NKp44	CD155, CD113
NKp46	B7-H6, BAG6, viral hemagglutinin, heparan sulfate
CD16	Fc region of IgG
Inhibitory	
NKG2A	HLA-E
KIR2DL1/2/3/4	HLA-A/B/C
LAIR1	Collagen

Several studies have highlighted the crucial role of NK cells in tumor immunosuppression. NK cell infiltration has been linked to better overall survival outcomes in various cancers, such as breast cancer and melanoma (115–117). Moreover, in mice, NK cells can eliminate various tumor types when injected at low doses into syngeneic mice and long-term depletion of NK cells resulted in significant increases in cancer severity (118–120). However, tumors often adapt a variety of escape mechanisms that prevent killing by NK cells. Suppressive cytokines, such as TGFβ, can downregulate the expression of activating receptors NKG2D and NKp30 (121). Another mechanism of escape is NK cell desensitization, where persistent stimulation by MHC-I deficient cells results in NK cells becoming desensitized after subsequent rounds of stimulation (122). A fundamental feature of NK cell recognition is their inhibition by receptors that bind MHC-I molecules. The function of these receptors is critical in preventing NK cell-mediated attacks against healthy cells. However, stressed cells such as virally infected or tumor cells with dysregulated MHC-I expression can become more susceptible to NK cell-mediated cytotoxicity, a process referred to as "missing-self recognition" (123). As a result, MHC-I deficient tumors, which are typically resistant to recognition by CD8+ T cells, may be promising targets for NK cell-mediated therapy.

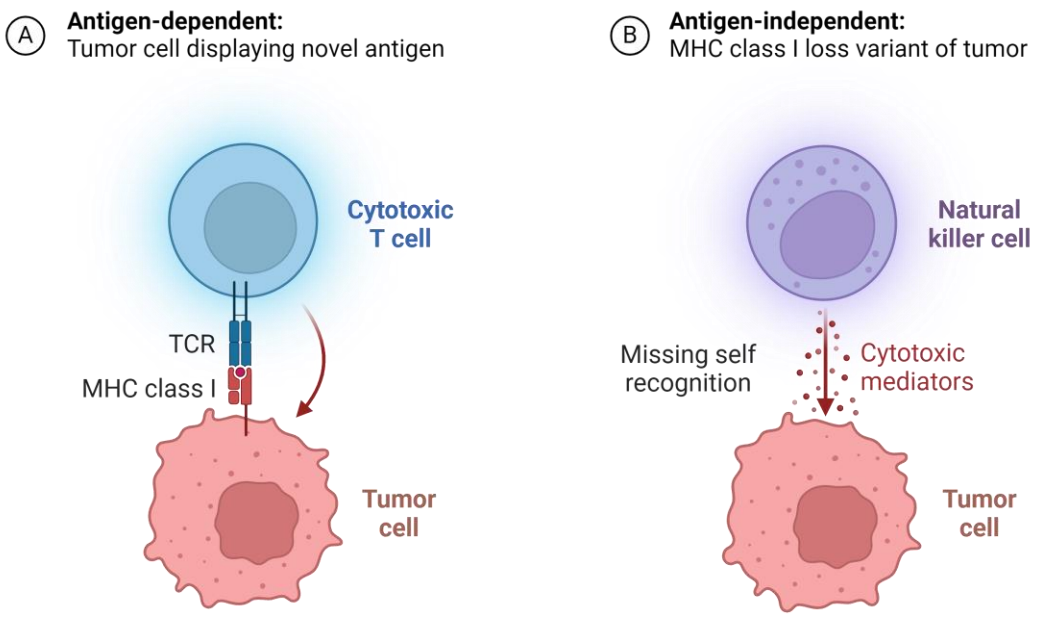

Figure 1.3: Immune cell mediated tumor destruction. CD8+ T cells and NK cells recognize target cells through distinct receptors. While both cytotoxic cells induce apoptosis in target cells, the mechanism of recognition by lymphocytes differs. NK cells kill target cells in an antigen-nonspecific manner regulated by a variety of inhibitory and activating surface receptors. In contrast, CD8+ T cells destroy target cells by recognizing MHC =class I restricted peptide antigens.

Inhibitory receptors specific for MHC-I signal through immunoreceptor tyrosine-based inhibitory motifs (ITIMs) in their cytoplasmic domains. In humans, killer cell immunoglobulin-like receptors (KIRs) and HLA molecules function as ligands to these receptors (124,125). Mice lack KIR genes, but instead, express the family of lectin-like 49 receptors that recognize different H-2 class I molecules (126). Moreover, the non-classical HLA-E molecule (known as Qa-1 in mice) can recognize the CD94-NKG2A heterodimer receptor, leading to the inhibition of NK cells. It is essential to note that these inhibitory receptors can distinguish between MHC-I allelic products, which may result in NK cells being unimpeded if they engage with a tumor cell that selectively downregulates certain MHC-I alleles (127,128). Tumors that express MHC-I can presumably be

sensitive to NK-mediated cytotoxicity if there are elevated levels of activating ligands that overcome this inhibitory signaling. This provides an avenue to explore the potential of NK cells in cancer therapy in both MHC-I deficient and MHC-I competent tumors.

There is a growing interest in using endogenous NK cells for cancer immunotherapies due to their potential to complement T cell therapy. Preclinical studies have shown that therapeutic intervention can lead to NK cell-mediated rejection of established solid tumors. However, further research is necessary to gain a better understanding of how the tumor microenvironment affects NK cell activation. These findings provide strong motivation to continue exploring the potential of NK cells in cancer therapy.

Immunotherapy in breast cancer

Breast cancer is the most prevalent malignancy among women worldwide and is associated with the highest mortality rates. Triple-negative breast cancer (TNBC), which lacks the expression of estrogen receptor (ER), progesterone receptor (PR), and human epidermal growth factor receptor 2 (Her-2), is characterized by low differentiation, high invasiveness, a propensity for local and distant metastases, poor prognosis, and high recurrence rates (**Figure 1.4**) (129). The tumor microenvironment in TNBC is composed of various immune cells, including tumor-infiltrating lymphocytes (TILs), antigen-presenting cells, and fibroblasts, which contribute to disease progression and metastasis. Immunotherapy has emerged as a promising treatment option for many refractory solid tumors, including breast cancer. Historically, breast cancer has been considered a "cold" tumor due to low T-cell infiltration and a low tumor mutation burden. However, TNBC is characterized by a higher presence of infiltrating lymphocytes, providing a favorable immune microenvironment for immune checkpoint inhibitors (ICIs). Additionally, TNBC has a relatively high tumor mutation load, providing an antigenic foundation for immune cell recognition. PD-L1 expression is notably elevated in TNBC, making it a promising target for ICIs (130). The combination of ICIs with chemotherapy has yielded

promising therapeutic outcomes in TNBC patients, highlighting the clinical relevance of immunotherapy for this aggressive subtype of breast cancer.

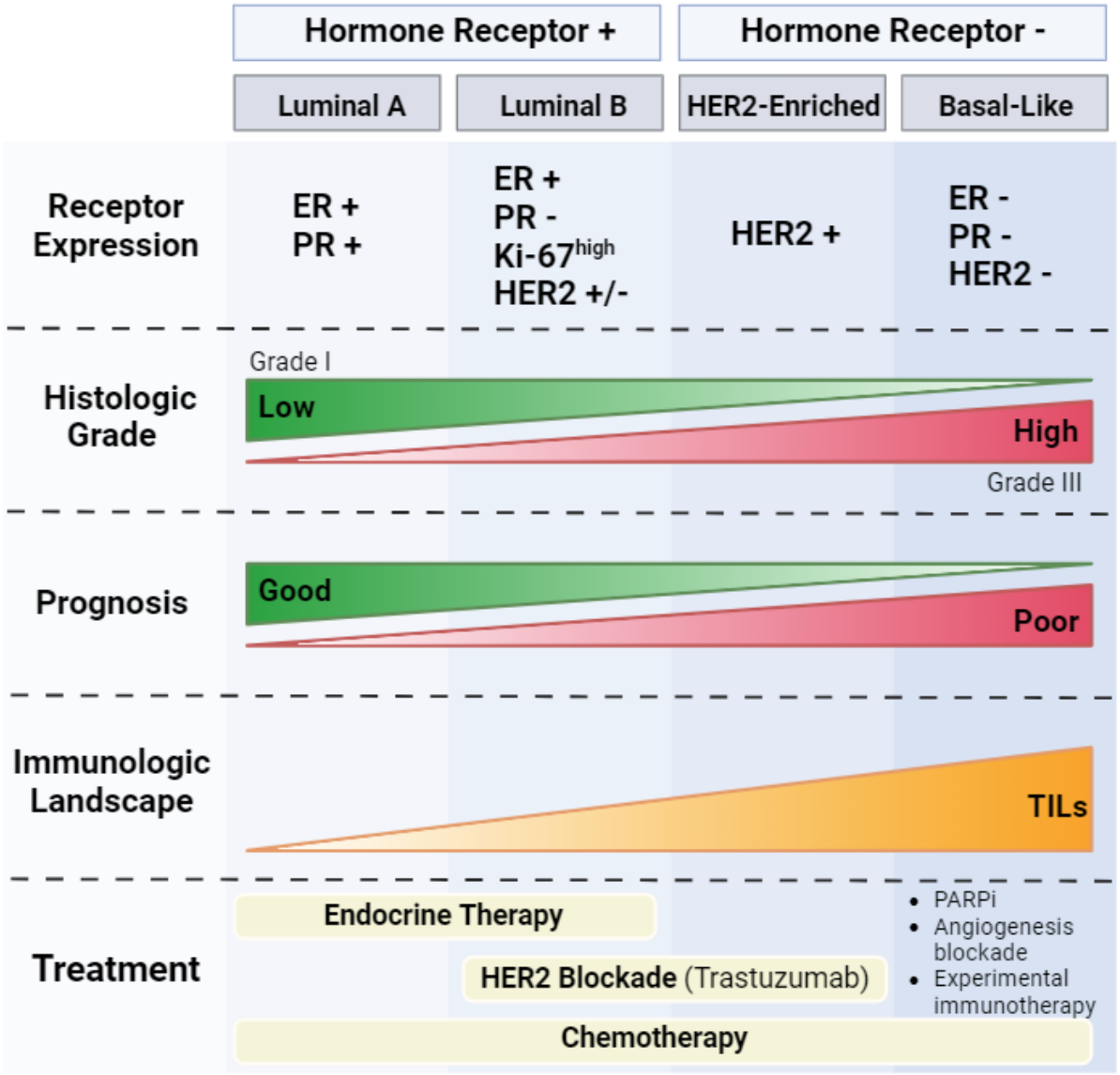

Figure 1.4: Breast cancer treatment and prognosis is informed by hormone receptor status. Breast cancer treatment and prognosis are influenced by the hormone receptor status, which is determined based on histological and molecular characteristics. Various classifications have been developed to aid in therapy decisions, with intrinsic subtypes being the most used in clinical settings. These subtypes rely on the expression of key proteins, including estrogen receptor (ER), progesterone receptor (PR), human epidermal growth factor receptor 2 (HER2), and the proliferation marker Ki67. Tumors expressing ER and/or PR are categorized as hormone receptor-positive, while tumors lacking expression of ER, PR, and HER2 are referred to as triple-negative.

In the phase III trial KEYNOTE-355, pembrolizumab plus chemotherapy improved PFS and OS in patients with advanced TNBC (131). The single-arm trial KEYNOTE-150 showed significant survival benefits in PD-L1-positive patients who had not received prior systemic therapy, using pembrolizumab in combination with chemotherapy in patients with metastatic TNBC (mTNBC) (132).

The safety and efficacy of atezolizumab plus nab-paclitaxel for TNBC patients who did not receive systemic therapy in the metastatic setting was validated by IMpassion130 (133). Atezolizumab significantly improved OS in the PD-L1-positive population by almost 2 years, leading to FDA approval in March 2019. However, in the phase III study IMpassion131, atezolizumab combined with paclitaxel showed no significant differences in PFS and may have even worsened OS in PD-L1-positive patients (134). Roche withdrew the indication for atezolizumab for the treatment of PD-L1 positive advanced TNBC due to the discrepancy between the two studies.

Multiple trials have demonstrated that administering pembrolizumab in conjunction with chemotherapy can enhance the rate of pathological complete response (pCR) in patients with early-stage triple-negative breast cancer (TNBC). In the I-SPY2 trial, a cohort assessed the effectiveness of pembrolizumab with paclitaxel- and anthracycline-based chemotherapy regimens in women with high-risk, early-stage HER-2-negative breast cancer, resulting in an increased pCR rate for TNBC patients (135). Furthermore, the KEYNOTE-522 phase III trial randomized previously untreated patients with early-stage TNBC to either the pembrolizumab–chemotherapy arm or the placebo–chemotherapy arm, with preliminary findings demonstrating a higher pCR rate in the pembrolizumab group (136). As of July 2021, the FDA has approved pembrolizumab in combination with chemotherapy as a neoadjuvant treatment for high-risk, early-stage TNBC and for continued use as a standalone agent in the adjuvant phase.

Despite some progress in the use of immune checkpoint inhibitors (ICIs) for TNBC, significant challenges still exist. Clinical outcomes demonstrate that only a small subset of TNBC patients benefit from immunotherapy, highlighting the need to identify the target population and expand the treatment's efficacy. Combination therapy is the most promising way forward, but the optimal combination regimen, sequence, dosage, and duration require further exploration. With an increasing number of preclinical and clinical studies in this area, we hope to achieve the ultimate goal of selecting the most suitable patients for immunotherapy, administering the most appropriate immunotherapy or immune-combination therapy, accurately evaluating treatment efficacy, and achieving optimal therapeutic outcomes with minimal toxicity.

Overview and significance of research

The studies in this dissertation aims to use a combination of murine and human correlative studies to gain a better understanding of how heterogeneity in antigen presentation affects the immune microenvironment in breast cancer and impacts the efficacy of immunotherapy combinations. Additionally, these studies explore innovative approaches to modify MHC-I expression levels and diversity, with the ultimate goal of developing combinatorial therapeutic strategies that leverage the immune microenvironment's adaptation to antigen presentation heterogeneity. Specifically, we will target inhibitory receptors on NK cells, which are already in clinical trials for other indications. The results of these studies will challenge past assumptions and offer new therapeutic strategies for molecular and immune cancer therapeutics.

CHAPTER II

Materials and Methods

Patient samples. The 314 tissue microarrays used to study tsMHC-I expression heterogeneity were from breast cancer patients enrolled in the BRE03103 repository trial: NCT00899301, IRB030747 and at the Instituto Nacional de Enfermedades Neoplásicas (Lima, Perú): INEN 10-018. The 84 mTNBC patients that were used to study the correlation between tsMHC-I expression and immunotherapy benefit were enrolled in NCT03206203.

Cell lines. Murine mammary cancer cell lines EMT6 and E0771 were obtained from ATCC. Cell lines were tested at least once quarterly for Mycoplasma contamination. All media components were purchased from commercial vendors and prepared/stored under sterile conditions. Cell lines are utilized within early passage (<30 passages from acquisition from ATCC) and are DNA fingerprinted through commercial services for validation. EMT6 cells were grown in DMEM (Gibco) supplemented with 10% fetal bovine serum (FBS) (Life Technologies). E0771 cells were grown in RPMI (Gibco) and supplemented with 10% FBS. B2m-KO-IFNγ EMT6 cells were maintained in DMEM-F12 (GIBCO) supplementers with 10% TET-System approved FBS (GIBCO). B2m and Qa1 knockout cell lines were generated using CRISPR plasmids (Santa Cruz) and flow sorted on GFP positive cells. Cell lines were verified to be complete knockout populations by flow cytometry.

Viral transduction. The pSHUTTLE-IFNγ (GeneCopoeia) was recombined into the pINDUCER-20 plasmid (62) using LR Clonase (Invitrogen), resulting in DOX-inducible IFNγ transgene expression. Lentiviral particles were produced by co-transfecting pINDUCER-IFNγ plasmid with pMD2G and psPAX helper plasmids into 293FT cells. Target cells were transduced in the presence of polybrene and selected by neomycin resistance. ELISA

Levels of IFNγ secreted from B2m-KO-IFNγ EMT6 cells were evaluated using an ELISA kit according to the manufacturer's instructions (Invitrogen).

Mice. All mice were housed at the Vanderbilt University Medical Center vivarium, which is accredited by the Association for Assessment and Accreditation of Laboratory Animal Care International (AAALAC). The Vanderbilt Division of Animal Care and Institutional Animal Care and Use Committee (IACUC) approved mouse procedures and studies. C57BL/6J and BALB/c mice were purchased from Envigo (Indianapolis, IN) and allowed to acclimatize for at least one week before tumor implantation and experimentation. IFNγ-/- mice were purchased from The Jackson Laboratory (002287) and genotyping was performed according to distributer protocol. For all experiments, 6- to 8-week-old female mice with 100 mm3 tumors were stratified into specific treatment groups.

Tumor implantation and treatment strategy. For mammary tumor models, 5x104 EMT6 or 1x105 E0771 cells were orthotopically injected into the fourth right mammary fat pad of female BALB/c (EMT6) or C57BL/6J (E0771) mice. Following the establishment of tumors (~100-200mm3) mice were stratified prior to therapy administration. The mice were treated via intraperitoneal (IP) injection with isotype IgG2a control (BioXcell, clone BE0089), anti-NKG2A (BioXcell, clone 20D5), or anti-PD-L1 (Genentech, clone 6E11) dosing at 200μg on day seven and 100μg on days 14, 21, 28, and 35. Mice used for each treatment arm are defined in respective figure legends. For tumor growth analysis, tumors were measured 3 times weekly with calipers, and volume was calculated in mm3 using the formula (length x width x width x width/2). Mice were humanely euthanized at defined end points or when the tumor volume reached 2 cm3 or tumor ulceration.

Fine-Needle Aspiration. Following previously published techniques 57, fine-needle aspiration (FNA) on mouse tumors using a sterile beveled needle attached to a 10ml syringe with a syringe holder. The needle was then agitated within the tumor and one to three needle passes were collected from each tumor. The FNA-acquired cells were then processed for flow cytometry analysis.

Depletion of CD8+ T cells and NK cells. For NK cell depletion, 100µL of polyclonal anti-asialo-GM1 (BioLegend, clone Poly21460) or 100µg of anti-NK1.1 (BioXcell, clone PK136) was injected IP into mice once weekly prior to tumor implantation. For the depletion of CD8+ T cells, 200µg of depleting anti-CD8α (BioXcell, clone 2.43) was administered via IP injection for the initial treatment and then 100µg once weekly. A rat IgG2b for anti-CD8α, k (BioXcell, clone BE0090) and rabbit polyclonal IgG (BioLegend, clone Poly29108) was used as an isotype control.

Flow cytometry. Samples were run on an Attune NxT Acoustic Focusing Cytometer (Life Technologies). Analysis was performed in FlowJo. Gating was first done on forward scatter and side scatter to exclude debris. Doublets were excluded by gating on FSC area vs. FSC height (**Supplementary Figure 2.1**) Zombie Violet (BioLegend) was used to exclude dead cells from analyses. Antibodies: CD3- AF488 (BioLegend,clone HIT3a), Cd8a-AF488 (BioLegend, clone 53-6.7), CD45-PerCP/Cy5.5 (BioLegend, clone GK1.5), CD45-APC(BioLegend, clone 30-F11), NK1.1- APC (BioLegend, clone PK136), NKp46- APC (BioLegend, clone 29A1.4), CD11b-PE/Cy7 (BioLegend, clone M1/70), CD11c-AF488(BioLegend, N418), IA/IE-AF700 (BioLegend M5/114.15.2), CD27 (BioLegend, clone LG.3A10), H-2- PE (BioLegend, clone M1/42), NKG2A-PE (Miltenyi Biotec, clone REA1161), H2-Dd-PE (BioLegend, clone 34-2-12), Qa-1b(b)-PE (BD Biosciences, clone 6A8.6F10.1A6), PD-L1-APC (BioLegend, clone 29E.2A3), CD49b- APC/Cy7 (Biolegend, clone DX5), and CD107b-FITC (BioLegend, clone 1D4B), IFNγ-PE (Biolegend, clone XMG1.2).

Tumor dissociation and immune cell isolation. EMT6 and E0771 tumors were harvested from mice at ~300-500mm3 (serum-free RPMI, Gibco) and dissociated using the Tumor Dissociation Kit (Miltenyi Biotec) according to manufacturer's specifications with the gentleMACs Octo dissociator (Miltenyi Biotec) default tumor protocol (40 minutes at 37°C under constant agitation). The dissociate was then passed through a 40µm filter and washed with 20-

30mL of PBS and ACK lysed. CD45+ cell isolation was performed using CD45 mouse microbeads (Miltenyi Biotec).

RNA isolation. After dissociation and CD45+ bead isolation, RNA was harvested from mouse tumors using the Maxwell 16 automated workstation (Promega) and the LEV simplyRNA Tissue Kit (Promega). RNA concentration was determined by spectrophotometry (NanoDrop2000, Thermo Fisher Scientific).

NanoString gene expression analysis. Gene expression analysis on untreated heterogeneous MHC-I EMT6 tumors (CD45+ bead sorted) were performed using the nanoString Pan-cancer immunology panel according to the manufacturer's specifications. Tumor dissociates were used for RNA preparation, and 50 ng of total RNA was used for input into nCounter hybridizations. Data were normalized according to endogenous housekeeper controls and transcript counts were log-transformed for statistical analysis. Original data from the NanoString is available at Supplementary Data 1.

Single-cell RNA sequencing. Immune cells were harvested from parental EMT6 and MHC-I^{HET} tumors and total tumor and CD45+ immune populations were collected from parental EMT6 tumors for single cell RNA sequencing. Each sample (targeting 15,000 cells per sample) was processed for single-cell 5′ RNA sequencing utilizing the 10x Chromium system. Libraries were prepared following the manufacturer's protocol. The libraries were sequenced using NovaSeq 6000 with 150 bp paired-end reads. RTA (v.2.4.11; Illumina) was used for base calling, and analysis was completed using 10x Genomics Cell Ranger software. Data was analyzed in R using the filtered h5 gene matrices in the Seurat package. In brief, samples were subset to include cells with >200 but <3,000 unique transcripts to exclude probable non-cellular RNA reads and doublets. Cells with >15% of reads coming from mitochondrial transcripts were also excluded as probable dying cells. Batch effect correction was introduced using Seurat built-in CCA method. SingleR was used to assist with cell-type annotation of clusters. Differential gene expression analysis was applied calling FindMarkers function with resulting volcano plot

produced with EnhancedVolvano. Single sample gene set enrichment analysis was performed on each individual cell using Escape package using Hallmark gene pathway.

Immunofluorescence and analysis methods. Immunofluorescent assays for CK/HLA-A/B/C +/-CD8 or CD56 and CK/HLA-E were developed and optimized at Vanderbilt University Medical Center using tyramine signal amplification (TSA) for increased antigen sensitivity. Briefly, formalin-fixed paraffin-embedded tissue was sectioned at 4 mm, deparaffinized, antigen retrieval performed with citrate buffer at pH 6, endogenous peroxidase blocked with hydrogen peroxide, and protein block applied. Sections were then incubated with the first primary antibody overnight at 4°C. Followed by incubation with an HRP-conjugated secondary antibody, and TSA reagent applied according to the manufacturer's recommendations. After washing, antigen retrieval, and protein blockade, incubation steps were repeated for the second and third primary antibodies as described. Primary antibodies: (panCK AE1/AE3 Biocare) at 1:1600, HLA-A/B/C C6 Santa Cruz at 1:1300, CD8 144B MM39-10 StatLab, CD56 E7X9M Cell Signaling at 1:600, HLA-E MEM-E/02 Abcam at 1:400. Counterstaining was performed with DAPI for nuclei identification. Tonsil and placenta were used as positive and negative control tissues. Specificity of the C6 antibody was confirmed by IHC analysis of K562 cells (MHC-I null) transduced with individual HLA-A, B, and C alleles. The C6 antibody recognizes most common types of HLA-A, B and C, and is therefore representative of a pan-MHC-I stain (Supplementary Figure 1A).

Whole slide images were digitally acquired using an AxioScan Z1 slide scanner (Carl Zeiss) at 20x. Automated quantification was performed via a pathologist-supervised machine learning algorithm using QuPath software. Cell segmentation was determined with the built-in cell detection algorithm. Briefly, nuclei were identified above an optimized threshold on DAPI and defined utilizing watershed segmentation. The cell cytoplasm and membrane were determined by 3µm cell expansion around the nuclei. Cells were labeled as objects in a hierarchical manner below the tissue annotation or TMA core, each with a xy coordinate. Measurements of intensity

and morphology were generated for every cell compartment and channel. Object classifiers were trained on annotated training regions from control tissue and tumor samples to define cellular phenotypes. Tumor cells were defined by panCK expression and subcellular characteristics. T-cell and NK cells were defined by CD8 and CD56 expression, respectively. Once the algorithm was performing at a satisfactory level, it was used for batch analysis. For cases with low, heterogeneous, or null CK expression in which the classifier's performance was not optimal, tumor areas were manually annotated. Out-of-focus areas, tissue folds, necrosis, normal breast, and in situ carcinoma were excluded from the analysis. A pathologist visually assessed each sample for the correct performance of the algorithm. Single cell data including sample ID, xy coordinate, cell phenotype, and HLA-A/B/C and HLA-E intensity were exported from QuPath for further analysis.

Human breast tumor MHC-I expression analysis. To measure if HLA-A/B/C expression is associated with immunotherapy benefit, a categorical variable of Top and Bottom 33% HLA-A/B/C expression was created. Patients from the carboplatin ± atezolizumab arms were ordered separately from high to low based on their average tumoral HLA-A intensity. For each arm, the top 33% of the rank were selected (for carboplatin + atezolizumab, 41/3=13.6 (round to 13 patients); for carboplatin, 39/3=13 patients) to compare their progression free survival. Similarly, 13 patients at the bottom of the rank were selected from each arm to compare their progression free survival. Single-cell resolution immunofluorescence data, including fluorescence intensity for HLA-A/B/C, CD8, CD56 (NK cell marker), and pancytokeratin on breast cancer tumors, and spatial cell coordinates were imported from immunofluorescence imaging data. The coefficient of variation (μ/σ) was calculated to measure tumor-specific HLA-A/B/C heterogeneity within the sample. To assess the modality of tumor-specific HLA-A/B/C expression, Hartigen's Dip test and the R package LaplacesDemon were applied to calculate a Bayesian form of test statistic for multimodality.

Human breast tumor spatial analysis. Tumor cells were categorized as MHC-I^{high} (mean HLA-A/B/C intensity + standard deviation), MHC-I^{low} (mean HLA-A/B/C intensity - standard deviation), or MHC-I^{mid}. Then, the Ripley's K function (R package: spatstat.core, v2.4-4) and the resulting area under the curve were calculated to measure the spatial distribution and clustering pattern. Clustering algorithms DBSCAN (R package: dbscan, v1.1) were applied, taking the tumor cells' spatial coordinates as input to create tumor clusters. The clusters were categorized as HLA-A/B/C^{high} (HLA-A/B/C median+IQR), HLA-A/B/Clow (HLA-A/B/C median-IQR), or HLA-A/B/Chet. To determine the effect of tumor MHC-I expressional heterogeneity on immune cell localization, immune cell spatial coordinates were superimposed on the tumor clusters. Each immune cell is linked with its nearest tumor cluster to create an immune:tumor pair. Each core was then summarized by counting the immune:MHC-Ihigh cluster pair, immune:MHC-Ilow cluster pair, and immune:MHC-Ihet cluster pair. The count was further adjusted by the number of corresponding tumor clusters, either HLA-A/B/C high, het, or low, and the number of immune cells in the specific core to reduce sampling bias.

adjusted count = (N of immune:tumor cluster pair)/

(N of corresponding tumor cluster × N of immune cells)

NK cell quantification was performed using CIBERSORTx deconvolution of TBCRC patient's tumor bulk RNAseq data. CD8 T cell quantification was collected from the mIF image result. The NK:CD8 ratio was calculated using formula log2NK/CD8.

To quantify the MHC-I heterogeneity within the tumor, dbscan unsupervised clustering to identify individual tumor clusters was performed. Each cluster was then classified as MHC-I high, het, and low based on the cluster's average HLA-A/B/C intensity. The percentage of MHC-I het clusters within the tumor was then calculated. To identify the optimal cutoff points that separate patient's progression free survival, the R package survminer (version 0.4.9) was used and an 85% MHC-I het cluster was chosen as the optimal cutoff point. Patients with tumors

containing >=85% MHC-I het clusters were labeled as having abundant MHC-I heterogeneity while tumors with <85% were labeled as having low MHC-I heterogeneity.

Statistical analysis. Statistical analyses were performed as indicated using R or GraphPad Prism (GraphPad Software). For two-group analyses, student's t-test was used to compare normally distributed means. Log or square root transformation or non-parametric testing was used if not normally distributed. For comparison within the patient or tumor, paired t-test or non-parametric testing was used. For multiple comparisons, ANOVA (analysis of variance) was accompanied by a posthoc Tukey test or a Kruskal-Wallis's test with a posthoc Dunn's test. For survival analysis, the log-ranked test is used. To access the data tailedness, excessive kurtosis parameter was calculated from base R function kurtosis. In a standard normal distribution, the kurtosis value is 3. Therefore, excess kurtosis is calculated by subtracting 3 from the original kurtosis value. For a data distribution that has very few outliers, like a uniform distribution in extreme cases, a negative excess kurtosis value is expected. A positive excess kurtosis value, such as in the case of a patient's HLA-A intensity, indicates that the data distribution tends to have heavy tails. A heavy-tailed distribution means there is a greater probability of encountering a tumor cell with HLA-A/B/C expression that is a certain standard deviation away from the mean tumoral HLA-A/B/C expression during random sampling of tumor cells.

CHAPTER III

Intratumor heterogeneity in MHC-I expression drives immunotherapy resistance in breast cancer and drives NK cell infiltration[2]

Abstract

Although immune checkpoint inhibition (ICI), such as anti-Programmed Death Ligand-1 (αPD-L1), has shown success in cancer therapy, intrinsic and acquired resistance to therapy are prevalent in triple-negative breast cancer (TNBC) patients, and the mechanisms underlying this resistance are not well understood. The recognition of MHC-I-peptide complexes (pMHC-I) by CD8+ cytotoxic T cells is critical for the response to ICIs in patients. Tumor cells can evade immunosurveillance and ICI by downregulating or deleting tumor-specific Major Histocompatibility Complex I (tsMHC-I). Tumors from TNBC patients show diverse MHC-I phenotypes, ranging from highly positive to weakly positive (or negative) MHC-I expression, even within the same tumor. Complete loss of MHC-I is known to impact anti-tumor immunity and ICI response. However, there is a lack of models that address heterogeneity in MHC-I expression, which is the more common clinical scenario. In fact, most studies have evaluated the role of MHC-I expression using complete Beta-2-microglobulin (B2m) knockout models to eliminate tumor MHC-I expression, which is uncommon in human disease. Our data show that this model misses unique immunologic features of the tumor-immune microenvironment that occur when MHC-I is heterogeneously expressed.

[2] Adapted from Taylor, B.C., Sun, X., Gonzalez-Ericsson, P., Sanchez, V., Sanders, M.E., Hanna, A., Wescott, E., Opalenik, S.R., Lehmann, B.D., Abramson, V.G., Pietenpol, J.A., Balko, J.M. NKG2A is a Therapeutic Vulnerability in Immunotherapy Resistant MHC-I Heterogenous Triple Negative Breast Cancer. Cancer Discovery. 2023.

Introduction

Immunotherapy, particularly immune checkpoint inhibitors (ICI), has become a standard treatment for many types of cancer(137). The anti-programmed death-1 (PD-1) monoclonal antibody pembrolizumab is approved for the treatment of early-stage or programmed death ligand-1 (PD-L1)-positive metastatic triple-negative breast cancer (TNBC) in combination with chemotherapy(131,133,136,138–140). However, only about 15% of early-stage TNBC patients experience benefit from adding ICI(136,141). Current biomarkers such as tumor-infiltrating immune cells and PD-L1 expression have shown limited or no utility in predicting ICI treatment outcomes in the early setting(136,141–143). Further research is needed to understand why ICI therapy is ineffective for most TNBC patients and to devise strategies to expand its clinical benefit.

CD8+ T cell recognition of major histocompatibility complex-I (MHC-I, comprised of classical HLA-A, -B, and -C in humans) molecules bearing antigens cognate to the unique T cell receptor is critical for anti-tumor immune clearance and efficacy of ICIs(3,144). Loss or dysfunction of MHC-I represents a common mechanism by which tumor cells can evade adaptive immunity and has been associated with resistance to immunotherapy(23,47,81,145,146). There are a variety of mechanisms whereby tumor-specific MHC-I (tsMHC-I) antigen presentation can be disrupted, including immune editing or selection against neoantigens(45,147), loss or lack of MHC-I allelic diversity(78,148,149), and development of mutations which limit interferon-sensing pathways and resulting MHC-I upregulation(23). Somatic genetic losses at HLA loci, or epigenetic suppression by promoter hypermethylation have also been described in breast cancer(150).

Mouse studies modeling the role of tsMHC-I in anti-tumor immunity and immunotherapy response frequently rely on complete (clonal) genomic loss of tumor *beta-2-microglobulin*

(*B2m*), an obligate heterodimeric partner for MHC-I. Genetic deletion of *B2m* results in an immunologically cold tumor microenvironment and complete lack of response to PD-1/L1-targeted therapy(23,85,151), or other therapies targeting adaptive responses requiring antigen recognition(47,77). However, clonal deletion of tsMHC-I or *B2m* is relatively uncommon in breast cancer, or in cancer in general(150,152,153), with a majority of tumors exhibiting sub-clonal lesions, increasing the complexity of tsMHC-I expression within the tumor microenvironment.

Heterogeneous loss or downregulation of tsMHC-I at the single-cell level is anticipated to have numerous consequences. Partial loss could render tumors less responsive or completely unresponsive to immunotherapies. Coordinate reduction in T cell infiltration and function could also occur. Finally, perhaps more unexpectedly, heterogeneity in the microenvironment could lead to spatial effects on tumor immunity not appreciated in either fully MHC-I-competent or -incompetent tumors (e.g., a neomorphic effect).

Results

Partial loss of tsMHC-I expression is associated with lack of immunotherapy benefit in TNBC

Transcriptional suppression or polymorphic loss of MHC-I is correlated with ICI resistance (41,74), due to downregulation and reduced diversity of tumor antigen presentation to CD8+ T cells. The association of tsMHC-I protein expression on ICI treatment outcomes in breast cancer patients has not been studied in detail. To test whether loss of MHC-I expression is associated with the efficacy of ICI therapy in breast cancer, multiplexed immunofluorescence (mIF) staining was conducted for DAPI, pan-cytokeratin (panCK, a marker for epithelial cells), and HLA-A/B/C (representing MHC-I), on pre-treatment biopsies from 84 metastatic TNBC patients in a recently completed randomized Phase II clinical trial evaluating carboplatin ± atezolizumab (NCT03206203) (**Figure 3.1A**). Improved progression-free survival (PFS) was observed

in patients with high tsMHC-I expression (top 33% HLA-A/B/C intensity, n=13) when treated with carboplatin in combination with atezolizumab compared to carboplatin alone. In contrast, there was no significant difference in PFS between the two treatment arms for patients with low tsMHC-I expression (bottom 33% HLA-A/B/C intensity, n=13) (**Figure 1B**). Our findings emphasize that adding anti-PD-1/L1 targeting immunotherapy is unlikely to benefit metastatic TNBC patients with low tsMHC-I expression. During this analysis, we observed that many breast cancers demonstrated heterogeneous expression of HLA-A/B/C, comprising regions of high and absent expression (see example in **Figure 3.1A**). Of note, we further validated the specificity of the antibody HLA-A C6 through IHC analysis of various HLA alleles. The C6 antibody recognized most common types of HLA-A, B, and C alleles, and is therefore representative of a pan HLA stain (**Supplementary Figure 3.1A**). To more specifically quantify the probability that individual tumor cells with high and low MHC-I expression were present within the same tumor, the tailedness of tsMHC-I expression was measured using the excess Kurtosis parameter. (**Supplementary Figure 3.1B**)**.** Most TNBC tumors displayed a leptokurtic distribution, demonstrating the coexistence of extreme outliers.

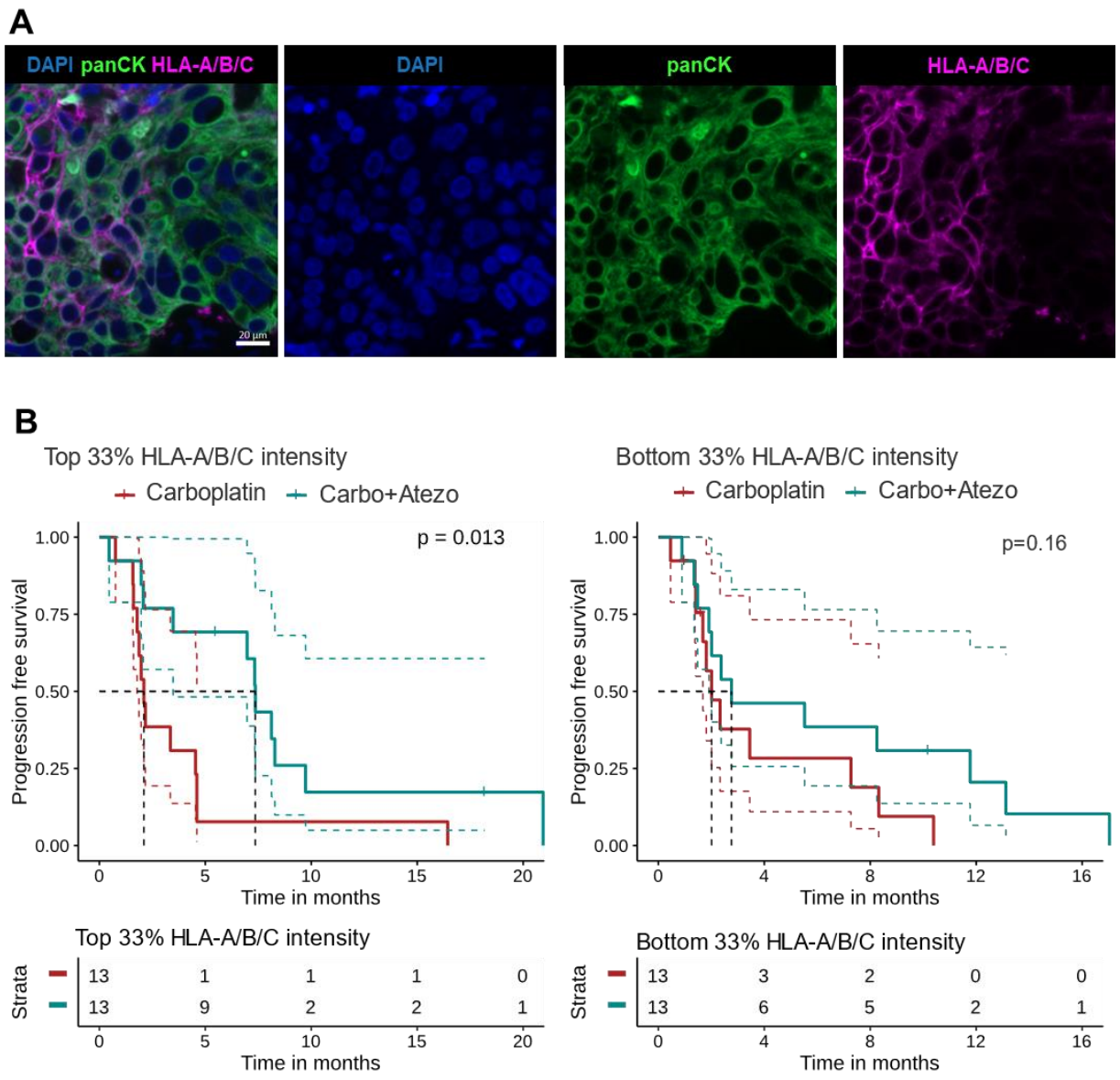

Figure 3.1: Low tsMHC-I expression is associated with lack of benefit to immunotherapy treated mTNBC. **A)** mIF for HLA-A/B/C (MHC-I) and panCK (merged and single channel example shown), was performed on 84 baseline/pre-therapy archived biopsy samples collected from patients with metastatic TNBC in a randomized Phase II clinical trial of carboplatin ± atezolizumab. **B)** Progression free survival was compared using the log-rank test between carboplatin ± atezolizumab metastatic TNBC patients with the highest tsMHC-I expression (top 33%) and those with the lowest tsMHC-I expression (bottom 33%). Confidence intervals for each arm are represented as red or green dotted lines and median survival for each arm are plotted as black dotted line.

TNBC displays high tsMHC-I expression heterogeneity

TNBC tumors demonstrate heterogeneous intratumor MHC-I expression, meaning tumor cells with high and low MHC-I expression co-exist within the same microenvironment. To investigate whether the heterogeneity of tsMHC-I expression is breast cancer subtype-specific, single-cell level mIF analysis was conducted for panCK and HLA-A/B/C on tumor microarrays comprising 314 breast cancer patients (n=227 ER+; 9 HER2+/ER+; 7 HER2+/ER-; 52 TNBC) (**Figure 3.2A**). Significant variability in tumor HLA-A/B/C expression was observed across breast cancer subtypes, with TNBC exhibiting the highest overall expression (**Figure 3.2B**). Moreover, TNBC tumors at the single cell level also demonstrated a high coefficient of variation, reaffirming tsMHC-I intra-patient heterogeneity in expression (**Figure 3.2C**). To assess the distribution of tsMHC-I fluorescence intensity, Hartigan's dip test(154) was utilized to measure the probability of unimodal versus multimodal distribution. Many TNBC tumor cells expressed HLA-A/B/C in a multimodal manner (**Figure 2D**), indicating the presence of HLA-A/B/C^{high} and HLA-A/B/C^{low} tumor cells within the same tumor. HER2+/ER+ tumors also expressed a high degree of multimodality but were poorly represented in this dataset.

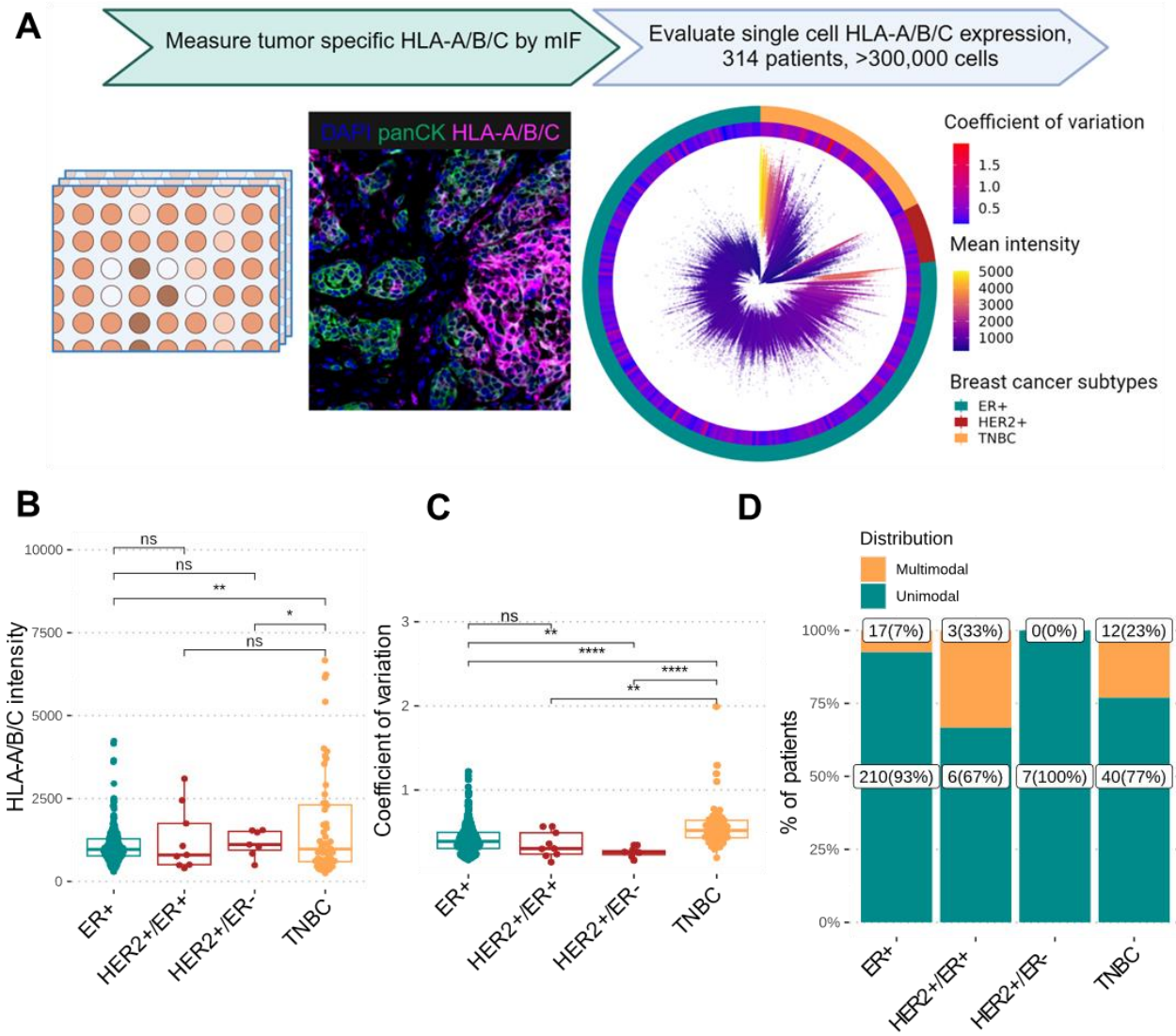

Figure 3.2: TNBCs display high tumor-specific MHC-I expression heterogeneity. A) mIF for HLA-A/B/C and panCK was performed on 314 breast tumor microarrays (n=227 ER+; 9 HER2+/ER+; 7 HER2+/ER-; 52 TNBC) to obtain single-cell resolution MHC-I expression. The circle plot is a summary of the patients' HLA-A/B/C expression. Each line in the center represents single patient tumors comprised of individual tumor cell HLA-A/B/C expression plotted as a dotted plot. Spikes are colored by the tumor's mean MHC-I intensity. The inner layer of the circle reflects the coefficient of variation of each tumor. The outer layer of the circle is labeled by breast cancer subtype. **B)** Total sample HLA-A/B/C IF intensity across breast cancer subtypes. **C)** Coefficient of variation of HLA-A/B/C expression within breast tumors. **D)** Hartigan's dip test was applied to determine whether the distribution of tsMHC-I expression is unimodal or multi-modal. ****P<0.0001, **P<0.01, Bonferroni-corrected t-test was used for statistical comparisons. Boxplots display the median, 25th, and 75th quantiles.

Modeling MHC-I heterogeneity and response to immunotherapy in vivo

Distinct patterns of MHC-I heterogeneity were observed in TNBC patient tumors, but the impact of this observation on immune cell infiltration and response to immunotherapy has not been studied in preclinical models. To assess how the immune microenvironment is shaped in response to tsMHC-I heterogeneity, CRISPR-Cas9 was used to knock out *B2m* in a BALB/c murine orthotopic mammary cancer model (EMT6), which has homogeneously high MHC-I expression at baseline (**Figure 3.3A**). As expected, clonal loss of *B2m* completely abrogated tumor sensitivity to anti-PD-L1 (**Figure 3.3B**), consistent with prior literature(155–158). To model MHC-I heterogeneity and response to anti-PD-L1, EMT6 MHC-I proficient and deficient isogenic lines were mixed at various ratios prior to injection (**Figure 3.3C)**. The EMT6 model displayed variability in response to single-agent anti-PD-L1, ranging from complete response (CR), acquired resistance (AR), and intrinsic resistance (IR) (**Figure 3.3D**). As little as 10% loss of MHC-I resulted in significantly decreased CRs and 50% loss of MHC-I resulted in no CRs (**Figure 3.3E**). Because the 50% loss of MHC-I abrogated CR to anti-PD-L1, this percentage was selected to model MHC-I heterogeneity, termed MHC-I^{HET} henceforth, to examine changes in the immune microenvironment with respect to MHC-I loss and resistance to anti-PD-L1.

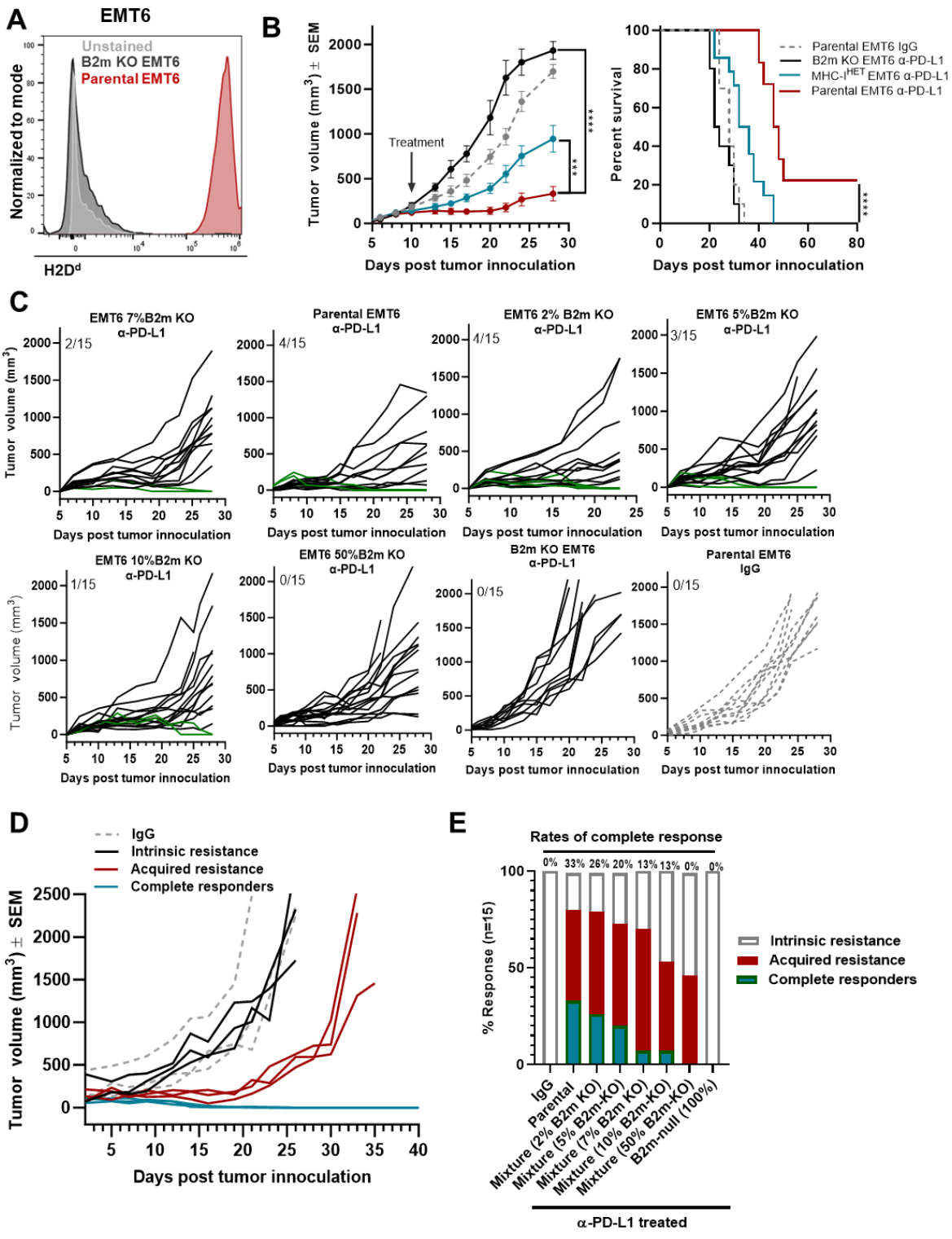

Figure 3.3: Modeling MHC-I heterogeneity and response to immunotherapy in vivo. A) Flow Cytometry histogram showing MHC-I (H2Dd) expression on live parental EMT6 and EMT6 B2m KO cells. **B)** Parental, MHC-I^{HET}, and B2m KO EMT6 tumor cells were injected subcutaneously in BALB/c mice. Mice were treated at 7-day intervals with IgG antibody or anti-PD-L1 antibody.

Graphs show combined tumor growth and survival curves. n=10 to 15 per group. **C)** Parental and B2m KO cells at varying inoculums (2% B2m KO EMT6 and 98% Parental EMT6; 5% B2m KO EMT6 and 95% Parental EMT6; 7% B2m KO EMT6 and 93% Parental EMT6; 10% B2m KO EMT6 and 90% Parental EMT6) were injected subcutaneously in BALB/c mice. Mice were treated at 7-day intervals with anti-PD-L1 antibody. Green lines represent CRs. n=15, with number of CRs observed annotated in graph. **D)** Representative individual mouse tumor curves for intrinsic resistance, acquired resistance, and complete response when treated at 7-day intervals with anti-PD-L1 antibody. These curves were picked to best represent resistance patterns in EMT6 tumors and are across multiple experiments. **E)** Percentage rates of complete response acquired resistance, and intrinsic resistance in parental, B2m KO, and the various inoculums of parental and B2m KO mixture EMT6 tumor cells injected subcutaneously in BALB/c mice. Mice were treated at 7-day intervals with IgG or anti-PD-L1 antibody. Data presented are represented of two individual experiments. n=15.

Enforcing heterogeneity in MHC-I expression reshapes NK cell infiltration

To determine how changes in MHC-I expression might reshape the immune microenvironment in untreated parental (high MHC-I), MHC-I^{HET} (heterogeneous MHC-I), and *B2m-KO* (MHC-I null) EMT6 tumors, RNA gene expression profiling was performed on CD45+ infiltrating immune cells for each tumor type. Gene expression analysis revealed that T cell markers and interferons (IFN) were coordinately expressed with increasing MHC-I expression (**Figure 3.4A** and **Supplementary Figure 3.4A-B**). Interestingly, MHC-I^{HET} tumors had a uniquely elevated level of NK cell-related genes (**Figure 3.4B-C**). Increased NK cell abundance in MHC-I^{HET} tumors was further confirmed using flow cytometry through direct measurement of immune cell populations and total tumor populations (**Figure 3.4D-F and Supplementary Figure 3.4C**). To describe these differences in NK cell infiltration among the models at various stages of tumor size, longitudinal assessment of tumor-infiltrating lymphocytes was performed by fine-needle aspiration. NK cells were present at the beginning of tumor formation, ~100mm^3, in the parental and *B2m-KO* tumors, but when tumors reached ~500mm^3, NK cells were no longer detected. In contrast, in the MHC-I^{HET} EMT6 tumor model, NK cells infiltrated at significantly higher numbers at ~100mm^3 and were still present at ~500mm^3 (**Supplementary Figure 3.4D**), indicating higher NK cell retention throughout tumor progression.

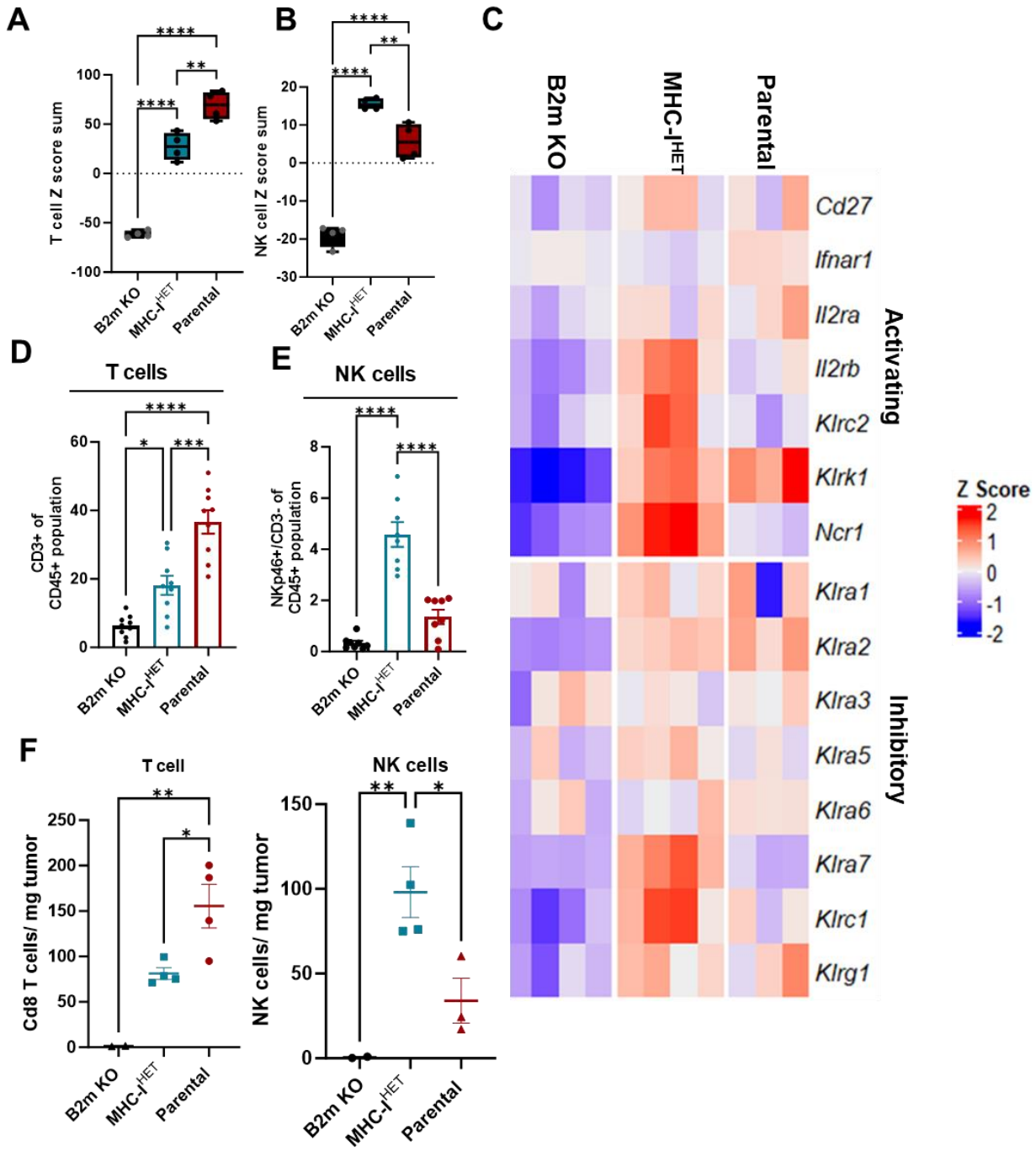

Figure 3.4: Enforcing heterogeneity in MHC-I expression reshapes NK cell infiltration. A-B*)* Calculated z-score sum of NK and T Cell related genes in untreated parental, MHC-I^{HET}, and *B2m* KO EMT6 tumors CD45+ microbead fractionated. *n=4* per group. **C**) Untreated parental, MHC-I^{HET}, and B2m KO EMT6 tumor CD45+ tumor-infiltrating leukocytes were bead isolated, RNA was extracted, and utilized for NanoString gene expression using the PanCancer Immune Pathways codeset (>700 immune-related genes). n=4. **D-E)** Flow cytometry analysis of tumor infiltrating CD3+ T cells and NK cells from untreated parental, MHC-I^{HET}, and *B2m* KO EMT6 tumors. CD45+ tumor-infiltrating leukocytes were bead isolated

Discussion

The mechanism of resistance to immunotherapy in TNBC remains poorly understood. Only 15% of patients with early-stage TNBC benefit from the addition of immunotherapy to standard neoadjuvant chemotherapy regimens, and in the metastatic setting, only about 20% of patients qualify for immunotherapy based on PD-L1 testing, with far fewer actually deriving benefit. Previous studies have attempted to validate potential biomarkers of response, such as tumor-infiltrating lymphocytes, mRNA signatures, and tumor mutation burden, but have largely been unsuccessful due to a lack of consideration for direct testing of tumor cells' antigen presentation capabilities.

Considering these failed studies, studies fail to consider direct testing of antigen presentation capabilities of tumor cells. CD8+ cytotoxic T cell recognition of MHC-I-peptide complexes (pMHC-I) is critical for an effective response to ICIs. However, tumor cells can evade immunosurveillance and ICI treatment through the downregulation or deletion of tumor-specific MHC-I (tsMHC-I). Most studies of MHC-I expression by tumor cells have been conducted using "purist" models of MHC-I loss, such as complete *B2m* knockout, which do not accurately replicate most human diseases. Surprisingly, few studies have explored the effects of heterogeneous MHC-I expression in the microenvironment, which is far more common in human breast cancers.

Our approach and model provide an innovative design that yields novel insights into the anti-tumor immune response and new ways of targeting cancer immune evasion. Our preliminary data demonstrate substantial heterogeneity in MHC-I expression in primary breast cancers, where immunotherapy has recently been approved in combination with chemotherapy (chemo-immunotherapy) for TNBC. There is a pressing need to gain a better understanding of how the existing and underappreciated heterogeneity in MHC-I expression by breast cancers may impact the immune microenvironment and how to overcome primary resistance to immunotherapy. To achieve this, further investigation into the specific loss of MHC-I alleles

versus just *B2m* loss is required. Additionally, a comparison of the effects of MHC-I "hard" lesion heterogeneity to "soft" lesion heterogeneity should be examined. Our model only represents hard lesions encoded in the DNA sequence, while soft lesions such as methylation appear to be even more predominant in human cancer and may have different effects on anti-tumor immunity.

A more detailed mechanistic understanding of how intra-tumor heterogeneity in antigen presentation shapes anti-tumor immunity will be critical for developing new therapeutic strategies to enhance immunotherapy regimens in breast cancer, with potential applications to other cancer types. Our data demonstrate a unique tumor-immune microenvironment in heterogeneous MHC-I-expressing tumors, supporting a deeper dive into how modulation of MHC-I expression shapes antitumor immunity in breast cancer. This observation should be extended rigorously into multiple models of mammary cancer, with multiple mechanisms of MHC-I downregulation/loss, and ultimately determining whether the same altered anti-tumor microenvironment can be observed in human breast cancers.

CHAPTER IV

NKG2A is a therapeutic vulnerability in immunotherapy resistant MHC-I heterogenous triple-negative breast cancer [3]

Abstract

Despite the success of immune checkpoint inhibition (ICI) in treating cancer, patients with triple-negative breast cancer (TNBC) often develop resistance to therapy, and the underlying mechanisms are unclear. MHC-I expression is essential for antigen presentation and T-cell–directed immunotherapy responses. This study demonstrates that TNBC patients display intratumor heterogeneity in regional MHC-I expression. In murine models, loss of MHC-I negates antitumor immunity and ICI response, whereas intratumor MHC-I heterogeneity leads to increased infiltration of natural killer (NK) cells in an IFNγ-dependent manner. Using spatial technologies, MHC-I heterogeneity is associated with clinical resistance to anti-programmed death (PD) L1 therapy and increased NK: T-cell ratios in human breast tumors. MHC-I heterogeneous tumors require NKG2A to suppress NK-cell function. Combining anti-NKG2A and anti–PD-L1 therapies restores complete response in heterogeneous MHC-I murine models, dependent on the presence of activated, tumor-infiltrating NK and CD8+ T cells. These results suggest that similar strategies may enhance patient benefit in clinical trials.

Introduction

As MHC-I expression varies greatly among breast cancers, innovative approaches are needed to enhance the effectiveness of immunotherapies targeting the host immune system for cancer

[3] Adapted from Taylor, B.C., Sun, X., Gonzalez-Ericsson, P., Sanchez, V., Sanders, M.E., Hanna, A., Wescott, E., Opalenik, S.R., Lehmann, B.D., Abramson, V.G., Pietenpol, J.A., Balko, J.M. NKG2A is a Therapeutic Vulnerability in Immunotherapy Resistant MHC-I Heterogenous Triple Negative Breast Cancer. Cancer Discovery. 2023.

treatment. Several strategies have been proposed to counteract the loss of MHC-I antigen presentation, including the use of bi-specific antibodies that bind to tumor-expressed molecules beyond MHC-I and harnessing other immune cell populations therapeutically when CD8+ T cell cytotoxicity is diminished, such as NK cells.

When target cells lack MHC-I, NK cells become activated through a process known as "missing-self recognition", which enables them to eliminate the target cells. For instance, bacteria, viruses, and impaired or infected cells may lack or downregulate MHC, leading to unhindered NK cell activity that is typically suppressed by inhibitory receptors on target cells. As a result, NK cells are more inclined to attack these target cells. Given the actions and abilities of NK cells, they have garnered significant attention, and their use holds great promise in the realm of cancer immunotherapy.

In Chapter II in murine tumors with controlled MHC-I heterogeneity, we observed a striking increase in NK cell infiltration. However, semi-linear resistance to anti-PD-L1 was still observed with increasing B2m-null content, suggesting that NK cell functionality is insufficient to adequately slow tumor growth regardless of ICI therapy. Nonetheless, the increased presence of NK cells suggests that if functionality could be restored therapeutically, this could be a tractable approach to translate to the clinic in TNBC. Klrc1(Nkg2a) and its heterodimeric partner Cd94 are C-type lectin receptors which are expressed predominantly on the surface of NK cells and some CD8+ T cells. Signaling via their ligand (HLA-E/Qa-1b, present or interferon-inducible on a variety of cells including tumor cells) suppresses NK cell functionality through abrogation of ‘missing-self’ signals. MHC-I heterogeneous tumors may recruit NK cells but drive their balance (e.g. Nkg2a:Nkg2d ratio) toward inhibition. Thus, we will determine whether NK cells can be targeted to overcome ICI resistance in MHC-I heterogeneous tumors.In this study, analyzing the spatial contexture of human breast tumors, we found that regions of tumors with heterogeneous MHC-I expression contained significantly higher levels of NK cells compared with regions with

uniformly high or low MHC-I expression. Murine mammary tumors with enforced MHC-I heterogeneity (MHC-I^{HET}) mirrored our findings in human TNBC and showed substantially increased NK-cell infiltration compared with MHC-I proficient or B2M-knockout (KO) tumors. Tumor-infiltrating NK cells targeted with combination anti-NKG2A and anti-PD-L1 treatment overcame anti–PD-L1 resistance and extended survival in multiple murine mammary cancer models. Furthermore, we have identified IFNγ as a crucial recruitment factor for tumor-infiltrating NK cells in MHC-I heterogeneous tumors. Collectively, we identified key changes in the tumor microenvironment of heterogeneous MHC-I TNBCs and candidate combination immunotherapy to overcome ICI resistance.

Results

NK cells in MHC-I heterogeneous tumors are enriched with Itga2 and IL2 signaling related genes

In Chapter III, we described unique changes in NK cell infiltration in MHC-I^{HET} tumors. We hypothesized that the lack of immune infiltration in *B2m-KO* tumors could be due to a paucity of key chemokine and cytokine signals such as IFNγ/α and Cxcl9/10 (**Supplementary Figure 4.1**). Since the expression of Cxcl9/10 was similar between parental and MHC-I^{HET} EMT6 tumor microenvironments, the level of these chemokines alone could not explain the differences in NK cell abundance. Therefore, single-cell RNA (scRNA seq) and NanoString gene expression profiling was utilized to characterize tumor-infiltrating NK cells from parental and MHC-I^{HET} EMT6 tumors to assess factors contributing to NK cell retention and recruitment. NK cells were characterized with SingleR and further confirmed by their *Ncr1* and *Klrc1* positivity and lack of *Cd3e* (**Figure 4.1A and Supplementary Figure 4.2A**). Differential gene expression analysis revealed NK cells from MHC-I^{HET} EMT6 tumors expressed elevated levels of *Itga2* (CD49b, conventional NK cells), an integrin subunit that forms a receptor for collagen (**Figure 4.1B**).

CD49b has recently been shown to help retain NK cells at the site of infection when binding to collagen, which is highly enriched within EMT6 tumors and surrounding fibroblasts (**Supplementary Figure 4.2B-C**) (159–161). In addition, enrichment of IL-2 signaling related genes (*Stat5b, Il2rb)*, and particularly higher Bcl2 expression, an anti-apoptotic factor that also serves as an activation or proliferation marker for NK cells (162), was observed in NK cells from MHC-I^{HET} EMT6 tumors compared to parental EMT6 tumors (**Figure 4.1B-C)**. These observations were further confirmed using NanoString gene profiling on CD45+ cells and flow cytometry (**Figure 4.1D-E**), suggesting that MHC-I^{HET} tumor-infiltrating NK cells bear specific phenotypes that lead to NK cell retention and maintenance. Although MHC-I^{HET} EMT6 tumors are resistant to anti-PD-L1 therapy, there are substantial changes in the amount of tumor-infiltrating NK cells, illustrating an opportunity to therapeutically exploit this phenotype.

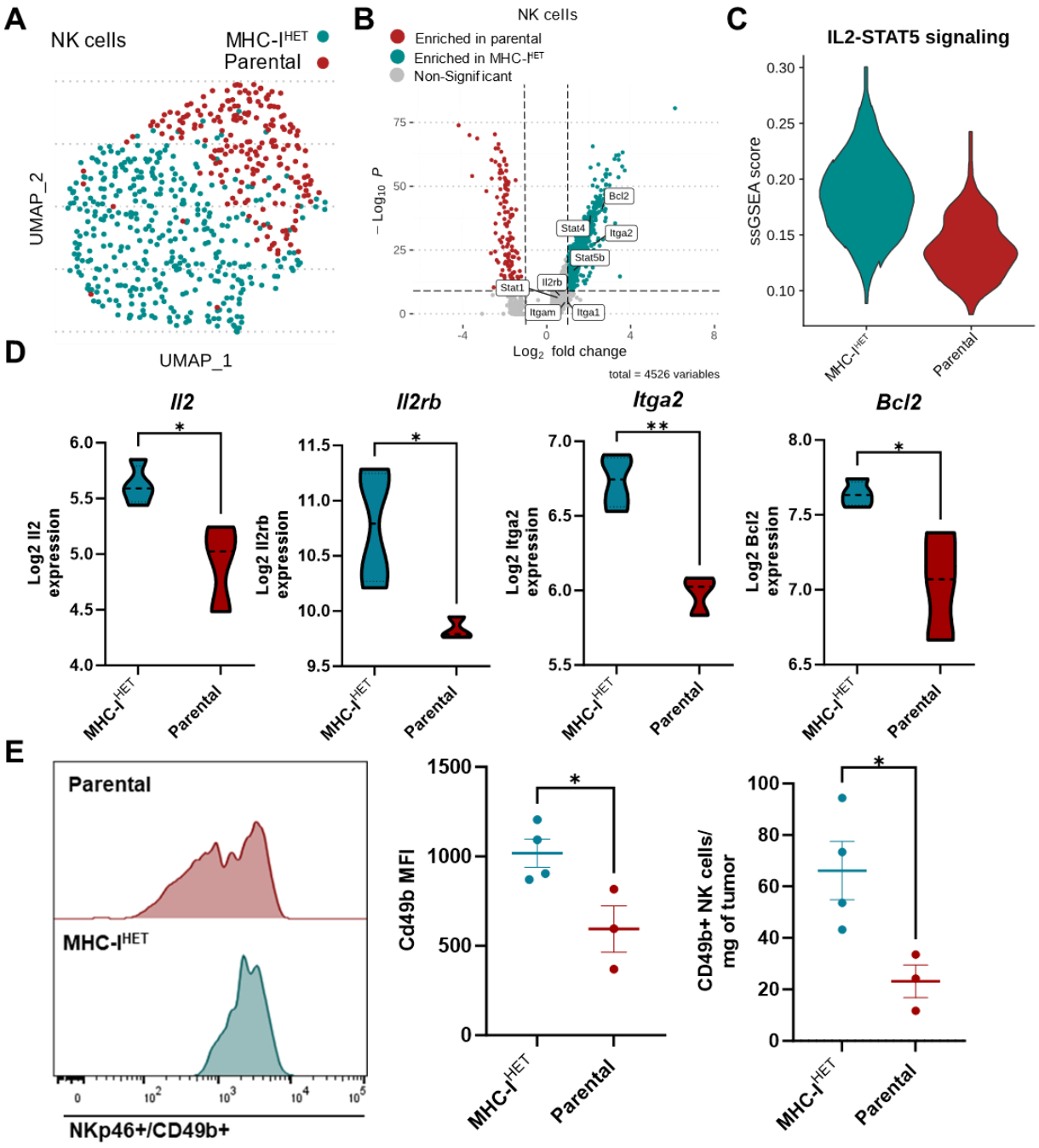

Figure 4.1: NK cells in MHC-I heterogeneous tumors are enriched with Itga2 and IL2 signaling related genes. A-C) Single cell RNA sequencing performed on untreated parental and MHC-I ^{HET}EMT6 tumors. **A)** UMAP of tumor infiltrating NK cells using SingleR. **B)** Differentially expressed genes compared between the NK cells in parental and MHC-I^{HET} EMT6 tumors (colored genes all show absolute log FC>1and pvalue<1e-5). **C)** IL2-STAT5 ssGSEA was performed on the NK cells taking individual cells as the sample (p<0.0001). **D)** Untreated parental and MHC-I^{HET} EMT6 tumors were CD45+ tumor infiltrating leukocytes bead isolated. RNA was extracted and utilized for NanoString gene expression using the PanCancer Immune Pathways codeset (>700 immune-related genes). Analyzed by student's t test. *n=4.* **E)** Flow cytometry analysis of

CD49b expression tumor infiltrating NK cells from untreated parental and MHC-I^{HET} EMT6 tumors. Mean shown with SEM. Analyzed by student's t test. *n*=3-4. *p≤0.05, **p≤0.01

MHC-I^{HET} tumor analysis reveals distinct changes in the immune microenvironment.

Previous studies have established that the presence of conventional type 1 dendritic cells (cDC1) in the tumor microenvironment are reliant on NK cells (163,164). Flow cytometry analysis revealed that cDC1s (defined here as Cd45+Cd11c+MHC-II-high) were significantly more abundant in MHC-I^{HET} EMT6 tumors compared to parental EMT6 tumors, consistent with the higher NK cell infiltration (**Figure 4.2A**). Transcriptomic analysis of CD8+ T cells in untreated MHC-I^{HET} and parental EMT6 tumors revealed T cells from MHC-I^{HET} EMT6 tumors displayed markers of naïve CD8+ T cells (*Tcf7, Ccr7, Sell)* and had reduced markers of cytotoxic function and activated CD8+ T cells (*Gzmb, Nkg7) (***Figure 4.2B-D)**. Thus, despite the increased potential for CD8+ T cell priming by more abundant cDCs, it is possible that the substantial reduction tumor cell-specific antigen presentation in MHC-I^{HET} tumors dominates the phenotype in basal conditions.

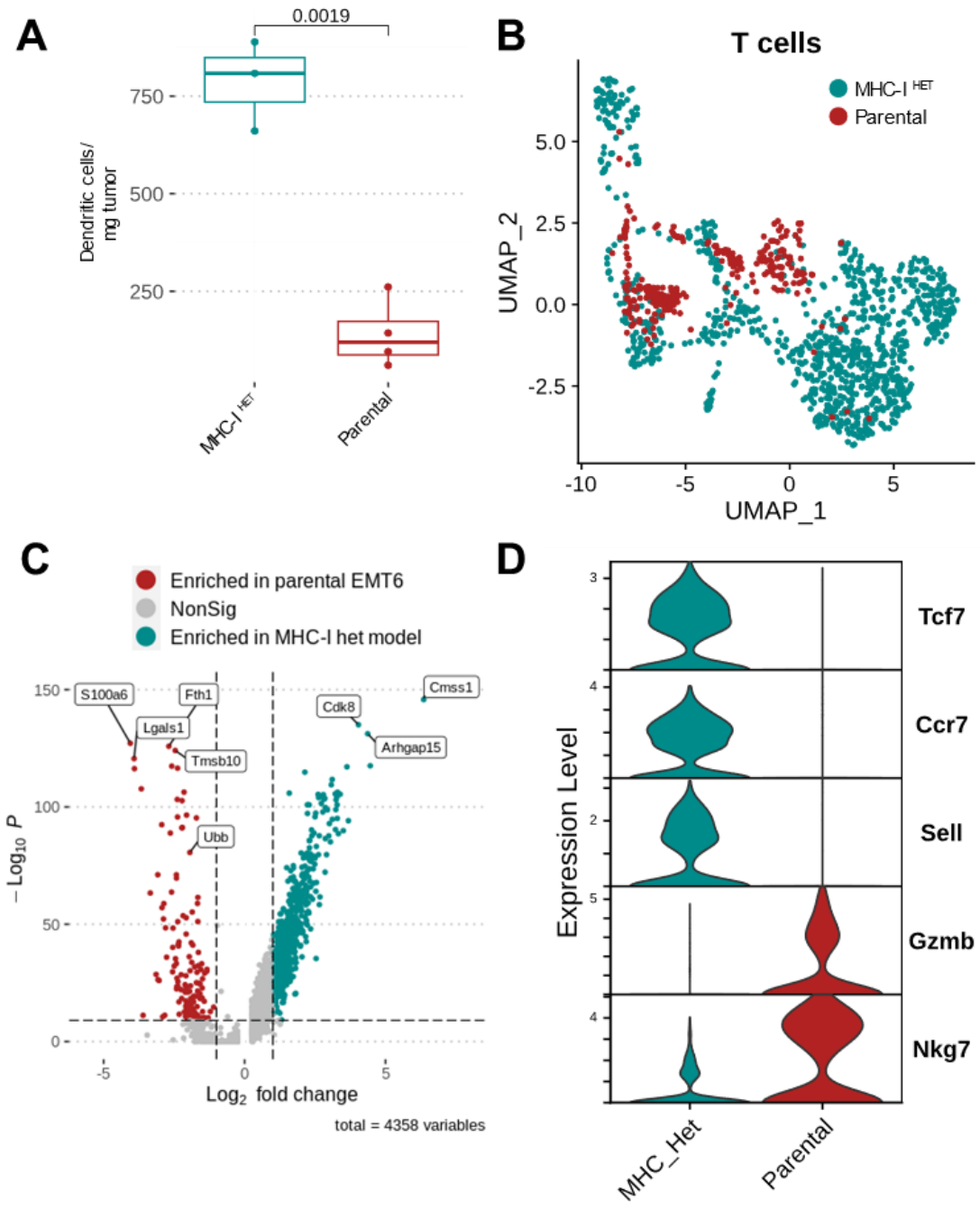

Figure 4.2: MHC-I^{HET} tumor analysis reveals distinct changes in the immune microenvironment. A) Flow cytometry analysis of tumor infiltrating normalized to tumor weight from untreated parental and MHC-I^{HET} EMT6 tumors. Dendritic cells are gated on live MHC-II+/CD11c+ tumor infiltrating dendritic cells was measured as number of cells per mg of tumor. *n=3-4.* Data analyzed by student T test. **B-C)** Single cell RNA sequencing performed on untreated parental and MHC-I ^{HET}EMT6 tumors. **B)** UMAP of tumor infiltrating T cells classified using SingleR. **C)** Comparison of T cell **d**ifferentially expressed genes from parental MHC-I ^{HET}EMT6 tumors (colored genes all show absolute log FC>1and p value<1e-5). **D)** Gene expression for markers of cytotoxic (Gzmb, Nkg7) and naïve (Sell, Ccr7, Tcf7) CD8 T cells.

Combined targeting of T cells and NK cells restores immunotherapy responses in MHC-I^{HET} tumors

We next hypothesized that therapeutic activation of tumor-infiltrating NK cells in MHC-I^{HET} EMT6 tumors could overcome resistance to anti-PD-L1 immunotherapy. The inhibitory receptor NKG2A is expressed on NK and T cells, recognizing the non-classical MHC-I molecule HLA-E in humans and Qa-1b (encoded by the *H2-T23* gene) in mice. Expression of Qa-1b was observed in MHC-I^{HET} EMT6 tumor cells (CD45-) *in vivo* (**Figure 4.3A**). NKG2A expression of NK and T cells in the tumor environment and control tissue (spleen) was examined. NKG2A expression of NK cells was constitutive, while it was increased on tumor infiltrating CD8+ T cells as compared to spleen (**Figure 4.3B**). To evaluate if activation of NK cells via NKG2A blockade in MHC-I^{HET} EMT6 tumor-bearing mice would improve response and overall survival, mice were treated with anti-NKG2A, anti-PD-L1, or a combination of both. While single-agent anti-NKG2A or anti-PD-L1 showed no improved survival or reduced tumor growth rates, a combination of NKG2A and PD-L1 blockade had a pronounced anti-tumor effect and restored CRs (CR=30%) in mice bearing MHC-I^{HET} EMT6 tumors (**Figure 4.3C**).

Comparable results were obtained in the basal-like C57BL/6 murine mammary cancer cell line E0771. When stimulated with IFNγ for 48 hours *in vitro*, E0771 cells display a naturally occurring heterogeneous expression of MHC-I (**Figure 4.3D**). Additionally, E0771 had similar levels of tumor-infiltrating NK and CD8+ T cells to the MHC-I^{HET} EMT6 model (**Figure 4.3E**). E0771 tumors are known to be resistant to anti-PD-L1 therapy (165). When E0771 tumor-bearing mice were treated with a combination of anti-PD-L1 and anti-NKG2A blockade, survival was significantly extended compared to single agent anti-PD-L1 and anti-NKG2A (**Figure 4.3F**).

Given that the combination blockade of NKG2A and PD-L1 improved response in MHC-I heterogeneous mammary tumors, it was investigated whether this strategy could also enhance

the response in parental or *B2m-KO* tumors. tumors While *B2m-KO* tumors showed no response to combination therapy, parental EMT6 tumors showed significant tumor reduction (CR=80%) in comparison to single agent anti-PD-L1 (CR=33%) (**Supplementary Figure 4.3A**). This suggests engagement by CD8+ T cells and potentially augmentation of limited populations of NK cells, which are enhanced after anti-PD-L1 treatment alone in parental EMT6 tumors (**Supplementary figure 4.3B**).

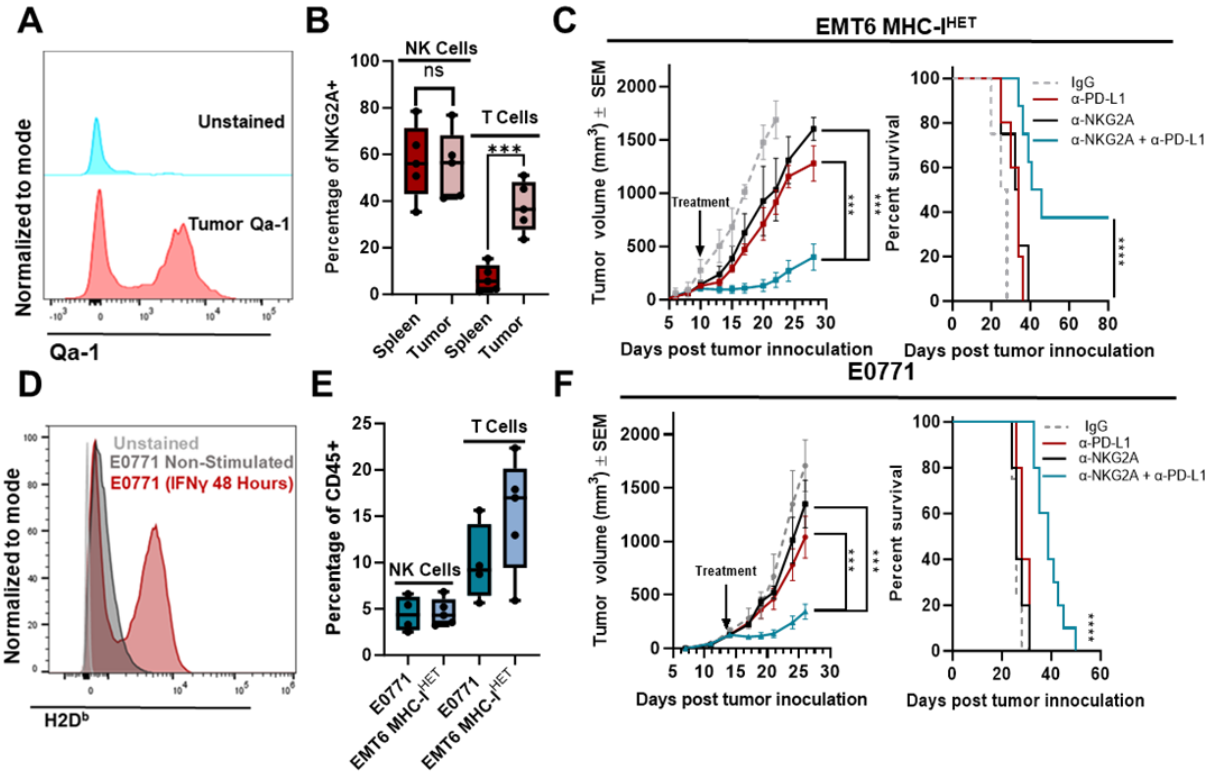

Figure 4.3: Combined targeting of T and NK cells restores immunotherapy responses in in heterogenous MHC-I murine mammary tumors. ***A)*** Flow cytometry analysis of Qa1b expression on MHC-I^{HET} tumors. Gated on live CD45- cells. ***B)*** Flow cytometry analysis of NKG2A expression on the surfaces of NK and CD8+ T cells in the spleen and MHC-I^{HET} EMT6 tumors. NK cells are gated on live CD45^{+}, NKp46^{+}, and CD3^{-}. CD3+ T cells are gated on live CD45^{+} and CD3^{+}. Student's t test was used for comparison. *n=5.* ***C)*** MHC-I^{HET} EMT6 tumor cells were injected subcutaneously in BALB/c mice. Mice were treated at 7-day intervals with IgG antibody, anti-PD-L1 antibody, anti-NKG2A antibody, or a combination of anti-NKG2A and anti-PD-L1 antibodies. Graphs show combined tumor growth and survival curves and analyzed by ANOVA followed by Tukey's post-hoc test and log-rank (Mantel-Cox) tests, respectively. *n=5 to 10* per group. ***D)*** Flow cytometry histogram showing MHC-I (H2D^{b}) expression on live E0771 cells after stimulation *in vitro for* 48 hours with 50 ng/mL of IFNγ. **E)** Flow cytometry analysis of tumor infiltrating NK and T cells from untreated E0771 and MHC-I^{HET} EMT6 tumors were CD45+ tumor-infiltrating leukocytes were bead isolated. NK cells are gated on live CD45^{+}, NK1.1^{+}, and CD3^{-}. T cells are

gated on live CD45+, CD3+. *n=4-5* per group. **F*)*** E0771 tumor cells were injected subcutaneously in C57BL/6 mice. Mice were treated at 7-day intervals with IgG antibody, anti-PD-L1 antibody, anti-NKG2A antibody, or a combination of anti-NKG2A and anti-PD-L1 antibodies. Graphs show combined tumor growth and survival curves and were analyzed by ANOVA followed by Tukey's post-hoc test and log-rank (Mantel-Cox) tests, respectively. *n=5 to 10* per group.

The NKG2A/Qa1 axis promotes immunotherapy resistance in MHC-I^{HET} tumors

To more rigorously assess whether PD-L1 therapeutic targeting in the MHC-I^{HET} tumors is thwarted by the Qa-1b: NKG2A axis, *Qa-1b,* the ligand for NKG2A*,* was deleted in parental EMT6 cells while leaving other MHC-I coding genes intact (**Figure 4.4A**). Treatment with anti-PD-L1 resulted in a significant reduction in tumor volume in Qa-1b KO tumors (**Figure 4.4B**), similar to the level of response observed in parental EMT6 tumors that received combination treatment with anti-NKG2A**.** The Qa-1b KO cells were then combined with *B2m-KO* cells (which cannot express Qa-1b due to lack of *B2m*) at a 50:50 ratio to create a tumor model that is MHC-I^{HET} /Qa-1b^{Neg}. Qa-1b knockout partially restored single-agent anti-PD-L1 response (**Figure 4.4C).** We hypothesize that the effect was only partial due to availability of Qa1 from other stromal cells in the tumor microenvironment but could also hint at alternative ligands for NKG2A. Thus, these data demonstrate the role of the NKG2A/Qa1 axis in promoting intrinsic resistance to anti-PD-L1 in MHC-I^{HET} tumors.

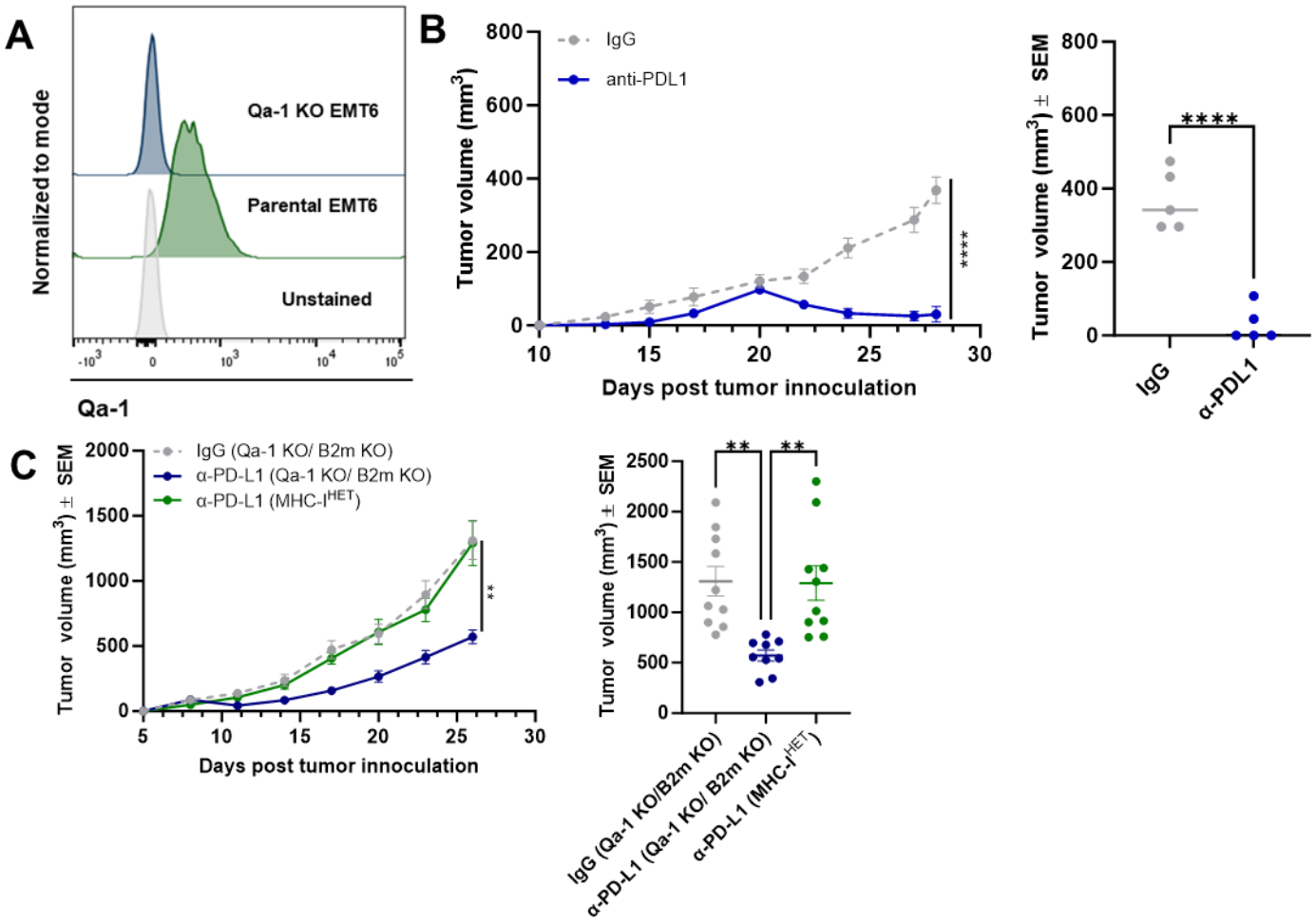

Figure 4.4 The NKG2A/Qa1 axis promotes immunotherapy resistance in MHC-I^{HET} tumors. A**)** Flow Cytometry histogram showing Qa-1 expression on live parental EMT6 and EMT6 Qa1 KO cells after stimulation *in vitro* for 48 hours with 50ng/ mL of IFNγ. **B)** Qa1 KO EMT6 cells were injected subcutaneously in BALB/c mice. Mice were treated at 7-day intervals with IgG antibody or anti-PD-L1 antibody. Graphs show combined tumor growth and individual tumor sizes on day 28 post tumor inoculation. *n= 5 per group.* **C**) Parental, MHC-I^{HET}, and *B2m* KO: Qa1 KO (50:50) EMT6 tumor cells were injected subcutaneously in BALB/c mice. Mice were treated at 7-day intervals with IgG antibody or anti-PD-L1 antibody. Graphs show combined tumor growth and individual tumor sizes on day 26 post tumor inoculation. *n=10 per group*. Bars represent SEM. Data analyzed by ANOVA followed by Tukey's post-hoc test. *p≤0.05, **p≤0.01; ***p≤0.001, ****p≤0.0001

Response to NKG2A and PD-L1 combination blockade is dependent on both NK cell and T cell activity

NKG2A is expressed on both CD8+ T cells and NK cells and is considered a therapeutic target in both cell types. To determine if the anti-tumor effect of combination therapy depended on NK

cells or CD8+ T cells, tumor-bearing mice were treated with antibodies for asialo-GM1 (*Balb/c* and *C57/BL6*) or NK1.1 (*C57BL6*) (depleting NK cells) or CD8α (depleting CD8+ cytotoxic T lymphocytes). Based on these studies both NK and CD8+ T cells are necessary for response to the combination of anti-NKG2A and anti-PD-L1 in MHC-I^{HET} EMT6 and E0771 tumors (**Figure 4.5A** and **Supplementary Figure 4.4A-B**). These data suggest that both therapies are targeting different populations of lymphocytes, each of which may be functionally eliminating different populations of tumor cells in the microenvironment. To test this, tumor MHC-I expression was examined by flow cytometry at tumor endpoint among the treatment groups. In both the MHC-I^{HET} EMT6 tumors and E0771 tumors, anti-PD-L1 treatment selected against MHC-I expressing cells, resulting in tumors that were MHC-I null, whereas anti-NKG2A selected for MHC-I expressing cells (**Figure 4.5B** and **Supplementary Figure 4.4D**). In EMT6 MHC-I^{HET} tumors, NK cells were significantly higher in single-agent-treated anti-NKG2A and combination-treated tumors on day three after treatment; however, by day seven, only NK cells in combination-treated tumors remained elevated (**Figure 4.5C**). The NK cells in tumors treated with anti-NKG2A exhibited higher degranulation as measured by CD107a (**Figure 4.5D**), whereas T cells in tumors treated with anti-PD-L1 had significantly higher degranulation (**Figure 4.5E**). These data suggest that anti-NKG2A and anti-PD-L1 may be a synergistic combination treatment to overcome immunotherapy resistance in TNBC models with heterogeneous MHC-I expression via cooperative elimination of MHC-I+ and MHC-I- cells.

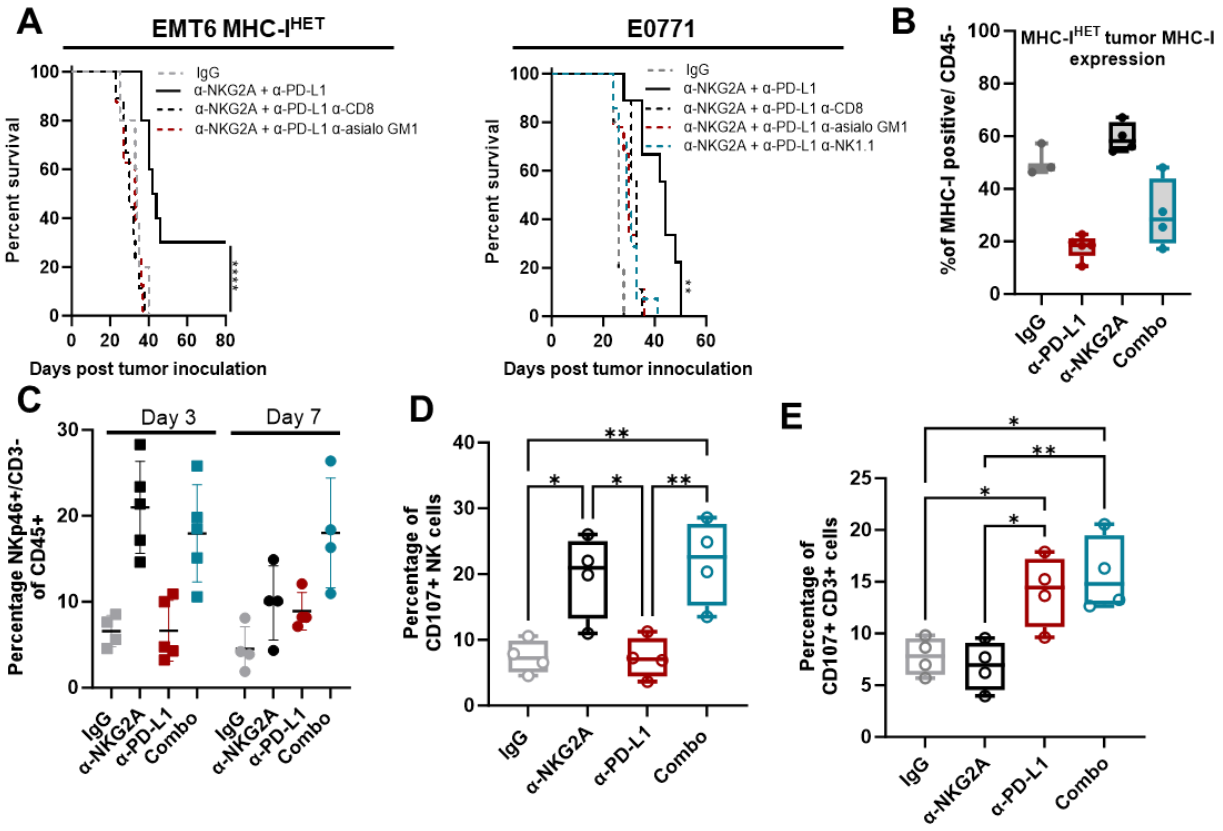

Figure 4.5: Response to NKG2A and PD-L1 combination blockade is dependent on both NK cell and T cell activity. ***A) MHC***-I^{HET} EMT6 or E0771 tumor cells were injected subcutaneously in BALB/c mice or C57BL/6 mice, respectively. Three days after tumor implantation, mice were treated with IgG, anti-CD8α, anti-NK1.1 or anti-aGM1 antibody. Mice were treated at 7-day intervals with IgG antibody, anti-PD-L1 antibody, anti-NKG2A antibody, or a combination of anti-NKG2A and anti-PD-L1 antibodies. Graphs show combined survival curves and were analyzed by log-rank (Mantel-Cox) tests. Significance shown is non-depleted IgG control compared to both anti-CD8 and anti-aGM1 treated mice. *n=5 to 10* per group. **B)** Flow cytometry analysis of MHC-I^{HET} tumor MHC-I expression after treatment with IgG, anti-PDL1, anti-NKG2A, or a combination of both anti-NKG2A and anti-PD-L1. EMT6 tumors resected at endpoint. Tumor cells are gated on live CD45^{-}, H2D^{+}. *n*= 5. ***C-E)*** Flow cytometry analysis of tumor infiltrating NK and CD3+ T cells in MHC-I^{HET} EMT6 tumors treated IgG antibody, anti-PD-L1 antibody, anti-NKG2A antibody, or a combination of anti-NKG2A and anti-PD-L1 antibodies day 3 and day 7 post treatment. CD45+ tumor-infiltrating leukocytes were bead isolated. **C)** NK cells are gated on live CD45^{+} and CD3^{-} NKp46+. Analyzed by ANOVA followed by Tukey's post-hoc test. *n=3-5* per group. ***D)*** Flow cytometry analysis of tumor infiltrating NK cell degranulation in MHC-I^{HET} EMT6 tumors. NK cells are gated on live CD45^{+} and CD3^{-} NKp46 +, CD107+. *n=3-5* per group. ***E)*** Flow cytometry analysis of tumor infiltrating CD3+ T cell degranulation in MHC-I^{HET} EMT6 tumors CD3 T cells are gated on live CD45^{+} and CD3+, CD107+. *n=3-5* per group. Analyzed by ANOVA followed by Tukey's post-hoc. *p≤0.05, **p≤0.01; ***p≤0.001, ****p≤0.0001

NK cell infiltration is dependent on the presence of IFNγ in the tumor

We next hypothesized that the absence of NK cells in *B2m-KO* tumors was attributed to the lack of IFNγ from antigen-responsive T cells leading to a cold tumor microenvironment. To investigate this, a doxycycline (dox) inducible IFNγ vector was transduced in *B2m-KO* EMT6 cells, which do not inherently secrete IFNγ (**Figure 4.6A-C**). *In vivo* dox-mediated induction of IFNγ in *B2m*-KO EMT6 tumors resulted in a significant increase of tumor-infiltrating NK cell in MHC-I null tumors (**Figure 4.6D**). Subsequent activation of these NK cells with anti-NKG2A significantly reduced tumor burden in the *B2m-KO* EMT6 tumors, which were previously shown to be unresponsive to multiple types of therapy (**Figure 4.6E**). Our findings suggest that although MHC-I null tumors lack inhibitory signals that could facilitate NK-mediated tumor clearance, the absence of critical stimulatory signals (e.g., IFNγ) results in poor NK cell recruitment. Consistent with this hypothesis, MHC-I^{HET} EMT6 tumors implanted into *IFNγ-/-* BALB/c mice resulted in a complete loss of NK cell infiltration into MHC-I^{HET} EMT6 tumors compared to those established in wildtype mice, while T cell infiltration remained unchanged (**Figure 4.6F**). Depletion of CD8+ T cells also abolished NK cell recruitment in MHC-I^{HET} EMT6 tumors grown in wildtype mice, suggesting that interferon from antigen-activated CD8+ T cells is a required signal for NK cell recruitment (**Figure 4.6G)**.

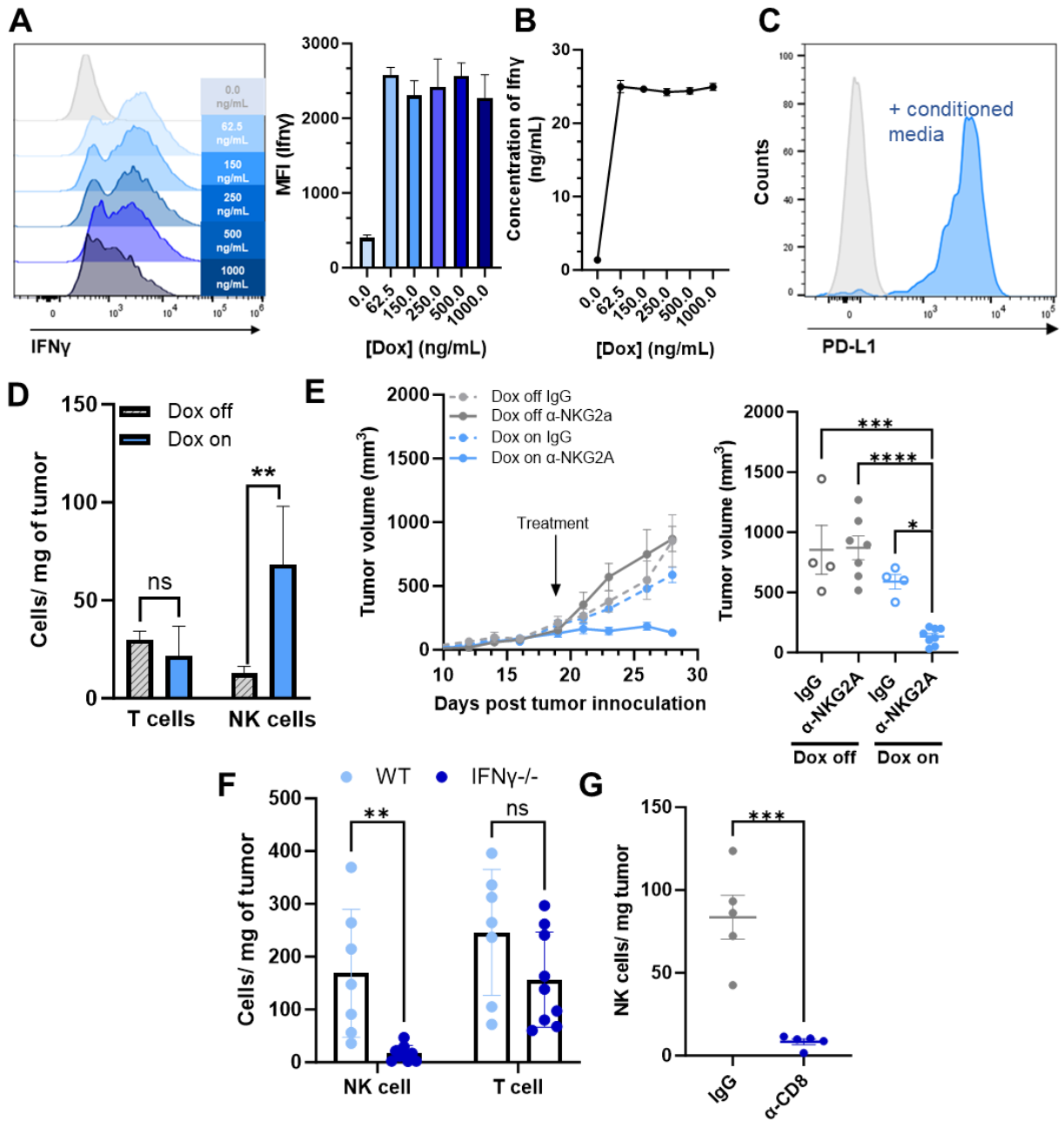

Figure 4.6: Tumor microenvironmental interferon gamma is required for NK cell recruitment to tumors lacking MHC-I expression A) Flow cytometry staining for intracellular IFNγ. *B2m* KO EMT6-IFNγ cells were treated with increasing doxycycline (Dox) concentrations (0, 62.5, 150, 250, 500, 1000 ng/mL) and incubated for 48 hours. **B)** IFNγ secretion after doxycycline treatment was measured in supernatant and detected by ELISA. Data represent mean ± SEM. **C)** *B2m* KO EMT6-IFNγ cells were treated with 62.5 ng/mL of doxycycline and collected after 48 hours. The supernatant containing secreted IFNγ was placed on parental EMT6 cells to induce PD-L1 expression. **D)** Flow cytometry analysis of *B2m* KO dox-inducible IFNγ EMT6 tumor infiltrating NK cells and CD8 T cells with or without doxycycline. NK cells are gated

on live $CD45^+$, $NKp46^+$, and $CD3^-$. T cells are gated on live CD45+, CD3+. Normalized to tumor weight. N=4. Analyzed by student T test. **E)** Doxycycline inducible IFNγ B2m KO EMT6 tumor cells were injected subcutaneously in BALB/c mice. Mice were given water with or without doxycycline and treated at 7-day intervals with IgG antibody or anti-NKG2A antibody. Graphs show combined tumor growth and individual tumor sizes on day 28 post tumor inoculation. n=4-10 per group. Data analyzed by ANOVA followed by Tukey's post-hoc test**. F)** Flow cytometry analysis of MHC-I^{HET} tumor infiltrating NK cells from MHC-I^{HET} tumors grown in wildtype or *Ifng* -/- BALB/c mice. **G)** Flow cytometry analysis of MHC-I^{HET} tumor infiltrating NK cells from mice treated with either IgG or anti-CD8α depletion antibody. *p≤0.05, **p≤0.01; ***p≤0.001, ****p≤0.0001

Regional tumor-specific MHC-I expression is associated with changes in the local immune microenvironment

To identify if the NKG2A/HLA-E axis is a relevant therapeutic target in TNBC, expression of tumor HLA-E and NKG2A in infiltrating NK cells was examined in a series of TNBCs. HLA-E was found to be widely expressed in TNBC tumors and was significantly correlated with the presence tumor-infiltrating NK and CD8+ T cells (**Figure 4.7 A-B)**. Furthermore, analysis of previously published scRNA sequencing data from human TNBC (166) revealed that NKG2A (gene name KLRC1) is highly enriched in NK and, to a lesser degree, CD8+ T cells, consistent with results in our *in vivo* model (**Supplementary Figure 4.5A**).

Based on the observed distinct immune cell infiltration pattern changes due to alterations in tsMHC-I expression in mice, we asked whether tsMHC-I expression is associated with similar tumor immune microenvironment features in humans. To test this, mIF assays were performed using panCK and HLA-A/B/C to evaluate tsMHC-I expression, and CD8 or CD56 (NK cell marker) to spatially assess immune cell infiltration patterns (**Figure 4.7C-D and Supplementary 4.5B-C**). At the bulk level, a positive correlation between tsMHC-I expression and CD8+ T cell infiltration was observed (**Supplementary Figure 4.5D**). However, there was no significant linear correlation between average MHC-I expression and the abundance of NK cells (**Supplementary Figure 4.5E**). Given the tsMHC-I heterogeneity observed in TNBC

tumors, the immune cell infiltration patterns around regions of high and low MHC-I expression and regions characterized by heterogeneous MHC-I expression were examined. Density-based spatial clustering of applications with noise (DBSCAN)(167) was used to cluster panCK+ cells from each tumor. Based on the average HLA-A/B/C intensity of the tumor clusters, the clusters were classified as HLA-A/B/C^{high}, HLA-A/B/C^{het}, and HLA-A/B/C^{low}. Using the nearest neighbor method, each tumor cluster was paired with its closest CD8+ T cell or NK cell (**Figure 4.7C and D**). To minimize sampling bias, the number of immune-tumor pairs was normalized by the number of immune cells and tumor clusters. CD8+ T cells tended to co-localize with HLA-A/B/C^{high} tumor clusters. In contrast, regions of HLA-A/B/C^{low} had the lowest infiltration of CD8+ T cells (**Figure 4.7E**). Consistent with our findings in the murine model, HLA-A/B/C^{het} tumor clusters exhibited the highest levels of infiltrating NK cells and intermediate level of CD8+ T cells (**Figure 4.7E and F**). Thus, regions of MHC-I heterogeneity are associated with increased NK cell localization, consistent with our murine models.

To investigate the impact of heterogeneity in MHC-I expression on the outcome of ICI treatment, the abundance of HLA-A/B/C^{het} tumor regions in pre-therapy biopsy samples from the clinical trial of carboplatin ± atezolizumab in metastatic TNBC was evaluated. Tumor cells were grouped using the DBSCAN algorithm, and the percentage of HLA-A/B/C^{het} regions out of total tumor clusters was calculated. Patients whose biopsies contained over 85% HLA-A/B/C^{het} regions were classified as “abundant heterogeneity,” while the remaining patients were labeled as “low heterogeneity”. Among chemoimmunotherapy-treated patients, the abundance of HLA-A/B/C^{het} regions was strongly associated with progression-free survival, but not in patients treated with chemotherapy alone (**Figure 4.7G**). In patients with abundant MHC-I heterogeneity, the NK:CD8 T cell ratio was higher (**Figure 4.7H**), indicating a relatively higher infiltration of NK cells that could be activated/targeted with anti-NKG2A immunotherapy. These findings highlight the importance of understanding the relationship between tsMHC-I expression

and immune cell infiltration in determining patient outcomes and identifying novel immunotherapy targets.

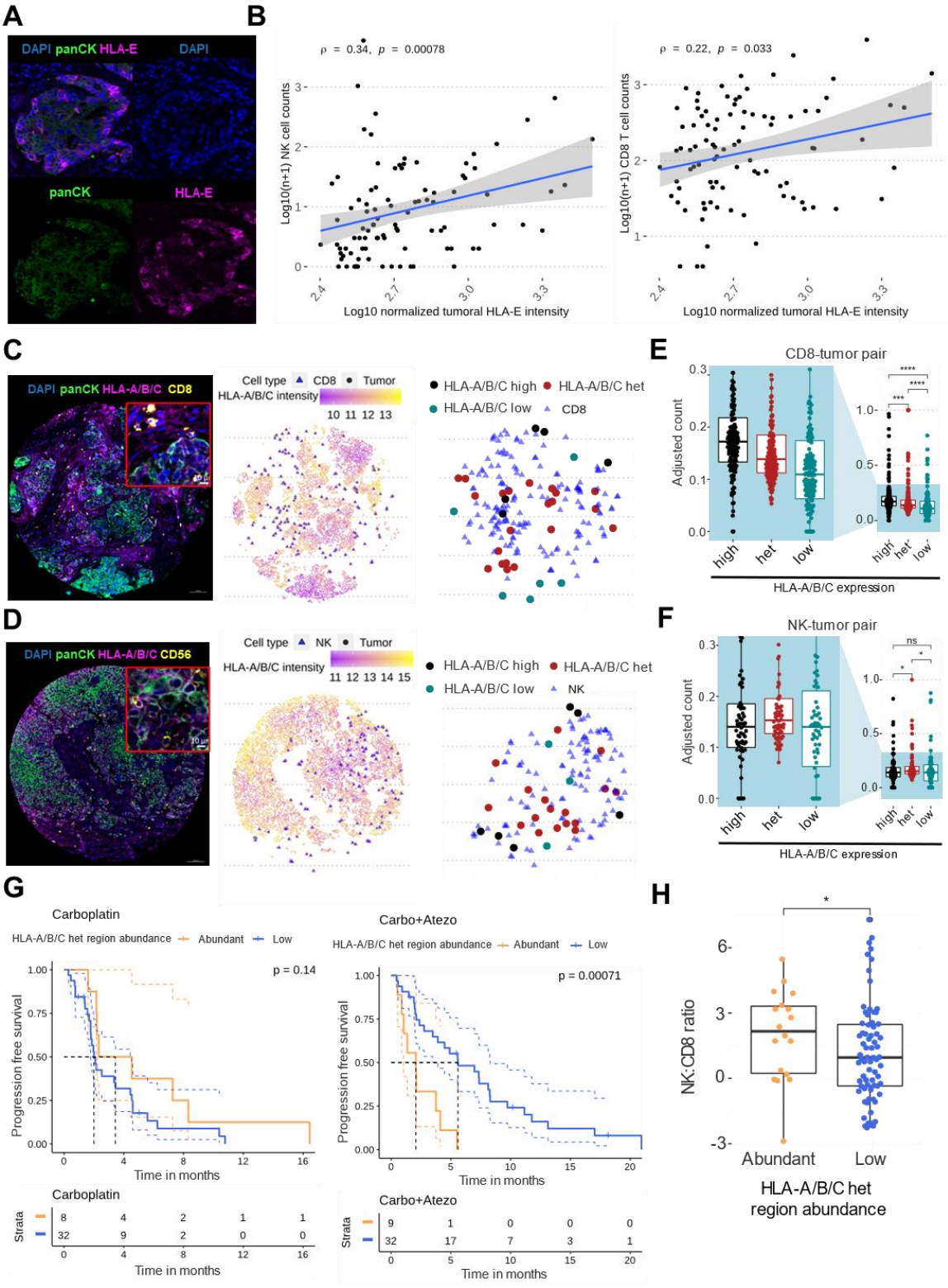

Figure 4.7: Tumor-specific MHC-I expression is associated with the regional NK cell and T cell infiltration A) mIF for HLA-E and panCK (merged and single channel example shown), was performed on 93 TNBC tumor microarrays. **B)** The expression HLA-E on tumor cells positively correlates with NK cell and CD8 T cell abundance (p=0.00078, spearman test). Log10 normalization was performed on HLA-E intensity, CD8 T cell counts, and NK cell counts to improve visualization. **C)** Representative mIF staining for DAPI, panCK, HLA-A/B/C and CD8 or CD56. Cell identity, spatial coordinates, and HLA-A/B/C expression were recorded for subsequent analysis of tumor microenvironment. Tumor cells were further clustered with DBSCAN algorithm to capture spatial tumor islands and the islands were labeled based on their MHC-I expression. **D)** CD8 T cells were clustered with their nearest tumor island to form CD8-tumor pair. Boxplot showing average of adjusted CD8-tumor pair count per patient. (****p<0.0001, ***p<0.001, Bonferroni-corrected paired t-test, ROI=154). **E)** NK cells were clustered with their nearest tumor island to form NK-tumor pair. **F)** Boxplot showing average of adjusted NK-tumor pair count per patient. (*p<0.05, Bonferroni-corrected paired t-test, ROI=69). **G)** Patients from the NCT03206203 clinical trial were classified as HLA-A/B/C^{het} region dominant (labeled as abundant) or HLA-A/B/C^{het} region low (labeled as low). Progression free survival was compared using the log-rank test between the two cohorts within carboplatin + atezolizumab arm (n=41, p=0.00071) and carboplatin arm (n=39, p=0.15). Confidence intervals for the corresponding patients were represented as yellow or blue dotted line and median survival for each cohort is plotted as black dotted line. **H)** NK and CD8 T cell infiltration was calculated using a normalized NK:CD8 ratio (*p<0.05, Wilcoxon test). All the boxplots capture the median, and 25^{th} and 75^{th} quantile.

Discussion

Anti-PD-1/PD-L1-based therapy can produce durable anti-tumor immune responses in some patients. However, adaptive, and innate immune responses impose selection pressure on tumor cells, which eventually lead to immune escape and immunotherapy resistance. Multiple cancer cell intrinsic immune escape mechanisms, such as low neoantigen load (168,169), loss of antigen presentation (23), and impaired response to interferon (170), have been correlated with immunotherapy outcome. Among these ICI resistance mechanisms, insufficient antigen presentation to T cells, exemplified by MHC-I downregulation, compromises a sizable proportion of patients (171,172). Our analysis of metastatic TNBC patients treated with chemotherapy ± immunotherapy demonstrated that high tsMHC-I heterogeneity is associated with lack of benefit to PD-L1 therapy. As heterogeneous tsMHC-I expression is common in breast cancer, particularly TNBC, our results highlight the need to overcome aberrant tsMHC-I expression to achieve higher rates of immunotherapy responses and benefit. While several approaches have been investigated to enhance MHC-I expression and reactivate anti-tumor immunity (94), our

objective was to exploit changes in the immune microenvironment resulting from tsMHC-I heterogeneous expression to overcome immunotherapy resistance. We found that this tumor-specific phenotype drives NK cell infiltration leading to our investigation of alternative checkpoint blockades, specifically NKG2A.

Our findings reinforce the growing interest in utilizing tumor-infiltrating NK cells as a potential therapeutic strategy for tumors with loss of MHC-I expression (173–175). Other reports have highlighted tumor cells with complete loss of MHC-I and increased sensitivity to NK cells because they fail to engage inhibitory KIR (176–178). While informative, these studies have not explored the relationship of NK cells and varied MHC-I expression, which is commonly the case we and others have found in breast cancer (150,152,153). This study provides evidence that heterogeneity in MHC-I expression, not complete loss of MHC-I, has the strongest correlation with NK cell infiltration in TNBC patient cohorts and murine models. The observed increase in NK cell abundance in heterogeneous MHC-I tumors is due to several factors: firstly, as we have shown here, tumor microenvironmental IFNγ is required for NK cell recruitment, coming from antigen-responsive T cells. Secondly, although not mechanistically shown here, an upregulation of IL-2 signaling, crucial for maintaining NK cell activity, appears to be associated with enhanced NK cell activity. Finally, we observed an enrichment of CD49b expression which facilitates NK cell retention within the tumor microenvironment. Interactions between collagen and CD49b in NK cells can promote the expression of CXCL10 and other chemokines in the presence of low levels of interferon (179). The $CD49b^{High}$ NK cells that infiltrate $MHC\text{-}I^{HET}$ tumors may actively engage with the collagen-rich environment, leading to an increase in CXCL9/10 expression. However, further investigation is necessary to explore the impact of NK-dependent chemokine expression in the $MHC\text{-}I^{HET}$ microenvironment on CD4/CD8 infiltration and retention.

Increased infiltration of NK cells has important implications for systemic anti-tumor immunity, as previous research has demonstrated that NK cells produce chemokines that attract cDC1s

(12,163,164). We observed higher dendritic cell infiltration in the NK cell abundant MHC-^{IHET} tumor models. However, markers of T cell activation that could be associated with cDC cross-priming were not observed. This phenomenon may be explained by differences in immunogenicity between our syngeneic tumor model and other spontaneous models, or the partial loss of MHC-I on tumor cells. Alternatively, cDC priming of CD4+ T cells leading to CD4-mediate cytokine support could also play a more dominant role under basal conditions in the absence of therapeutic checkpoint blockade.

Other studies have highlighted the importance of NK and CD8+ T cell activation through NKG2A blockade therapy (180–182). Monalizumab (anti-NKG2A, AstraZeneca) has become the center of several clinical trials in various cancer types (NCT04307329, NCT04590963, NCT05221840, NCT02671435, NCT05061550, NCT03833440). Our findings indicate that HLA-E expression is frequently detected in TNBC tumors and is positively correlated with infiltration of NK and CD8+ T cells. These findings suggest that combining anti-NKG2A with anti-PD-L1 therapy may represent a promising yet underexplored approach for treating TNBC tumors. Future research could involve spatial profiling to measure the distance between HLA-E positive tumors and NK/CD8+ T cells, with the aim of developing potential biomarkers to predict patient response to NKG2A blockade.

These data reinforce the growing interest on how tumor-specific antigen presentation via MHC-I plays a role in modifying anti-tumor immunity and ICI response. Together, they endorse the unmet translational and clinical need to address heterogeneity in MHC-I expression as a variable in understanding breast cancer anti-tumor immunity and response to immunotherapy. Moreover, these data highlight the potential to harness NK cell function in advancing cancer immunotherapy combinations.

Chapter V

Conclusions and Future Directions

MHC-I heterogeneity and immunotherapy response in TNBC

PD-1/L1-targeting therapies function by inhibiting suppressive signals to activated T effector cells, particularly CD8+ cytotoxic cells (172,183). The suppressive signal occurs when PD-1 binds to PD-L1 on T cells, which is commonly present on infiltrating myeloid cells but can also be expressed by tumor cells and other components of the adaptive and innate immune systems. Recognition of peptide-bound MHC-I molecules by CD8+ T cells is essential for antitumor immune clearance and the efficacy of ICIs (183,184). MHC-I is expressed ubiquitously on all nucleated cells and can be induced by inflammatory signals, such as interferons (e.g., interferon-gamma; IFNγ), to enhance antigen presentation to T cells in the microenvironment. Although tumor immune-editing of neoantigens is an established mechanism of escape from CD8+ T cells, the expression of MHC-I by tumor cells is the most critical step in this process. Therefore, loss or deregulation of MHC-I represents a straightforward method for tumor cells to evade adaptive immunity. There are few studies that have systematically explored MHC-I loss in breast cancers, specifically in the tumor compartment; however, our data suggest it is far more common than expected.

Loss or downregulation of MHC-I is a well-known mechanism of immune evasion, and in some cases, it has been associated with resistance to immunotherapy (185). For instance, genomic loss of beta-2-microglobulin (B2M), which is a necessary partner for stabilizing and expressing classical HLA-A/B/C and non-classical HLAs on the cell surface, has been observed in melanomas that have developed acquired resistance to anti-PD-1 therapy (23). Preclinical studies on MHC-I and B2M function have demonstrated that loss of these molecules through genetic deletion or CRISPR/Cas9-mediated KO in tumor cells results in an overwhelmingly "cold" immune microenvironment and negates the response to most T cell-targeted

therapeutics. However, these studies typically rely on complete loss or "purist" biological approaches to understanding the consequences of MHC-I loss. Therefore, further research is necessary to fully comprehend the complexity of MHC-I regulation in cancer and its impact on immunotherapy efficacy.

In chapter III above, I describe our work on MHC-I heterogeneity in triple-negative breast cancer and immunotherapy response. To evaluate heterogeneity in MHC-I expression at the single-cell level, we performed multiplexed immunofluorescence for HLA-A/B/C and pan-cytokeratin (panCK) to colocalize MHC-I signal to tumor cells. A series of >300 early breast cancers from diverse subtypes were analyzed. We found that TNBC had the highest average intensity/expression level across tumor cells, but also the highest variability and probability of demonstrating bimodal MHC-I expression. To examine the impact of MHC-I expression heterogeneity on the outcomes of ICI treatment, the abundance of HLA-A/B/C in tumor regions was evaluated in pre-therapy biopsy samples obtained from a clinical trial of carboplatin ± atezolizumab in mTNBC [NCT03206203]. DBSCAN was used to cluster panCK+ cells from each tumor, and the percentage of HLA-A/B/C regions out of the total tumor clusters was determined. Patients whose biopsies contained over 85% HLA-A/B/C regions were classified as having "abundant heterogeneity," while the rest were labeled as having "low heterogeneity." Among patients who received atezolizumab treatment, the abundance of HLA-A/B/C regions was strongly correlated with PFS, but not in patients treated with carboplatin alone.

Based on our findings in human disease, we developed an informative model to illustrate how heterogeneity in MHC-I expression could impact anti-tumor immunity. We utilized CRISPR-guided *B2m* knockout (*B2m*-null) in a murine orthotopic model (EMT6) and combined MHC-I-proficient and MHC-I-deficient isogenic lines at various ratios to simulate how pre-existing populations of absolute MHC-I loss would affect the immune microenvironment. Our results showed that heterogeneity in MHC-I expression led to considerable resistance to anti-PD-L1 therapy, which

was consistent with our observations in patients. Additionally, this resulted in a significantly different tumor-immune microenvironment compared to the complete absence (*B2m*-null) or presence (MHC-I-proficient) of MHC-I in the tumor inoculums.

NK cell interactions with MHC-I heterogenous tumors

In breast cancers, new strategies are required to broaden the applicability of therapeutics that target the host immune system for cancer treatment. While tumors with low or diminished MHC-I expression can escape adaptive CD8+ T cell cytotoxicity, NK cells provide an alternative innate immunologic approach to target these tumors for elimination. This is due to the "missing-self" hypothesis, which states that NK cells identify and remove tumor cells that do not express MHC-I. Furthermore, NK cells produce chemokines and cytokines that can facilitate adaptive immune responses, such as dendritic cell recruitment for antigen priming and the elimination of adjacent MHC-I expressing tumor cells. While NK cells may be crucial in controlling and eliminating cancer cells, our understanding of the extent of NK cell cytotoxic response in heterogeneous MHC-I TNBC tumors is limited.

In chapter IV, our work described the role of NK cells in heterogeneous MHC-I tumors and how they can be utilized to overcome immunotherapy resistance. In human breast tumors, we utilized multiplexed immunofluorescence for panCK, HLA-A/B/C, and either CD8 or CD56 to observe changes in the immune microenvironment. We found that cytotoxic T cells were regionally linked to high MHC-I expression, while NK cells were spatially organized to heterogeneous regions. In murine tumors with controlled MHC-I heterogeneity, we observed a notable increase in NK cell infiltration. However, resistance to anti-PD-L1 therapy persisted, indicating that the functionality of NK cells alone is insufficient to effectively slow tumor growth, regardless of ICI therapy. Nonetheless, the elevated presence of NK cells suggested that if NK cell functionality could be restored therapeutically, this could be a practical approach overcome immunotherapy resistance. In a transcriptional analysis of CD45+ infiltrating cells, we noticed a

unique increase in the expression of Klrc1(Nkg2a) and its heterodimeric partner Cd94 in MHC-I heterogeneous tumors. These molecules are C-type lectin receptors, which are expressed on the surface of NK cells and some CD8+ T cells. Signaling via their ligand (HLA-E/Qa-1, present or interferon-inducible on various cells including tumor cells suppresses NK cell functionality through abrogation of "missing-self" signals. Treatment with anti-NKG2A therapeutic antibodies restored sensitivity to anti-PD-L1 therapy in EMT6 MHC-I^{HET} Additionally, KO of NKG2A ligand Qa-1 re-sensitized MHC-I^{HET} tumors to α-PD-L1 therapy.

Future Directions

Our findings strongly indicate that the expression of MHC-I can significantly impact the immune response against tumors, and its dysregulation may play a crucial role in immunotherapy resistance, specifically in TNBC. These insights advance our understanding of immunotherapy response and highlight the potential for combining multiple biomarkers to enhance predictive values for clinical use. Notably, MHC-II is a promising biomarker of response that could work synergistically with MHC-I.

Intriguingly, a subset of tumors, from many sites of origin, express MHC-II, which presents antigen to CD4+ T cells and is canonically thought to only be expressed by professional antigen presenting cells (pAPCs), such as B cells, macrophages, and dendritic cells (DCs). Our lab has previously identified that the expression of MHC-II on tumor cells was a biomarker for anti- PD-1/L1 response in melanoma (186). Additionally, other studies have shown that tsMHC-II expression is linked to an improved response to nivolumab in Classical Hodgkin Lymphoma and increased CD8+ infiltrate, leading to better survival in ovarian cancer (97). CD4+ T cell help is needed for effective priming and maintenance of a CD8+ T cell response. Therefore, stimulating CD4+ T cells may lead to a more effective anti-cancer immune response than activating CD8+ T cells alone.

In previous studies of our lab, we demonstrated that upregulating tsMHC-II could enhance anti-tumor immunity. Building on this, we hypothesized that MHC-II expression could serve as a functional antigen-presenting molecule, promoting CD4 T-helper cell aid to the anti-tumor environment and potentially overcome the loss of MHC-I. To investigate the therapeutic potential of MHC-II, we enforced tumor cell expression of *Class II Major Histocompatibility Complex Transactivator (CIITA)* in EMT6 B2m KO cells, which lack MHC-I expression (**Figure 5.1A**). Upon implantation into syngeneic immunocompetent mice, we observed that the enforced expression of MHC-II and its associated machinery could not effectively restore the response to immunotherapy in tumors that lacked MHC-I expression (**Figure 5.1B**).

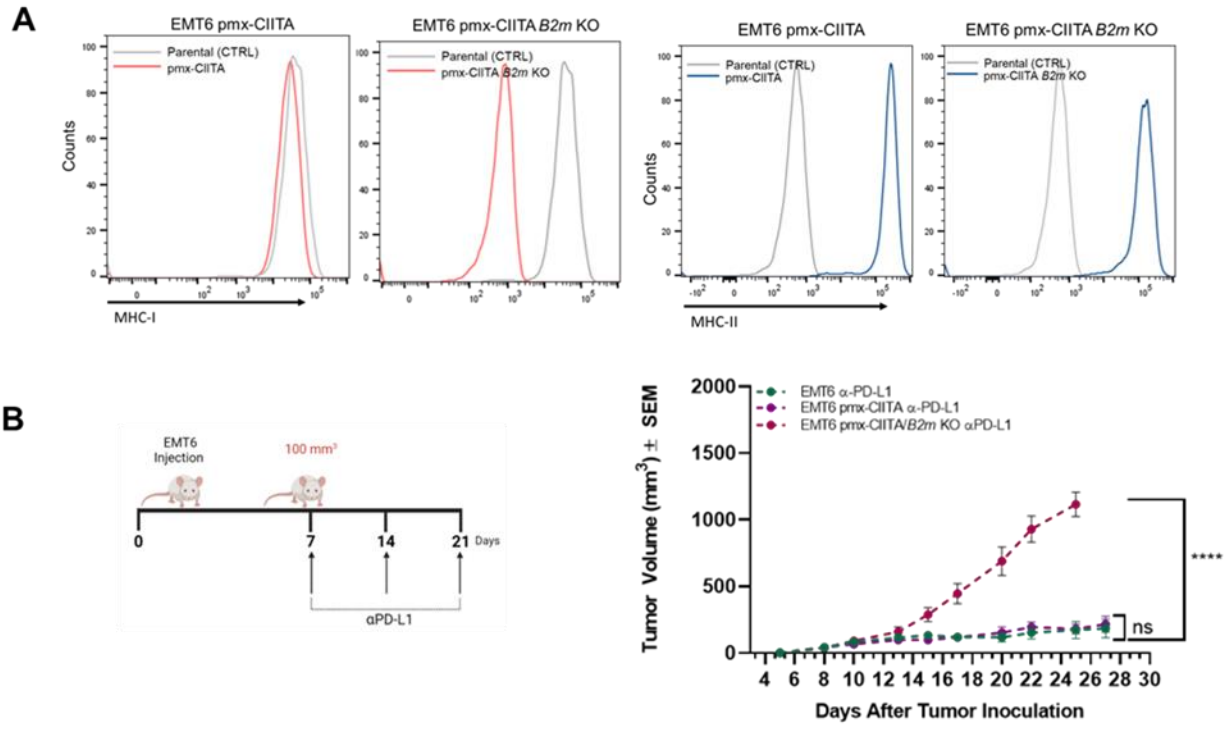

Figure 5.1. Enforced MHC-II expression in MHC-I null tumors fails to rescue response to anti-PD-L1 therapy. A) Parental EMT6 and B2m KO EMT6 cells were transduced with pmx-CIITA. Flow plots show MHC-I and MHC-II expression. B) Anti-PD-L1 treatment schema. C) EMT6 pmx-CIITA-B2m KO tumor cells were injected subcutaneously in BALB/c mice. Mice were treated at 7-day intervals with IgG antibody or anti-PD-L1 antibody. Graphs show combined tumor growth and survival curves. n=10 to 15 per group.

While the functional role of MHC-II may not be sufficient to overcome MHC-I loss, it could serve as a non-functional marker of the inflammatory state of the tumor environment. Combining assessments of MHC-I and MHC-II competence could improve predictive capacity and patient selection for future immunotherapy combination trials. While the clinical trial discussed in chapters III and IV (NCT03206203) did not find MHC-II to be a reliable predictor of immunotherapy efficacy on its own, the combination of MHC-I and MHC-II evaluations revealed a subset of patients who exhibited a favorable response to the addition of atezolizumab (**Figure 5.2A-B**).

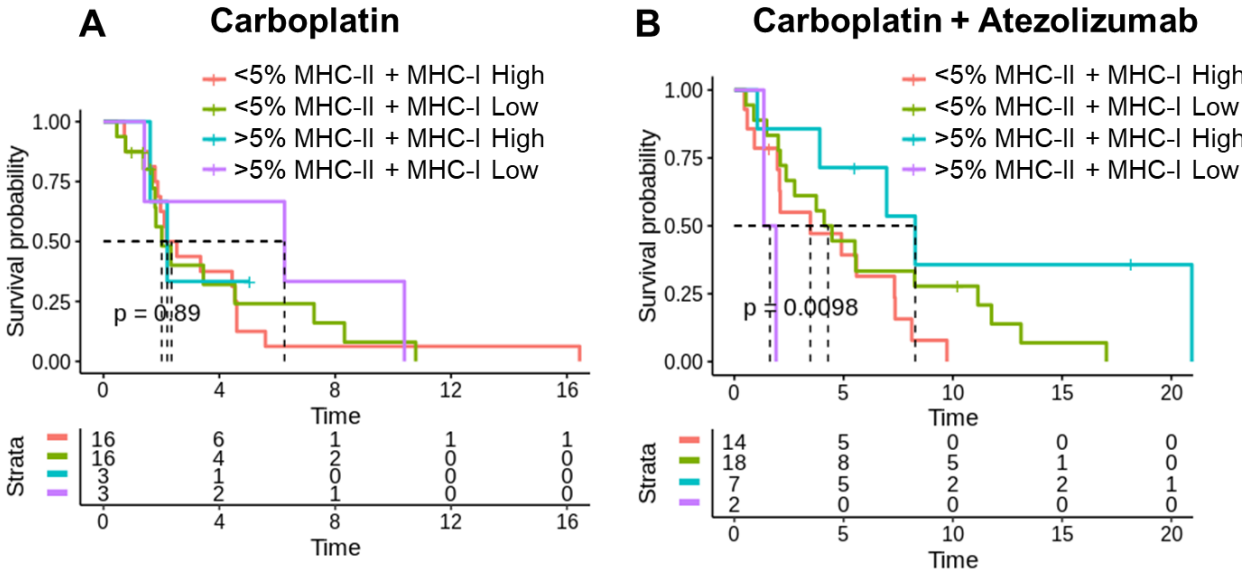

Figure 5.2. In metastatic TNBC, MHC-II predicts immunotherapy benefit only in MHC-I competent tumors. A-B) Analysis of progression-free survival in metastatic TNBC patients treated with carboplatin ± atezolizumab. Patient MHC-I/MHC-II expression is scored IHC.

Based on these initial findings, there is ample evidence to warrant further investigation into the potential correlation between a combined biomarker of tumor-specific HLA-DR/MHC-II expression and HLA-A/MHC-I expression and the clinical benefits of immunotherapy combination therapies in patients with early-stage or metastatic triple-negative breast cancer. . While we have not yet evaluated MHC-I expression in the early-stage setting, we anticipate that untreated early-stage tumors may exhibit a lesser degree of MHC-I loss. Therefore, it could be

proposed that combining MHC-I and MHC-II analyses could enhance our ability to predict patient response in the early setting as well. One potential approach to investigate this further would be to conduct a retrospective analysis using tissue samples from multiple institutions. This would involve collecting data from patients with early-stage and metastatic breast cancer who have received immunotherapy treatment and performing multiplexed immunofluorescence analysis on pre-treatment or metastatic tumor biopsies to measure tumor-specific MHC-II (HLA-DR/panCK), T cell activation (CD4/CD8/GZMB), and MHC-I (HLA-A/panCK). The primary aim of this analysis is to determine whether these markers are predictive of patient outcomes, with clinical response being assessed through measures such as progression-free survival (PFS), overall survival (OS), and pathological complete response (pCR). There is a scarcity of publicly available breast cancer datasets that include information on immunotherapy response. Therefore, this study has the potential to make significant contributions to the field, leading to future discoveries that could positively impact patients. Furthermore, the ongoing advancements in MHC-I/II biomarkers could potentially result in the first clinically-indicated immunotherapy biomarkers in the neoadjuvant (TNBC) setting. Ultimately, the findings of this study could serve as the foundation for the development of novel clinical trials, which will help further refine precision medicine approaches based on the data generated here.

An additional area of investigation for this project is to explore alternative combination therapies to address the problem of MHC-I loss. Since MHC-II antigen presentation facilitates CD4-T helper responses, tumor-MHC-II expression may lead to a more diverse antigen presentation profile. LAG-3 is an immune checkpoint molecule that competes with CD4 for binding to antigenic MHC-II molecules. Our research shows that many anti-PD-1/L1-responsive tumors express high levels of MHC-II, suggesting that LAG-3 expression on infiltrating leukocytes could be a direct mechanism of intrinsic or acquired resistance to anti-PD-1/L1 therapies. To test this, we enforced murine Ciita expression in the EMT6 tumor model and examined the effects of combining anti-PD-L1 with anti-LAG-3 monoclonal antibodies. Our findings indicate that the

addition of anti-LAG3 resulted in lower tumor burden and improved survival rates (**Figure 5.3**). Future directions for this research include conducting in vivo studies on our MHC-IHET model to determine if the combination of LAG-3 and PD-L1 targeted therapy can complement each other to aid in immunotherapy resistance. Overcoming therapeutic resistance to immune therapy, particularly anti-PD-1/PD-L1, is one of the major challenges in current cancer biology/therapy. As such, identifying and overcoming therapeutic resistance in MHC-I heterogenous tumors has the potential to significantly impact a large population of patients by extending the benefits of anti-PD-1-based therapy.

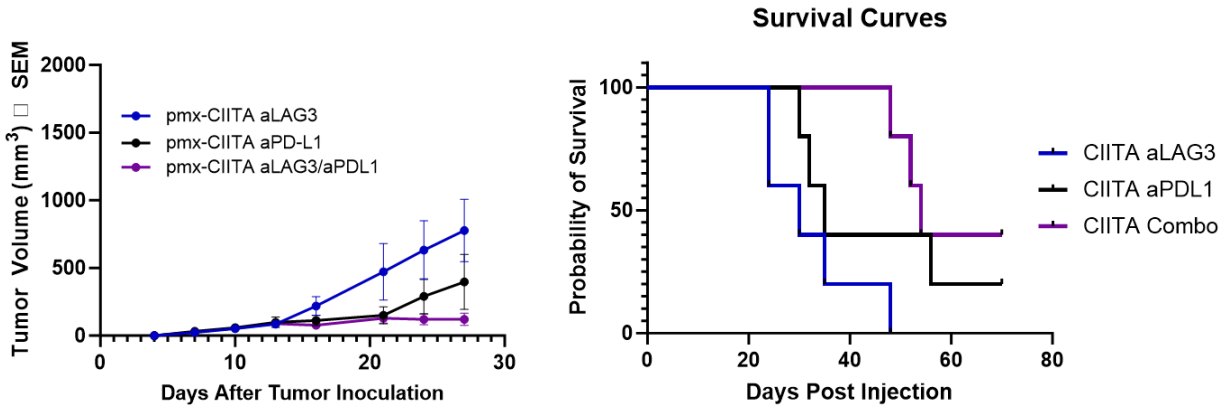

Figure 5.3. Combination blockade of PD-L1 and LAG3 in MHC-II high tumors extend survival. EMT6 pmx-CIITA- tumor cells were injected subcutaneously in BALB/c mice. Mice were treated at 7-day intervals with anti-PD-L1, anti-LAG3, or a combination of both. Graphs show combined tumor growth and survival curves. n=5 to 10 per group.

Concluding thoughts

This study utilizes a comprehensive approach that includes in vitro, in vivo, and human correlative studies to gain a better understanding of how heterogeneity in antigen presentation impacts the immune microenvironment in breast cancer, and consequently, modifies the likelihood of benefit from immunotherapies and chemoimmunotherapy combinations used in patient care. To develop combinatorial therapeutic strategies, we employed innovative techniques that modify MHC-I diversity and expression levels. Our strategies focus on

leveraging the immune microenvironment's adaptation to heterogeneity in antigen presentation, with a specific emphasis on targeting inhibitory receptors such as NK cells, which are already under clinical trial for other indications. The results of this work will provide novel insights into anti-tumor immunity, biomarkers for T cell-targeted and NK-targeted immunotherapy, and strategic design of future clinical trials in breast cancer.

References

1. Trowsdale J. Genomic structure and function in the MHC. Trends in Genetics. 1993;9:117–22.

2. Anderson P, Aptsiauri N, Ruiz-Cabello F, Garrido F. HLA class I loss in colorectal cancer: implications for immune escape and immunotherapy. Cell Mol Immunol. 2021;18:556–65.

3. Hazini A, Fisher K, Seymour L. Deregulation of HLA-I in cancer and its central importance for immunotherapy. J Immunother Cancer. BMJ Specialist Journals; 2021;9:e002899.

4. Hurkmans DP, Kuipers ME, Smit J, van Marion R, Mathijssen RHJ, Postmus PE, et al. Tumor mutational load, CD8+ T cells, expression of PD-L1 and HLA class I to guide immunotherapy decisions in NSCLC patients. Cancer Immunol Immunother. 2020;69:771–7.

5. Montesion M, Murugesan K, Jin DX, Sharaf R, Sanchez N, Guria A, et al. Somatic HLA Class I Loss Is a Widespread Mechanism of Immune Evasion Which Refines the Use of Tumor Mutational Burden as a Biomarker of Checkpoint Inhibitor Response. Cancer Discov. American Association for Cancer Research; 2021;11:282–92.

6. Cornel AM, Mimpen IL, Nierkens S. MHC Class I Downregulation in Cancer: Underlying Mechanisms and Potential Targets for Cancer Immunotherapy. Cancers (Basel) [Internet]. 2020 [cited 2020 Dec 10];12. Available from: https://www.ncbi.nlm.nih.gov/pmc/articles/PMC7409324/

7. Paul S, Weiskopf D, Angelo MA, Sidney J, Peters B, Sette A. HLA class I alleles are associated with peptide binding repertoires of different size, affinity, and immunogenicity. J Immunol. 2013;191:10.4049/jimmunol.1302101.

8. Michalek MT, Grant EP, Gramm C, Goldberg AL, Rock KL. A role for the ubiquitin-dependent proteolytic pathway in MHC class l-restricted antigen presentation. Nature. Nature Publishing Group; 1993;363:552–4.

9. Roelse J, Grommé M, Momburg F, Hämmerling G, Neefjes J. Trimming of TAP-translocated peptides in the endoplasmic reticulum and in the cytosol during recycling. Journal of Experimental Medicine. 1994;180:1591–7.

10. Kaer LV, Ashton-Rickardt PG, Ploegh HL, Tonegawa S. TAP1 mutant mice are deficient in antigen presentation, surface class I molecules, and CD4−8+ T cells. Cell. 1992;71:1205–14.

11. Chapman DC, Williams DB. ER quality control in the biogenesis of MHC class I molecules. Seminars in Cell & Developmental Biology. 2010;21:512–9.

12. Gutiérrez-Martínez E, Planès R, Anselmi G, Reynolds M, Menezes S, Adiko AC, et al. Cross-Presentation of Cell-Associated Antigens by MHC Class I in Dendritic Cell Subsets. Front Immunol [Internet]. Frontiers; 2015 [cited 2021 Jun 15];6. Available from: https://www.frontiersin.org/articles/10.3389/fimmu.2015.00363/full

13. Jongsma MLM, Guarda G, Spaapen RM. The regulatory network behind MHC class I expression. Molecular Immunology. 2019;113:16–21.

14. Gobin SJP, Keijsers V, Zutphen M van, Elsen PJ van den. The Role of Enhancer A in the Locus-Specific Transactivation of Classical and Nonclassical HLA Class I Genes by Nuclear Factor κB. The Journal of Immunology. American Association of Immunologists; 1998;161:2276–83.

15. Gobin SJP, Peijnenburg A, Keijsers V, van den Elsen PJ. Site α Is Crucial for Two Routes of IFNγ-Induced MHC Class I Transactivation: The ISRE-Mediated Route and a Novel Pathway Involving CIITA. Immunity. 1997;6:601–11.

16. Perkins N d., Edwards N l., Duckett C s., Agranoff A b., Schmid R m., Nabel G j. A cooperative interaction between NF-kappa B and Sp1 is required for HIV-1 enhancer activation. The EMBO Journal. John Wiley & Sons, Ltd; 1993;12:3551–8.

17. Chang C-H, Hammer J, Loh JE, Fodor WL, Flavell RA. The activation of major histocompatibility complex class I genes by interferon regulatory factor-1 (IRF-1). Immunogenetics. 1992;35:378–84.

18. Watanabe N, Sakakibara J, Hovanessian AG, Taniguchi T, Fujita T. Activation of IFN- β element by IRF-1 requires a post-translational event in addition to IRF-1 synthesis. Nucleic Acids Research. 1991;19:4421–8.

19. Lorenzi S, Forloni M, Cifaldi L, Antonucci C, Citti A, Boldrini R, et al. IRF1 and NF-kB Restore MHC Class I-Restricted Tumor Antigen Processing and Presentation to Cytotoxic T Cells in Aggressive Neuroblastoma. PLOS ONE. Public Library of Science; 2012;7:e46928.

20. Downs I, Vijayan S, Sidiq T, Kobayashi KS. CITA/NLRC5: A critical transcriptional regulator of MHC class I gene expression. BioFactors. 2016; 42:349–57.

21. Meissner TB, Li A, Liu Y-J, Gagnon E, Kobayashi KS. The nucleotide-binding domain of NLRC5 is critical for nuclear import and transactivation activity. Biochemical and Biophysical Research Communications. 2012; 418:786–91.

22. Yoshihama S, Roszik J, Downs I, Meissner TB, Vijayan S, Chapuy B, et al. NLRC5/MHC class I transactivator is a target for immune evasion in cancer. Proc Natl Acad Sci U S A. 2016;113:5999–6004.

23. Zaretsky JM, Garcia-Diaz A, Shin DS, Escuin-Ordinas H, Hugo W, Hu-Lieskovan S, et al. Mutations Associated with Acquired Resistance to PD-1 Blockade in Melanoma. New England Journal of Medicine. Massachusetts Medical Society; 2016;375:819–29.

24. Mehta AM, Jordanova ES, Kenter GG, Ferrone S, Fleuren G-J. Association of antigen processing machinery and HLA class I defects with clinicopathological outcome in cervical carcinoma. Cancer Immunol Immunother. 2008;10.

25. Cabrera T, Fernandez MA, Sierra A, Garrido A, Herruzo A, Escobedo A, et al. High frequency of altered HLA class I phenotypes in invasive breast carcinomas. Human Immunology. 1996;50:127–34.

26. Menon AG, Morreau H, Tollenaar RAEM, Alphenaar E, van Puijenbroek M, Putter H, et al. Down-Regulation of HLA-A Expression Correlates with a Better Prognosis in Colorectal Cancer Patients. Laboratory Investigation. Nature Publishing Group; 2002;82:1725–33.

27. Park HS, Cho U, Im SY, Yoo CY, Jung JH, Suh YJ, et al. Loss of Human Leukocyte Antigen Class I Expression Is Associated with Poor Prognosis in Patients with Advanced Breast Cancer. J Pathol Transl Med. 2019;53:75–85.

28. Watson NFS, Ramage JM, Madjd Z, Spendlove I, Ellis IO, Scholefield JH, et al. Immunosurveillance is active in colorectal cancer as downregulation but not complete loss of MHC class I expression correlates with a poor prognosis. International Journal of Cancer. 2006;118:6–10.

29. Hanagiri T, Shigematsu Y, Kuroda K, Baba T, Shiota H, Ichiki Y, et al. Prognostic implications of human leukocyte antigen class I expression in patients who underwent surgical resection for non-small-cell lung cancer. J Surg Res. 2013;181:e57-63.

30. Cordon-Cardo C, Fuks Z, Drobnjak M, Moreno C, Eisenbach L, Feldman M. Expression of HLA-A,B,C Antigens on Primary and Metastatic Tumor Cell Populations of Human Carcinomas. Cancer Res. American Association for Cancer Research; 1991;51:6372–80.

31. Seliger B, Höhne A, Knuth A, Bernhard H, Ehring B, Tampé R, et al. Reduced membrane major histocompatibility complex class I density and stability in a subset of human renal cell carcinomas with low TAP and LMP expression. Clin Cancer Res. American Association for Cancer Research; 1996;2:1427–33.

32. Kaklamanis L, Townsend A, Doussis-Anagnostopoulou IA, Mortensen N, Harris AL, Gatter KC. Loss of major histocompatibility complex-encoded transporter associated with antigen presentation (TAP) in colorectal cancer. Am J Pathol. 1994;145:505–9.

33. Seliger B, Maeurer MJ, Ferrone S. TAP off — tumors on. Immunology Today. 1997;18:292–9.

34. Bernal M, García-Alcalde F, Concha A, Cano C, Blanco A, Garrido F, et al. Genome-wide differential genetic profiling characterizes colorectal cancers with genetic instability and specific routes to HLA class I loss and immune escape. Cancer Immunol Immunother. 2012;61:803–16.

35. Vitale M, Rezzani R, Rodella L, Zauli G, Grigolato P, Cadei M, et al. HLA Class I Antigen and Transporter Associated with Antigen Processing (TAP1 and TAP2) Down-Regulation in High-Grade Primary Breast Carcinoma Lesions. Cancer Res. American Association for Cancer Research; 1998;58:737–42.

36. Shionoya Y, Kanaseki T, Miyamoto S, Tokita S, Hongo A, Kikuchi Y, et al. Loss of tapasin in human lung and colon cancer cells and escape from tumor-associated antigen-specific CTL recognition. OncoImmunology. Taylor & Francis; 2017;6:e1274476.

37. Stratikos E, Stamogiannos A, Zervoudi E, Fruci D. A Role for Naturally Occurring Alleles of Endoplasmic Reticulum Aminopeptidases in Tumor Immunity and Cancer Pre-Disposition. Front Oncol [Internet]. Frontiers; 2014 [cited 2021 Apr 18];4. Available from: https://www.frontiersin.org/articles/10.3389/fonc.2014.00363/full

38. Maleno I, López-Nevot M, Cabrera T, Salinero J, Garrido F. Multiple mechanisms generate HLA class I altered phenotypes in laryngeal carcinomas: high frequency of HLA haplotype loss associated with loss of heterozygosity in chromosome region 6p21. Cancer Immunol Immunother. 2002;51:389–96.

39. McGranahan N, Swanton C. Clonal Heterogeneity and Tumor Evolution: Past, Present, and the Future. Cell. 2017;168:613–28.

40. Yu S, Zhao Z, Chen L, Gu T, Yu H, Tang H, et al. HLA loss of heterozygosity-mediated discordant responses to immune checkpoint blockade in squamous cell lung cancer with renal metastasis. Immunotherapy. Future Medicine; 2021;13:195–200.

41. Chowell D, Morris LGT, Grigg CM, Weber JK, Samstein RM, Makarov V, et al. Patient HLA class I genotype influences cancer response to checkpoint blockade immunotherapy. Science. 2018;359:582–7.

42. Lobashevsky AL, Krueger-Sersen M, Britton RM, Littrell CA, Singh S, Cui CP, et al. Pretransplant HLA typing revealed loss of heterozygosity in the major histocompatibility complex in a patient with acute myeloid leukemia. Human Immunology. 2019;80:257–62.

43. Tran E, Robbins PF, Lu Y-C, Prickett TD, Gartner JJ, Jia L, et al. T-Cell Transfer Therapy Targeting Mutant KRAS in Cancer. New England Journal of Medicine. Massachusetts Medical Society; 2016;375:2255–62.

44. Toth DF, Raderer M, Wadsak W, Karanikas G. Beta-2 Microglobulin as a Diagnostic Parameter in Non-Hodgkin Lymphoma: A Comparative Study with FDG-PET. Anticancer Research. International Institute of Anticancer Research; 2013;33:3341–5.

45. Castro A, Ozturk K, Pyke RM, Xian S, Zanetti M, Carter H. Elevated neoantigen levels in tumors with somatic mutations in the HLA-A, HLA-B, HLA-C and B2M genes. BMC Med Genomics. 2019;12:107.

46. Le DT, Durham JN, Smith KN, Wang H, Bartlett BR, Aulakh LK, et al. Mismatch repair deficiency predicts response of solid tumors to PD-1 blockade. Science. American Association for the Advancement of Science; 2017;357:409–13.

47. Sade-Feldman M, Jiao YJ, Chen JH, Rooney MS, Barzily-Rokni M, Eliane J-P, et al. Resistance to checkpoint blockade therapy through inactivation of antigen presentation. Nat Commun [Internet]. 2017 [cited 2021 Jan 12];8. Available from: https://www.ncbi.nlm.nih.gov/pmc/articles/PMC5656607/

48. Spel L, Nieuwenhuis J, Haarsma R, Stickel E, Bleijerveld OB, Altelaar M, et al. Nedd4-Binding Protein 1 and TNFAIP3-Interacting Protein 1 Control MHC-1 Display in Neuroblastoma. Cancer Res. 2018;78:6621–31.

49. Yan Y, Zheng L, Du Q, Yan B, Geller DA. Interferon regulatory factor 1 (IRF-1) and IRF-2 regulate PD-L1 expression in hepatocellular carcinoma (HCC) cells. Cancer Immunol Immunother. 2020;69:1891–903.

50. Kriegsman BA, Vangala P, Chen BJ, Meraner P, Brass AL, Garber M, et al. Frequent Loss of IRF2 in Cancers Leads to Immune Evasion through Decreased MHC Class I Antigen Presentation and Increased PD-L1 Expression. The Journal of Immunology. American Association of Immunologists; 2019;203:1999–2010.

51. Burr ML, Sparbier CE, Chan KL, Chan Y-C, Kersbergen A, Lam EYN, et al. An Evolutionarily Conserved Function of Polycomb Silences the MHC Class I Antigen Presentation Pathway and Enables Immune Evasion in Cancer. Cancer Cell. 2019;36:385-401.e8.

52. Ye Q, Shen Y, Wang X, Yang J, Miao F, Shen C, et al. Hypermethylation of HLA class I gene is associated with HLA class I down-regulation in human gastric cancer. Tissue Antigens. 2010;75:30–9.

53. Nie Y, Yang G, Song Y, Zhao X, So C, Liao J, et al. DNA hypermethylation is a mechanism for loss of expression of the HLA class I genes in human esophageal squamous cell carcinomas. Carcinogenesis. 2001;22:1615–23.

54. Cho SX, Vijayan S, Yoo J-S, Watanabe T, Ouda R, An N, et al. MHC class I transactivator NLRC5 in host immunity, cancer and beyond. Immunology. 2021;162:252–61.

55. Yoshihama S, Cho SX, Yeung J, Pan X, Lizee G, Konganti K, et al. NLRC5/CITA expression correlates with efficient response to checkpoint blockade immunotherapy. Sci Rep. Nature Publishing Group; 2021;11:3258.

56. Luo N, Nixon MJ, Gonzalez-Ericsson PI, Sanchez V, Opalenik SR, Li H, et al. DNA methyltransferase inhibition upregulates MHC-I to potentiate cytotoxic T lymphocyte responses in breast cancer. Nat Commun [Internet]. 2018 [cited 2021 Jan 7];9. Available from: https://www.ncbi.nlm.nih.gov/pmc/articles/PMC5770411/

57. Fonsatti E, Nicolay HJM, Sigalotti L, Calabrò L, Pezzani L, Colizzi F, et al. Functional up-regulation of human leukocyte antigen class I antigens expression by 5-aza-2'-deoxycytidine in cutaneous melanoma: immunotherapeutic implications. Clin Cancer Res. 2007;13:3333–8.

58. Srivastava P, Paluch BE, Matsuzaki J, James SR, Collamat-Lai G, Taverna P, et al. Immunomodulatory action of the DNA methyltransferase inhibitor SGI-110 in epithelial ovarian cancer cells and xenografts. Epigenetics. Taylor & Francis; 2015;10:237–46.

59. Saleh MH, Wang L, Goldberg MS. Improving cancer immunotherapy with DNA methyltransferase inhibitors. Cancer Immunol Immunother. 2016;65:787–96.

60. Moufarrij S, Srivastava A, Gomez S, Hadley M, Palmer E, Austin PT, et al. Combining DNMT and HDAC6 inhibitors increases anti-tumor immune signaling and decreases tumor burden in ovarian cancer. Sci Rep. 2020;10:3470.

61. Siebenkäs C, Chiappinelli KB, Guzzetta AA, Sharma A, Jeschke J, Vatapalli R, et al. Inhibiting DNA methylation activates cancer testis antigens and expression of the antigen processing and presentation machinery in colon and ovarian cancer cells. PLOS ONE. Public Library of Science; 2017;12:e0179501.

62. Glozak MA, Seto E. Histone deacetylases and cancer. Oncogene. Nature Publishing Group; 2007;26:5420–32.

63. Sun T, Li Y, Yang W, Wu H, Li X, Huang Y, et al. Histone deacetylase inhibition up-regulates MHC class I to facilitate cytotoxic T lymphocyte-mediated tumor cell killing in glioma cells. J Cancer. 2019;10:5638–45.

64. Mora-García M de L, Duenas-González A, Hernández-Montes J, De la Cruz-Hernández E, Pérez-Cárdenas E, Weiss-Steider B, et al. Up-regulation of HLA class-I antigen expression and antigen-specific CTL response in cervical cancer cells by the demethylating agent hydralazine and the histone deacetylase inhibitor valproic acid. J Transl Med. 2006;4:55.

65. Suraweera A, O'Byrne KJ, Richard DJ. Combination Therapy with Histone Deacetylase Inhibitors (HDACi) for the Treatment of Cancer: Achieving the Full Therapeutic Potential of HDACi. Front Oncol. 2018;8:92.

66. Lazaridou M-F, Gonschorek E, Massa C, Friedrich M, Handke D, Mueller A, et al. Identification of miR-200a-5p targeting the peptide transporter TAP1 and its association with the clinical outcome of melanoma patients. OncoImmunology. Taylor & Francis; 2020;9:1774323.

67. Mari L, Hoefnagel SJM, Zito D, van de Meent M, van Endert P, Calpe S, et al. microRNA 125a Regulates MHC-I Expression on Esophageal Adenocarcinoma Cells, Associated with Suppression of Antitumor Immune Response and Poor Outcomes of Patients. Gastroenterology. 2018;155:784–98.

68. Colangelo T, Polcaro G, Ziccardi P, Pucci B, Muccillo L, Galgani M, et al. Proteomic screening identifies calreticulin as a miR-27a direct target repressing MHC class I cell surface exposure in colorectal cancer. Cell Death Dis. 2016;7:e2120–e2120.

69. Yi M, Xu L, Jiao Y, Luo S, Li A, Wu K. The role of cancer-derived microRNAs in cancer immune escape. Journal of Hematology & Oncology. 2020;13:25.

70. Ribas A, Wolchok JD. Cancer immunotherapy using checkpoint blockade. Science. American Association for the Advancement of Science; 2018;359:1350–5.

71. Leach DR, Krummel MF, Allison JP. Enhancement of Antitumor Immunity by CTLA-4 Blockade. Science [Internet]. American Association for the Advancement of Science; 1996 [cited 2022 Jan 19]; Available from: https://www.science.org/doi/abs/10.1126/science.271.5256.1734

72. Bai R, Chen N, Li L, Du N, Bai L, Lv Z, et al. Mechanisms of Cancer Resistance to Immunotherapy. Front Oncol [Internet]. 2020 [cited 2021 May 18];10. Available from: https://www.ncbi.nlm.nih.gov/pmc/articles/PMC7425302/

73. Postow MA, Sidlow R, Hellmann MD. Immune-Related Adverse Events Associated with Immune Checkpoint Blockade. New England Journal of Medicine. Massachusetts Medical Society; 2018;378:158–68.

74. Lee JH, Shklovskaya E, Lim SY, Carlino MS, Menzies AM, Stewart A, et al. Transcriptional downregulation of MHC class I and melanoma de- differentiation in resistance to PD-1 inhibition. Nat Commun [Internet]. 2020 [cited 2021 Jan 12];11. Available from: https://www.ncbi.nlm.nih.gov/pmc/articles/PMC7171183/

75. Lauss M, Donia M, Harbst K, Andersen R, Mitra S, Rosengren F, et al. Mutational and putative neoantigen load predict clinical benefit of adoptive T cell therapy in melanoma. Nat Commun. Nature Publishing Group; 2017;8:1738.

76. Rodig SJ, Gusenleitner D, Jackson DG, Gjini E, Giobbie-Hurder A, Jin C, et al. MHC proteins confer differential sensitivity to CTLA-4 and PD-1 blockade in untreated metastatic melanoma. Science Translational Medicine [Internet]. American Association for the Advancement of Science; 2018 [cited 2021 Jun 14];10. Available from: https://stm.sciencemag.org/content/10/450/eaar3342

77. Paulson KG, Voillet V, McAfee MS, Hunter DS, Wagener FD, Perdicchio M, et al. Acquired cancer resistance to combination immunotherapy from transcriptional loss of class I HLA. Nat Commun. 2018;9:3868.

78. Roerden M, Nelde A, Heitmann JS, Klein R, Rammensee H-G, Bethge WA, et al. HLA Evolutionary Divergence as a Prognostic Marker for AML Patients Undergoing Allogeneic Stem Cell Transplantation. Cancers. Multidisciplinary Digital Publishing Institute; 2020;12:1835.

79. Gurjao C, Liu D, Hofree M, AlDubayan SH, Wakiro I, Su M-J, et al. Intrinsic Resistance to Immune Checkpoint Blockade in a Mismatch Repair–Deficient Colorectal Cancer. Cancer Immunol Res. American Association for Cancer Research; 2019;7:1230–6.

80. Grasso CS, Giannakis M, Wells DK, Hamada T, Mu XJ, Quist M, et al. Genetic Mechanisms of Immune Evasion in Colorectal Cancer. Cancer Discov. American Association for Cancer Research; 2018;8:730–49.

81. Shin DS, Zaretsky JM, Escuin-Ordinas H, Garcia-Diaz A, Hu-Lieskovan S, Kalbasi A, et al. Primary Resistance to PD-1 Blockade Mediated by JAK1/2 Mutations. Cancer Discov. American Association for Cancer Research; 2017;7:188–201.

82. Luo N, Formisano L, Gonzalez-Ericsson PI, Sanchez V, Dean PT, Opalenik SR, et al. Melanoma response to anti-PD-L1 immunotherapy requires JAK1 signaling, but not JAK2. Oncoimmunology [Internet]. 2018 [cited 2021 Jun 14];7. Available from: https://www.ncbi.nlm.nih.gov/pmc/articles/PMC5975601/

83. Chew G-L, Campbell AE, De Neef E, Sutliff NA, Shadle SC, Tapscott SJ, et al. DUX4 suppresses MHC Class I to promote cancer immune evasion and resistance to checkpoint blockade. Dev Cell. 2019;50:658-671.e7.

84. Manguso RT, Pope HW, Zimmer MD, Brown FD, Yates KB, Miller BC, et al. In vivo CRISPR screening identifies Ptpn2 as a cancer immunotherapy target. Nature. Nature Publishing Group; 2017;547:413–8.

85. Zhao Y, Cao Y, Chen Y, Wu L, Hang H, Jiang C, et al. B2M gene expression shapes the immune landscape of lung adenocarcinoma and determines the response to immunotherapy. Immunology [Internet]. [cited 2021 Jun 14];n/a. Available from: https://onlinelibrary.wiley.com/doi/abs/10.1111/imm.13384

86. Propper DJ, Chao D, Braybrooke JP, Bahl P, Thavasu P, Balkwill F, et al. Low-Dose IFN-γ Induces Tumor MHC Expression in Metastatic Malignant Melanoma. Clin Cancer Res. American Association for Cancer Research; 2003;9:84–92.

87. Shukla A, Cloutier M, Appiya Santharam M, Ramanathan S, Ilangumaran S. The MHC Class-I Transactivator NLRC5: Implications to Cancer Immunology and Potential Applications to Cancer Immunotherapy. International Journal of Molecular Sciences. Multidisciplinary Digital Publishing Institute; 2021;22:1964.

88. Zhao M-Z, Sun Y, Jiang X-F, Liu L, Liu L, Sun L-X. Promotion on NLRC5 upregulating MHC-I expression by IFN-γ in MHC-I–deficient breast cancer cells. Immunol Res. 2019;67:497–504.

89. George PM, Badiger R, Alazawi W, Foster GR, Mitchell JA. Pharmacology and therapeutic potential of interferons. Pharmacology & Therapeutics. 2012;135:44–53.

90. Hemmerle T, Neri D. The Dose-Dependent Tumor Targeting of Antibody–IFNγ Fusion Proteins Reveals an Unexpected Receptor-Trapping Mechanism In Vivo. Cancer Immunol Res. American Association for Cancer Research; 2014;2:559–67.

91. Segars JH, Nagata T, Bours V, Medin JA, Franzoso G, Blanco JC, et al. Retinoic acid induction of major histocompatibility complex class I genes in NTera-2 embryonal carcinoma cells involves induction of NF-kappa B (p50-p65) and retinoic acid receptor beta-retinoid X receptor beta heterodimers. Mol Cell Biol. 1993;13:6157–69.

92. Farina AR, Masciulli M-P, Tacconelli A, Cappabianca L, De Santis G, Gulino A, et al. All-trans-retinoic acid induces nuclear factor kappaB activation and matrix metalloproteinase-9 expression and enhances basement membrane invasivity of differentiation-resistant human SK-N-BE 9N neuroblastoma Cells. Cell Growth Differ. 2002;13:343–54.

93. Kalbasi A, Tariveranmoshabad M, Hakimi K, Kremer S, Campbell KM, Funes JM, et al. Uncoupling interferon signaling and antigen presentation to overcome immunotherapy resistance due to JAK1 loss in melanoma. Science Translational Medicine [Internet]. American Association for the Advancement of Science; 2020 [cited 2022 Jan 19]; Available from: https://www.science.org/doi/abs/10.1126/scitranslmed.abb0152

94. Gu SS, Zhang W, Wang X, Jiang P, Traugh N, Li Z, et al. Therapeutically increasing MHC-I expression potentiates immune checkpoint blockade. Cancer Discov [Internet]. American Association for Cancer Research; 2021 [cited 2021 Feb 23]; Available from: https://cancerdiscovery.aacrjournals.org/content/early/2021/02/15/2159-8290.CD-20-0812

95. Brea EJ, Oh CY, Manchado E, Budhu S, Gejman RS, Mo G, et al. Kinase Regulation of Human MHC Class I Molecule Expression on Cancer Cells. Cancer Immunol Res. 2016;4:936–47.

96. Seliger B, Harders C, Lohmann S, Momburg F, Urlinger S, Tampé R, et al. Down-regulation of the MHC class I antigen-processing machinery after oncogenic transformation of murine fibroblasts. European Journal of Immunology. 1998;28:122–33.

97. Loi S, Dushyanthen S, Beavis PA, Salgado R, Denkert C, Savas P, et al. RAS/MAPK Activation Is Associated with Reduced Tumor-Infiltrating Lymphocytes in Triple-Negative Breast Cancer: Therapeutic Cooperation Between MEK and PD-1/PD-L1 Immune Checkpoint Inhibitors. Clin Cancer Res. 2016;22:1499–509.

98. Franklin DA, James JL, Axelrod ML, Balko JM. MEK inhibition activates STAT signaling to increase breast cancer immunogenicity via MHC-I expression. Cancer Drug Resist. 2020;3:603–12.

99. Lulli D, Carbone ML, Pastore S. The MEK Inhibitors Trametinib and Cobimetinib Induce a Type I Interferon Response in Human Keratinocytes. International Journal of Molecular Sciences. Multidisciplinary Digital Publishing Institute; 2017;18:2227.

100. Hastings K, Yu HA, Wei W, Sanchez-Vega F, DeVeaux M, Choi J, et al. EGFR mutation subtypes and response to immune checkpoint blockade treatment in non-small-cell lung cancer. Annals of Oncology. 2019;30:1311–20.

101. Meric-Bernstam F, Sandhu SK, Hamid O, Spreafico A, Kasper S, Dummer R, et al. Phase Ib study of MIW815 (ADU-S100) in combination with spartalizumab (PDR001) in patients (pts) with advanced/metastatic solid tumors or lymphomas. JCO. Wolters Kluwer; 2019;37:2507–2507.

102. Inoue M, Mimura K, Izawa S, Shiraishi K, Inoue A, Shiba S, et al. Expression of MHC Class I on breast cancer cells correlates inversely with HER2 expression. Oncoimmunology. 2012;1:1104–10.

103. Mimura K, Ando T, Poschke I, Mougiakakos D, Johansson CC, Ichikawa J, et al. T cell recognition of HLA-A2 restricted tumor antigens is impaired by the oncogene HER2. International Journal of Cancer. 2011;128:390–401.

104. Garrido G, Rabasa A, Garrido C, Chao L, Garrido F, García-Lora ÁM, et al. Upregulation of HLA Class I Expression on Tumor Cells by the Anti-EGFR Antibody Nimotuzumab. Front Pharmacol. 2017;8:595.

105. Srivastava RM, Trivedi S, Concha-Benavente F, Hyun-bae J, Wang L, Seethala RR, et al. STAT1-Induced HLA Class I Upregulation Enhances Immunogenicity and Clinical Response to Anti-EGFR mAb Cetuximab Therapy in HNC Patients. Cancer Immunol Res. 2015;3:936–45.

106. Pollack BP, Sapkota B, Cartee TV. Epidermal Growth Factor Receptor Inhibition Augments the Expression of MHC Class I and II Genes. Clin Cancer Res. 2011;17:4400–13.

107. Yamamoto K, Venida A, Yano J, Biancur DE, Kakiuchi M, Gupta S, et al. Autophagy promotes immune evasion of pancreatic cancer by degrading MHC-I. Nature. Nature Publishing Group; 2020;581:100–5.

108. Fang Y, Wang L, Wan C, Sun Y, Jeught KV der, Zhou Z, et al. MAL2 drives immune evasion in breast cancer by suppressing tumor antigen presentation. J Clin Invest [Internet]. American Society for Clinical Investigation; 2021 [cited 2021 Jun 21];131. Available from: https://www.jci.org/articles/view/140837#SEC2

109. Kobayashi M, Nagashio R, Jiang S-X, Saito K, Tsuchiya B, Ryuge S, et al. Calnexin is a novel sero-diagnostic marker for lung cancer. Lung Cancer. 2015;90:342–5.

110. Okayama A, Miyagi Y, Oshita F, Nishi M, Nakamura Y, Nagashima Y, et al. Proteomic Analysis of Proteins Related to Prognosis of Lung Adenocarcinoma. J Proteome Res. American Chemical Society; 2014;13:4686–94.

111. Alam A, Taye N, Patel S, Thube M, Mullick J, Shah VK, et al. SMAR1 favors immunosurveillance of cancer cells by modulating calnexin and MHC I expression. Neoplasia. 2019;21:945–62.

112. Hodge JW, Garnett CT, Farsaci B, Palena C, Tsang K-Y, Ferrone S, et al. Chemotherapy-induced immunogenic modulation of tumor cells enhances killing by cytotoxic T lymphocytes and is distinct from immunogenic cell death. International Journal of Cancer. 2013;133:624–36.

113. Tseng C-W, Hung C-F, Alvarez RD, Trimble C, Huh WK, Kim D, et al. Pretreatment with Cisplatin Enhances E7-Specific CD8+ T-Cell–Mediated Antitumor Immunity Induced by DNA Vaccination. Clin Cancer Res. American Association for Cancer Research; 2008;14:3185–92.

114. Iwai T, Sugimoto M, Wakita D, Yorozu K, Kurasawa M, Yamamoto K. Topoisomerase I inhibitor, irinotecan, depletes regulatory T cells and up-regulates MHC class I and PD-L1 expression, resulting in a supra-additive antitumor effect when combined with anti-PD-L1 antibodies. Oncotarget. 2018;9:31411–21.

115. Varn FS, Wang Y, Mullins DW, Fiering S, Cheng C. Systematic Pan-Cancer Analysis Reveals Immune Cell Interactions in the Tumor Microenvironment. Cancer Research. 2017;77:1271–82.

116. Cózar B, Greppi M, Carpentier S, Narni-Mancinelli E, Chiossone L, Vivier E. Tumor-Infiltrating Natural Killer Cells. Cancer Discovery. 2021;11:34–44.

117. Cursons J, Souza-Fonseca-Guimaraes F, Foroutan M, Anderson A, Hollande F, Hediyeh-Zadeh S, et al. A Gene Signature Predicting Natural Killer Cell Infiltration and Improved Survival in Melanoma Patients. Cancer Immunology Research. 2019;7:1162–74.

118. Seaman WE, Sleisenger M, Eriksson E, Koo GC. Depletion of natural killer cells in mice by monoclonal antibody to NK-1.1. Reduction in host defense against malignancy without loss of cellular or humoral immunity. The Journal of Immunology. 1987;138:4539–44.

119. Street SEA, Hayakawa Y, Zhan Y, Lew AM, MacGregor D, Jamieson AM, et al. Innate Immune Surveillance of Spontaneous B Cell Lymphomas by Natural Killer Cells and γδ T Cells. Journal of Experimental Medicine. 2004;199:879–84.

120. Cerwenka A, Baron JL, Lanier LL. Ectopic expression of retinoic acid early inducible-1 gene (RAE-1) permits natural killer cell-mediated rejection of an MHC class I-bearing tumor in vivo. Proceedings of the National Academy of Sciences. Proceedings of the National Academy of Sciences; 2001;98:11521–6.

121. Gao Y, Souza-Fonseca-Guimaraes F, Bald T, Ng SS, Young A, Ngiow SF, et al. Tumor immunoevasion by the conversion of effector NK cells into type 1 innate lymphoid cells. Nat Immunol. Nature Publishing Group; 2017;18:1004–15.

122. Joncker NT, Shifrin N, Delebecque F, Raulet DH. Mature natural killer cells reset their responsiveness when exposed to an altered MHC environment. Journal of Experimental Medicine. 2010;207:2065–72.

123. Sun JC, Lanier LL. NK cell development, homeostasis, and function: parallels with CD8+ T cells. Nat Rev Immunol. Nature Publishing Group; 2011;11:645–57.

124. Raulet DH. Missing self recognition and self tolerance of natural killer (NK) cells. Seminars in Immunology. 2006;18:145–50.

125. Pende D, Falco M, Vitale M, Cantoni C, Vitale C, Munari E, et al. Killer Ig-Like Receptors (KIRs): Their Role in NK Cell Modulation and Developments Leading to Their Clinical Exploitation. Frontiers in Immunology [Internet]. 2019 [cited 2024 Jan 19];10. Available from: https://www.frontiersin.org/articles/10.3389/fimmu.2019.01179

126. Carlyle JR, Mesci A, Fine JH, Chen P, Bélanger S, Tai L-H, et al. Evolution of the Ly49 and Nkrp1 recognition systems. Seminars in Immunology. 2008;20:321–30.

127. Johansson S, Johansson M, Rosmaraki E, Vahlne G, Mehr R, Salmon-Divon M, et al. Natural killer cell education in mice with single or multiple major histocompatibility complex class I molecules. Journal of Experimental Medicine. 2005;201:1145–55.

128. Lin Z, Bashirova AA, Viard M, Garner L, Quastel M, Beiersdorfer M, et al. HLA class I signal peptide polymorphism determines the level of CD94/NKG2–HLA-E-mediated regulation of effector cell responses. Nat Immunol. Nature Publishing Group; 2023;24:1087–97.

129. Bianchini G, De Angelis C, Licata L, Gianni L. Treatment landscape of triple-negative breast cancer — expanded options, evolving needs. Nat Rev Clin Oncol. Nature Publishing Group; 2022;19:91–113.

130. Heeke AL, Tan AR. Checkpoint inhibitor therapy for metastatic triple-negative breast cancer. Cancer Metastasis Rev. 2021;40:537–47.

131. Cortes J, Rugo HS, Cescon DW, Im S-A, Yusof MM, Gallardo C, et al. Pembrolizumab plus Chemotherapy in Advanced Triple-Negative Breast Cancer. New England Journal of Medicine. Massachusetts Medical Society; 2022;387:217–26.

132. Tolaney SM, Kalinsky K, Kaklamani VG, D'Adamo DR, Aktan G, Tsai ML, et al. Eribulin Plus Pembrolizumab in Patients with Metastatic Triple-Negative Breast Cancer (ENHANCE 1): A Phase Ib/II Study. Clinical Cancer Research. 2021;27:3061–8.

133. Schmid P, Adams S, Rugo HS, Schneeweiss A, Barrios CH, Iwata H, et al. Atezolizumab and Nab-Paclitaxel in Advanced Triple-Negative Breast Cancer. New England Journal of Medicine. Massachusetts Medical Society; 2018;379:2108–21.

134. Miles D, Gligorov J, André F, Cameron D, Schneeweiss A, Barrios C, et al. Primary results from IMpassion131, a double-blind, placebo-controlled, randomised phase III trial

of first-line paclitaxel with or without atezolizumab for unresectable locally advanced/metastatic triple-negative breast cancer. Annals of Oncology. Elsevier; 2021;32:994–1004.

135. Wang H, Yee D. I-SPY 2: a Neoadjuvant Adaptive Clinical Trial Designed to Improve Outcomes in High-Risk Breast Cancer. Curr Breast Cancer Rep. 2019;11:303–10.

136. Schmid P, Cortes J, Pusztai L, McArthur H, Kümmel S, Bergh J, et al. Pembrolizumab for Early Triple-Negative Breast Cancer. New England Journal of Medicine [Internet]. Massachusetts Medical Society; 2020 [cited 2020 Aug 11]; Available from: https://www.nejm.org/doi/10.1056/NEJMoa1910549?url_ver=Z39.88-2003&rfr_id=ori%3Arid%3Acrossref.org&rfr_dat=cr_pub++0pubmed

137. Sharma P, Allison JP. Immune Checkpoint Targeting in Cancer Therapy: Toward Combination Strategies with Curative Potential. Cell. 2015;161:205–14.

138. Cortes J, Cescon DW, Rugo HS, Nowecki Z, Im S-A, Yusof MM, et al. Pembrolizumab plus chemotherapy versus placebo plus chemotherapy for previously untreated locally recurrent inoperable or metastatic triple-negative breast cancer (KEYNOTE-355): a randomised, placebo-controlled, double-blind, phase 3 clinical trial. The Lancet. 2020;396:1817–28.

139. Schmid P, Cortes J, Dent R, Pusztai L, McArthur H, Kümmel S, et al. Event-free Survival with Pembrolizumab in Early Triple-Negative Breast Cancer. New England Journal of Medicine. Massachusetts Medical Society; 2022;386:556–67.

140. Nanda R, Liu MC, Yau C, Shatsky R, Pusztai L, Wallace A, et al. Effect of Pembrolizumab Plus Neoadjuvant Chemotherapy on Pathologic Complete Response in Women with Early-Stage Breast Cancer: An Analysis of the Ongoing Phase 2 Adaptively Randomized I-SPY2 Trial. JAMA Oncology. 2020;6:676–84.

141. Mittendorf EA, Zhang H, Barrios CH, Saji S, Jung KH, Hegg R, et al. Neoadjuvant atezolizumab in combination with sequential nab-paclitaxel and anthracycline-based chemotherapy versus placebo and chemotherapy in patients with early-stage triple-negative breast cancer (IMpassion031): a randomised, double-blind, phase 3 trial. The Lancet. 2020;396:1090–100.

142. Loibl S, Untch M, Burchardi N, Huober J, Sinn BV, Blohmer J-U, et al. A randomised phase II study investigating durvalumab in addition to an anthracycline taxane-based neoadjuvant therapy in early triple-negative breast cancer: clinical results and biomarker analysis of GeparNuevo study. Annals of Oncology. 2019;30:1279–88.

143. Sharma P, Hu-Lieskovan S, Wargo JA, Ribas A. Primary, Adaptive, and Acquired Resistance to Cancer Immunotherapy. Cell. 2017;168:707–23.

144. Taylor BC, Balko JM. Mechanisms of MHC-I Downregulation and Role in Immunotherapy Response. Frontiers in Immunology [Internet]. 2022 [cited 2022 Jul 25];13. Available from: https://www.frontiersin.org/articles/10.3389/fimmu.2022.844866

145. Torrejon DY, Abril-Rodriguez G, Champhekar AS, Tsoi J, Campbell KM, Kalbasi A, et al. Overcoming Genetically Based Resistance Mechanisms to PD-1 Blockade. Cancer Discovery. 2020;10:1140–57.

146. Gettinger S, Choi J, Hastings K, Truini A, Datar I, Sowell R, et al. Impaired HLA Class I Antigen Processing and Presentation as a Mechanism of Acquired Resistance to Immune Checkpoint Inhibitors in Lung Cancer. Cancer Discov. 2017;7:1420–35.

147. Goodman AM, Castro A, Pyke RM, Okamura R, Kato S, Riviere P, et al. MHC-I genotypes, and tumor mutational burden predict response to immunotherapy. Genome Medicine. 2020;12:45.

148. McGranahan N, Rosenthal R, Hiley CT, Rowan AJ, Watkins TBK, Wilson GA, et al. Allele-Specific HLA Loss and Immune Escape in Lung Cancer Evolution. Cell. 2017;171:1259-1271.e11.

149. Sivapalan L, Anagnostou V. Genetic variation in antigen presentation and cancer immunotherapy. Immunity. 2022;55:3–6.

150. Garcia-Recio S, Hinoue T, Wheeler GL, Kelly BJ, Garrido-Castro AC, Pascual T, et al. Multiomics in primary and metastatic breast tumors from the AURORA US network finds microenvironment and epigenetic drivers of metastasis. Nat Cancer. Nature Publishing Group; 2023;4:128–47.

151. Cindy Yang SY, Lien SC, Wang BX, Clouthier DL, Hanna Y, Cirlan I, et al. Pan-cancer analysis of longitudinal metastatic tumors reveals genomic alterations and immune landscape dynamics associated with pembrolizumab sensitivity. Nat Commun. Nature Publishing Group; 2021;12:5137.

152. Dusenbery AC, Maniaci JL, Hillerson ND, Dill EA, Bullock TN, Mills AM. MHC Class I Loss in Triple-negative Breast Cancer: A Potential Barrier to PD-1/PD-L1 Checkpoint Inhibitors. The American Journal of Surgical Pathology. 2021;45:701.

153. Kaneko K, Ishigami S, Kijima Y, Funasako Y, Hirata M, Okumura H, et al. Clinical implication of HLA class I expression in breast cancer. BMC Cancer. 2011;11:454.

154. Hartigan JA, Hartigan PM. The Dip Test of Unimodality. The Annals of Statistics. Institute of Mathematical Statistics; 1985;13:70–84.

155. Carretero FJ, del Campo AB, Flores-Martín JF, Mendez R, García-Lopez C, Cozar JM, et al. Frequent HLA class I alterations in human prostate cancer: molecular mechanisms and clinical relevance. Cancer Immunol Immunother. 2016;65:47–59.

156. Aptsiauri N, Garrido F. The Challenges of HLA Class I Loss in Cancer Immunotherapy: Facts and Hopes. Clinical Cancer Research. 2022;28:5021–9.

157. Paschen A, Méndez RM, Jimenez P, Sucker A, Ruiz-Cabello F, Song M, et al. Complete loss of HLA class I antigen expression on melanoma cells: A result of successive mutational events. International Journal of Cancer. 2003;103:759–67.

158. Garrido F, Ruiz-Cabello F, Aptsiauri N. Rejection versus escape: the tumor MHC dilemma. Cancer Immunol Immunother. 2017;66:259–71.

159. Garrod KR, Wei SH, Parker I, Cahalan MD. Natural killer cells actively patrol peripheral lymph nodes forming stable conjugates to eliminate MHC-mismatched targets. Proceedings of the National Academy of Sciences. Proceedings of the National Academy of Sciences; 2007;104:12081–6.

160. Coombes JL, Han S-J, van Rooijen N, Raulet DH, Robey EA. Infection-Induced Regulation of Natural Killer Cells by Macrophages and Collagen at the Lymph Node Subcapsular Sinus. Cell Reports. 2012;2:124–35.

161. Bunting MD, Vyas M, Requesens M, Langenbucher A, Schiferle EB, Manguso RT, et al. Extracellular matrix proteins regulate NK cell function in peripheral tissues. Science Advances. American Association for the Advancement of Science; 2022;8:eabk3327.

162. Jiang S, Munker R, Andreeff M. Bcl-2 is expressed in human natural killer cells and is regulated by interleukin-2. Nat Immun. 1996;15:312–7.

163. Böttcher JP, Bonavita E, Chakravarty P, Blees H, Cabeza-Cabrerizo M, Sammicheli S, et al. NK Cells Stimulate Recruitment of cDC1 into the Tumor Microenvironment Promoting Cancer Immune Control. Cell. 2018;172:1022-1037.e14.

164. Barry KC, Hsu J, Broz ML, Cueto FJ, Binnewies M, Combes AJ, et al. A natural killer–dendritic cell axis defines checkpoint therapy–responsive tumor microenvironments. Nat Med. Nature Publishing Group; 2018;24:1178–91.

165. Yang Y, Yang HH, Hu Y, Watson PH, Liu H, Geiger TR, et al. Immunocompetent mouse allograft models for development of therapies to target breast cancer metastasis. Oncotarget. Impact Journals; 2017;8:30621–43.

166. Wu SZ, Al-Eryani G, Roden DL, Junankar S, Harvey K, Andersson A, et al. A single-cell and spatially resolved atlas of human breast cancers. Nat Genet. Nature Publishing Group; 2021;53:1334–47.

167. Hahsler M, Piekenbrock M, Doran D. dbscan: Fast Density-Based Clustering with R. Journal of Statistical Software. 2019;91:1–30.

168. Snyder A, Makarov V, Merghoub T, Yuan J, Zaretsky JM, Desrichard A, et al. Genetic Basis for Clinical Response to CTLA-4 Blockade in Melanoma. New England Journal of Medicine. Massachusetts Medical Society; 2014;371:2189–99.

169. Rizvi NA, Hellmann MD, Snyder A, Kvistborg P, Makarov V, Havel JJ, et al. Mutational landscape determines sensitivity to PD-1 blockade in non–small cell lung cancer. Science. American Association for the Advancement of Science; 2015;348:124–8.

170. Gao J, Shi LZ, Zhao H, Chen J, Xiong L, He Q, et al. Loss of IFN-γ Pathway Genes in Tumor Cells as a Mechanism of Resistance to Anti-CTLA-4 Therapy. Cell. 2016;167:397-404.e9.

171. Rosenthal R, Cadieux EL, Salgado R, Bakir MA, Moore DA, Hiley CT, et al. Neoantigen-directed immune escape in lung cancer evolution. Nature. Nature Publishing Group; 2019;567:479–85.

172. Liu D, Schilling B, Liu D, Sucker A, Livingstone E, Jerby-Arnon L, et al. Integrative molecular and clinical modeling of clinical outcomes to PD1 blockade in patients with metastatic melanoma. Nat Med. Nature Publishing Group; 2019;25:1916–27.

173. Myers JA, Miller JS. Exploring the NK cell platform for cancer immunotherapy. Nat Rev Clin Oncol. Nature Publishing Group; 2021;18:85–100.

174. Cerwenka A, Lanier LL. Natural killers join the fight against cancer. Science. American Association for the Advancement of Science; 2018;359:1460–1.

175. Vivier E, Ugolini S, Blaise D, Chabannon C, Brossay L. Targeting natural killer cells and natural killer T cells in cancer. Nat Rev Immunol. Nature Publishing Group; 2012;12:239–52.

176. Bern MD, Parikh BA, Yang L, Beckman DL, Poursine-Laurent J, Yokoyama WM. Inducible down-regulation of MHC class I results in natural killer cell tolerance. Journal of Experimental Medicine. 2018;216:99–116.

177. Nicolai CJ, Wolf N, Chang I-C, Kirn G, Marcus A, Ndubaku CO, et al. NK cells mediate clearance of CD8+ T cell–resistant tumors in response to STING agonists. Science Immunology. American Association for the Advancement of Science; 2020;5:eaaz2738.

178. Anfossi N, André P, Guia S, Falk CS, Roetynck S, Stewart CA, et al. Human NK Cell Education by Inhibitory Receptors for MHC Class I. Immunity. 2006;25:331–42.

179. Bunting MD, Vyas M, Requesens M, Langenbucher A, Schiferle EB, Manguso RT, et al. Extracellular matrix proteins regulate NK cell function in peripheral tissues. Sci Adv. 2022;8:eabk3327.

180. Salomé B, Sfakianos JP, Ranti D, Daza J, Bieber C, Charap A, et al. NKG2A and HLA-E define an alternative immune checkpoint axis in bladder cancer. Cancer Cell. 2022;40:1027-1043.e9.

181. van Montfoort N, Borst L, Korrer MJ, Sluijter M, Marijt KA, Santegoets SJ, et al. NKG2A blockade potentiates CD8 T-cell immunity induced by cancer vaccines. Cell. 2018;175:1744-1755.e15.

182. André P, Denis C, Soulas C, Bourbon-Caillet C, Lopez J, Arnoux T, et al. Anti-NKG2A mAb Is a Checkpoint Inhibitor that Promotes Anti-tumor Immunity by Unleashing Both T and NK Cells. Cell. 2018;175:1731-1743.e13.

183. Tumeh PC, Harview CL, Yearley JH, Shintaku IP, Taylor EJM, Robert L, et al. PD-1 blockade induces responses by inhibiting adaptive immune resistance. Nature. 2014;515:568–71.

184. Anagnostou V, Smith KN, Forde PM, Niknafs N, Bhattacharya R, White J, et al. Evolution of Neoantigen Landscape during Immune Checkpoint Blockade in Non–Small Cell Lung Cancer. Cancer Discovery. 2017;7:264–76.

185. Dhatchinamoorthy K, Colbert JD, Rock KL. Cancer Immune Evasion Through Loss of MHC Class I Antigen Presentation. Frontiers in Immunology [Internet]. 2021 [cited 2024 Feb 5];12. Available from: https://www.frontiersin.org/journals/immunology/articles/10.3389/fimmu.2021.636568

186. Johnson DB, Estrada MV, Salgado R, Sanchez V, Doxie DB, Opalenik SR, et al. Melanoma-specific MHC-II expression represents a tumour-autonomous phenotype and predicts response to anti-PD-1/PD-L1 therapy. Nat Commun. Nature Publishing Group; 2016;7:10582.

Appendices

Chapter II Appendix

Supplementary material for chapter II: Materials and methods

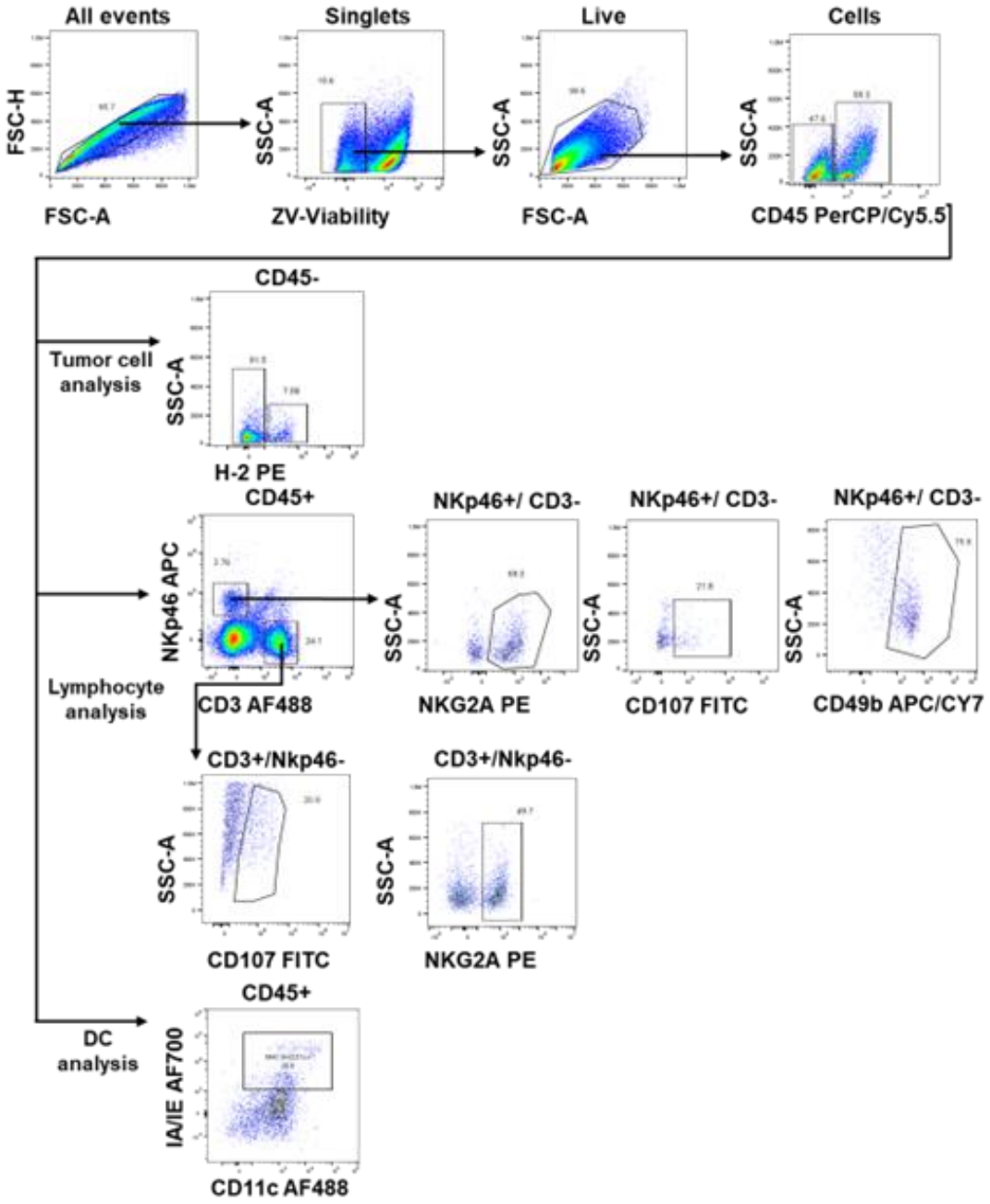

Supplementary Figure 2.1: Gating strategy for immune cell and tumor cell identification using tumor and lymphocyte-focused antibody panels.

Chapter III Appendix

Supplementary material for chapter III: Intratumor heterogeneity in MHC-I expression drives immunotherapy resistance in breast cancer

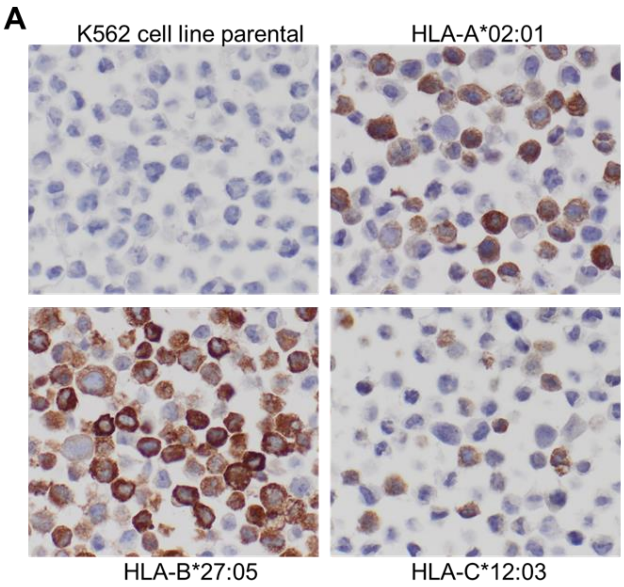

HLA Allele	Positive/Negative
Parental (K562)	Negative
HLA-B*08:01	Positive
HLA-A*24:02	Positive
HLA-A*26:01	Positive
HLA-A*03:01	Positive
HLA-B*27:05	Positive
HLA-B*35:01	Positive
HLA-B*44:02	Positive
HLA-B*44:03	Positive
HLA-B*49:01	Positive
HLA-B*53:01	Positive
HLA-B*56:01	Positive
HLA-C*01:02	Positive
HLA-C*07:01	Positive
HLA-C*12:03	Positive
HLA-A*02:01	Positive

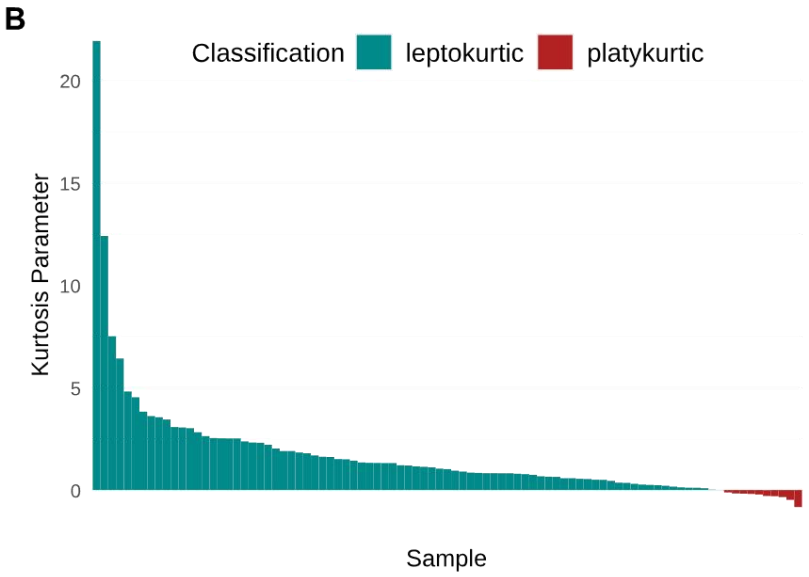

Supplementary Figure 3.1: A) Representative IHC examples of K562 cells transduced with various individual HLA alleles stained using the HLA-A C6 antibody and complete list of transduced alleles. B) Tailedness of tsMHC-I expression is measured by excess Kurtosis parameter, with parameter>0 as leptokurtic distribution and <0 as platykurtic distribution.

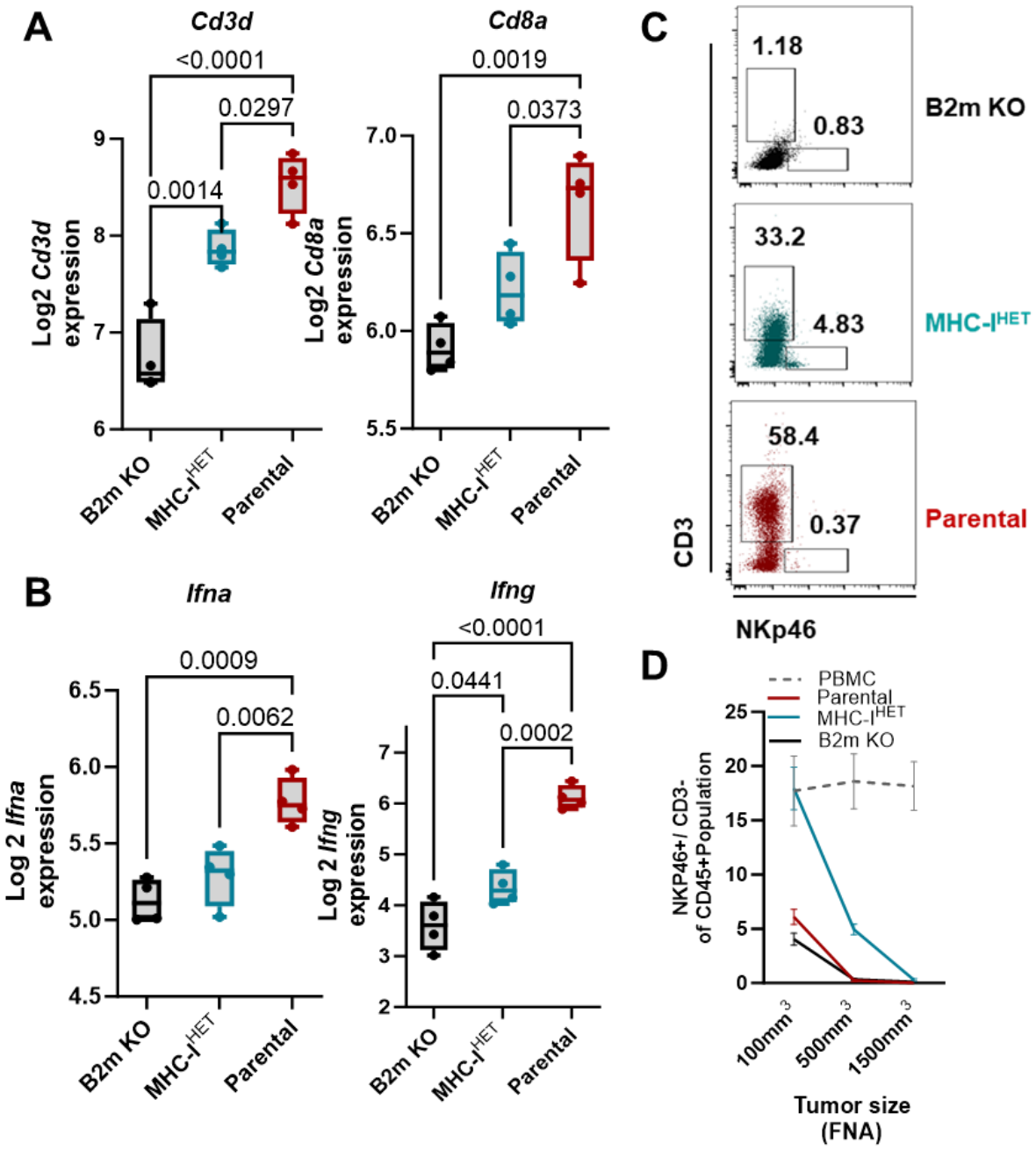

Supplementary Figure 3.4: A-B) Untreated parental, MHC-IHET, and B2m KO EMT6 tumor CD45+ tumor-infiltrating leukocytes were bead isolated, RNA was extracted, and utilized for NanoString gene expression using the PanCancer Immune Pathways codeset (>700 immune-related genes). n=4. C) . Representative NK cell and CD3+ T cell flow cytometry for CD45+ microbead-fractionated EMT6 tumors. D) Flow cytometry analysis of tumor infiltrating NK cells via non-terminal tumor sampling with FNA at various tumor sizes (100mm3, 500mm3, and 1500mm3) from untreated parental, MHC-IHET, and B2m KO EMT6 tumors. Matched NK cell levels in PBMC are included as a control. NK cells are gated on live CD45+, NKp46+, and CD3-. n= 5-8 per group. Analyzed by ANOVA followed by Tukey's post-hoc test and log-rank (Mantel-Cox) tests.

Chapter IV Appendix

Supplementary material for chapter IV: NKG2A is a therapeutic vulnerability in immunotherapy resistant MHC-I heterogenous triple-negative breast cancer

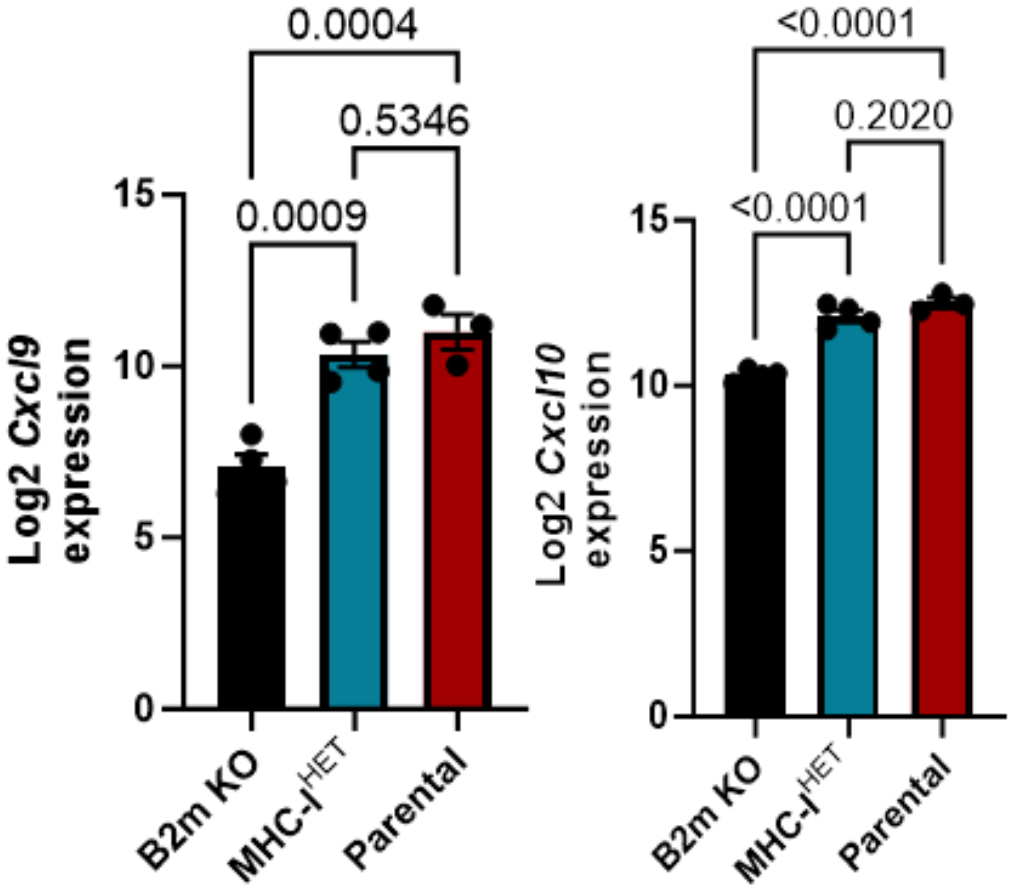

Supplementary Figure 4.1: Untreated parental, MHC-I^{HET}, and *B2m* KO EMT6 tumor CD45+ tumor-infiltrating leukocytes were bead isolated, RNA was extracted, and utilized for NanoString gene expression using the PanCancer Immune Pathways codeset (>700 immune-related genes). *n=4.*

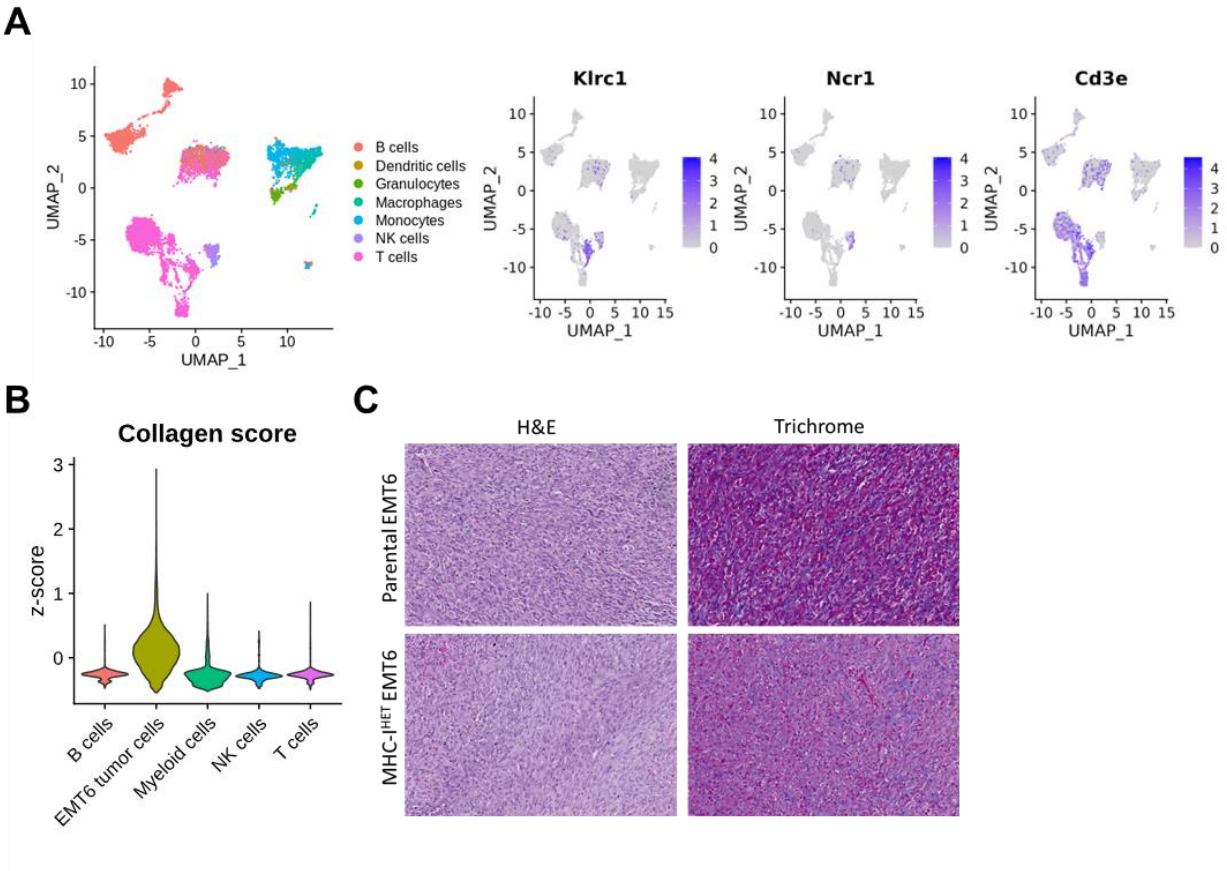

Supplementary Figure 4.2: A) The immune cell population was selected, and cell type labeling was performed using SingleR. NK cell status was confirmed based on Klrc1, Ncr1, and Cd3e expression. **B)** The z-score sum of genes encoding collagen type I/III/IV was calculated across different cell types. Among the EMT6 tumor cells, the expression of collagen genes is detected. **C)** Representative H&E and Masson's trichrome blue stains of parental and MHC-I^{HET} EMT6 tumors.

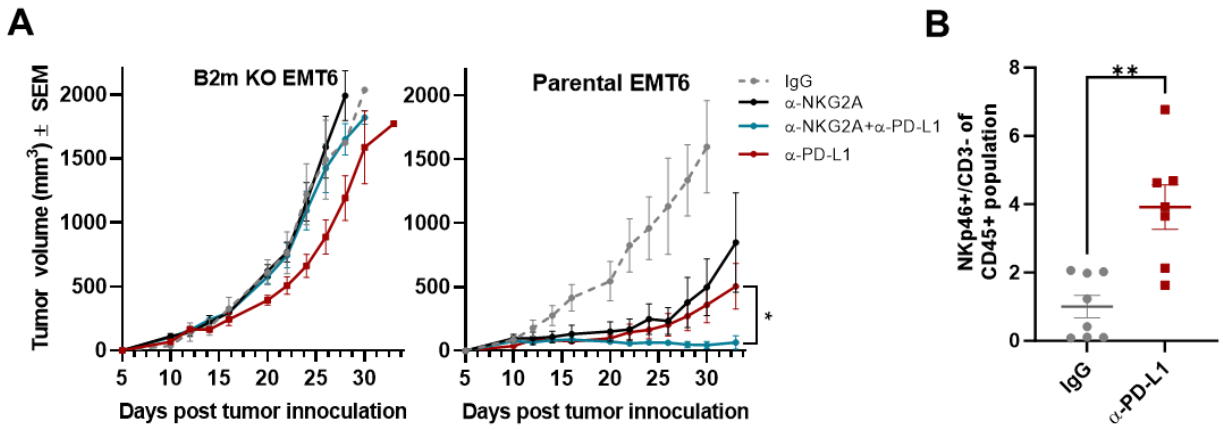

Supplementary Figure 4.3: A) Parental and *B2m* KO EMT6 tumor cells were injected subcutaneously in BALB/c mice. Mice were treated at 7-day intervals with IgG antibody, anti-PD-L1, anti-NKG2A, or a combination of anti-NKG2A and anti-PD-L1 antibodies. The data presented are representative of two independent experiments. Graphs show combined tumor growth curves and analyzed by ANOVA followed by Tukey's post-hoc test. *n=5 to 10* per group. **B)** Flow cytometry analysis of tumor infiltrating NK cells in parental EMT6 tumors treated IgG antibody or anti-PD-L1 antibody day 7 post treatment. CD45+ tumor-infiltrating leukocytes were bead isolated. NK cells are gated on live $CD45^{+}$ and $CD3^{-}$ NKp46+. Student's t test was used for comparison. Bars represent SEM.

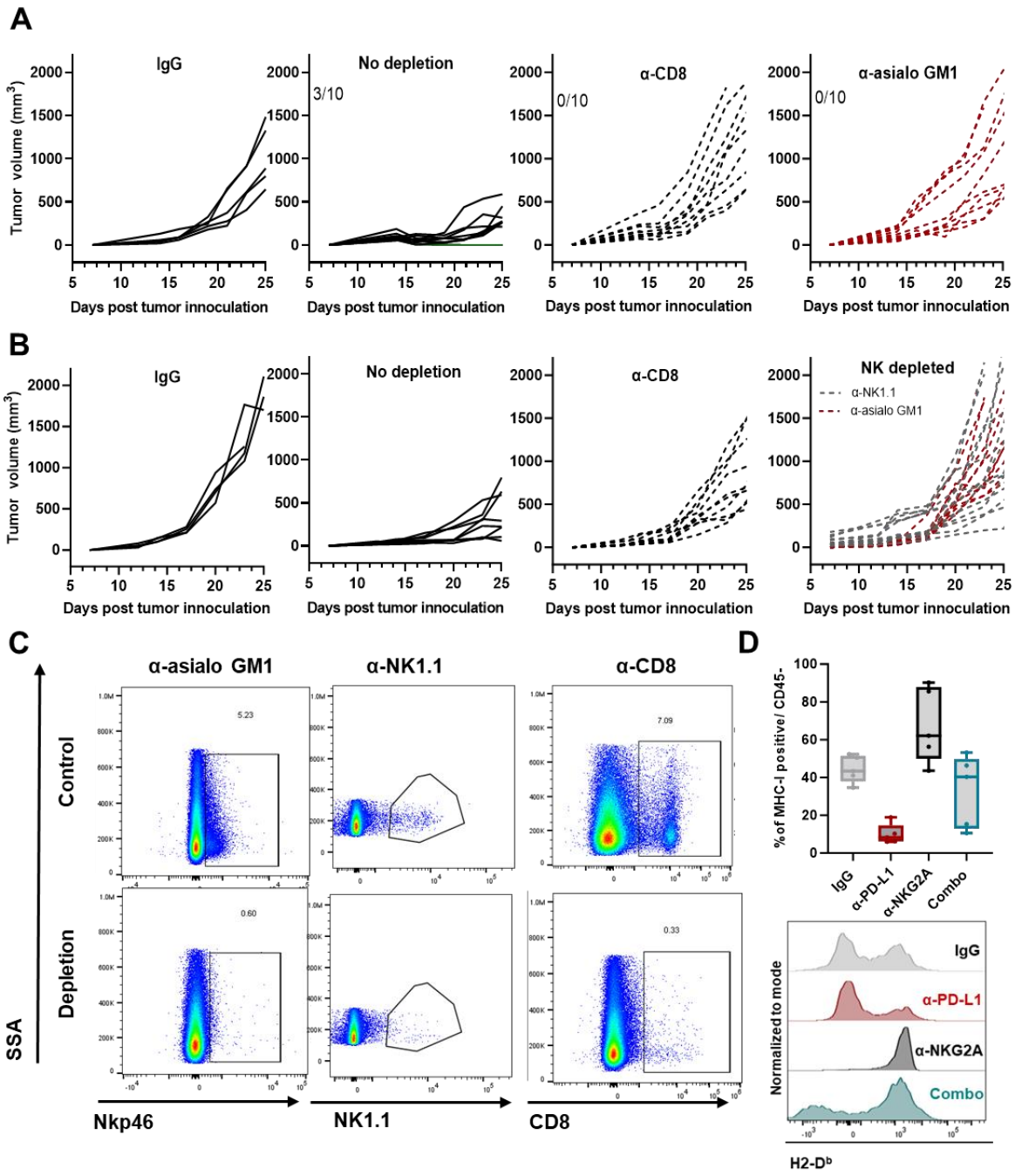

Supplementary Figure 4.4: A-B) A) MHC-I^{HET} EMT6 or **B) E**0771 tumor cells were injected subcutaneously in BALB/c or C57BL/6 mice, respectively. See attached with IgG, anti-CD8α, ant-NK1.1 or anti-aGM1 antibody. Mice were treated at 7-day intervals with IgG antibody, anti-PD-L1 antibody, anti-NKG2A antibody, or a combination of anti-NKG2A and anti-PD-L1 antibodies. Graphs show individual mouse tumor growth curves. Green lines represent CR. **C)** Representative flow cytometry on CD8 and NK depleted splenocytes compared to whole splenocytes. **D)** Flow cytometry analysis of E0771 tumor MHC-I expression after treatment with IgG, anti-PD-L1, anti-NKG2A, or a combination of both anti-NKG2A and anti-PD-L1. E0771 tumors were resected at endpoint. Tumor cells are gated on live CD45^{-}, H2D^{+}. *n= 5.*

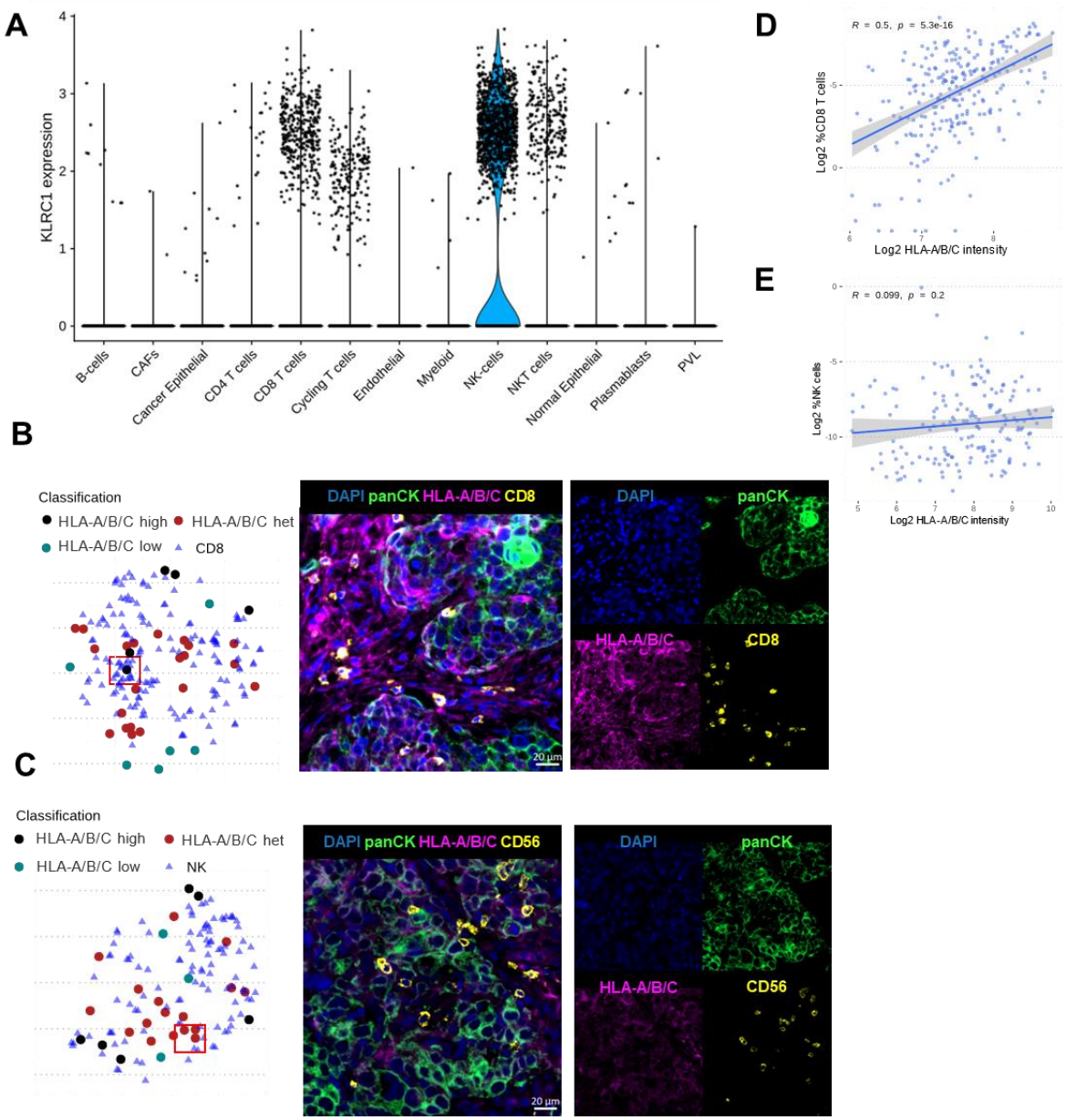

Supplementary Figure 4.5: A) The expression of KLRC1 (gene encoding NKG2A) was accessed in an annotated human TNBC single cell RNA seq dataset. B-C) Representative mIF staining for DAPI, panCK, HLA-A/B/C and B) CD8 or C) CD56 showing CD8 clusters around HLA-A/B/C high tumor islands in A and NK cells around HLA-A/B/C heterogenous tumor islands in B. Area marked by red square. D-E) The correlation between CD8 T cell and NK cell abundance and average MHC-I expression was measured with Pearson test. Log2 normalization was performed on HLA-A intensity, %CD8 T cells, and % NK cells to improve visualization. D) %CD8 T cell correlated with average tsMHC-I expression ($p<0.0001$, Pearson test). E) %NK cell correlated with average tsMHC-I expression ($p=0.2$, Pearson test).